1949 JUL 22 15:03
TECH LIBRARY KAFB, NM
0144599

NACA TN No. 1455

2808

NATIONAL ADVISORY COMMITTEE FOR AERONAUTICS

TECHNICAL NOTE

No. 1455

AN INVESTIGATION OF AIRCRAFT HEATERS

XXXI - SUMMARY OF LABORATORY TESTING OF SEVERAL EXHAUST-GAS AND AIR HEAT EXCHANGERS

By L. M. K. Boelter, A. G. Guibert, F. E. Romie,
V. D. Sanders, and J. M. Rademacher

University of California

Washington
July 1949

AFMDC
TECHNICAL LIBRARY
AFL 2811

319.98/41

0144599

NATIONAL ADVISORY COMMITTEE FOR AERONAUTICS

TECHNICAL NOTE NO. 1455

AN INVESTIGATION OF AIRCRAFT HEATERS

XXXI - SUMMARY OF LABORATORY TESTING OF SEVERAL EXHAUST-GAS AND AIR HEAT EXCHANGERS

By L. M. K. Boelter, A. G. Guibert, F. E. Romie,
V. D. Sanders, and J. M. Rademacher

SUMMARY

A comparison of the thermal performance and pressure-drop characteristics of heat exchangers tested on the University of California heat-exchanger test stand is presented. These exchangers included both parallel and cross-flow units as well as extended-surface and all-prime-surface units. All the heater performances were reduced to a uniform basis for purposes of comparison. This uniform basis was obtained by fixing the temperature difference of the exhaust gas and of the ventilating air at inlet and by choosing fixed exhaust-gas and ventilating-air weight rates. The results are presented in tabular form and in a series of performance charts for each heater. When several heaters were tested with two or more air shrouds, a comparison was made on the basis of results obtained with only one shroud in order to avoid duplication.

A description of the testing techniques used during these tests and a discussion of the measurement of the variables - temperature, weight rate, and pressure drop - are presented.

INTRODUCTION

The investigation of aircraft heaters at the University of California has resulted in the testing of a number of heat exchangers; the test data for most of these exchangers have been published in references 1 to 10. Because of the variety in the types of heat exchangers tested, a report in which all these data would be condensed, and from which the relative merits of the heaters could be estimated by direct comparison of all the factors involved, was thought desirable. Inasmuch as all these heat exchangers were tested at different exhaust-gas rates, the experimental data were plotted and, by interpolation, the heater performance at an exhaust-gas weight rate of 5000 pounds per hour was chosen as the basis of comparison. The inlet temperatures of the fluids were taken as 1600° F for the exhaust gas and 50° F for the ventilating air, corresponding to an inlet temperature difference of 1550° F. The experimental data were adjusted to these conditions by calculation.

A report (reference 11) has been published which presents results obtained at the Ames Aeronautical Laboratory (referred to as Ames in the present report) on the performance of several heat exchangers, some of which were also tested here. Because all the heat exchangers for which performance data are presented in this report were not tested at Ames, the same method of heater designation is not used. In all cases where the heat exchanger was also tested by Ames, however, the Ames designation is given in table I to facilitate identification. A point of difference between the Ames data and the data in this report is that the exhaust-gas weight rate used as the basis of comparison is not the same, the value in the Ames report being 3300 pounds per hour and the value in this report being 5000 pounds per hour. This is an undesirable feature, but it was unavoidable because of the fact that the majority of the heat exchangers in the present work had been tested at exhaust-gas rates higher than 3300 pounds per hour, and extrapolation to 5000 pounds per hour was preferable to extrapolation to 3300 pounds per hour. In addition, the instrumentation of the test setups differed because the Ames tests were flight tests of the heat exchangers and consequently the spatial limitations were different. In the Ames tests, the exhaust-gas flow was from an aircraft engine, metered by a venturi section, and all pressure drops (both isothermal and nonisothermal) were measured using static-pressure wall taps and static-pressure tubes.

If the heater thermal performances obtained at Ames are compared with those obtained at this laboratory (at equivalent conditions), it is found that the Ames results are about 12 percent lower, on the average. This deviation may be due in part to the differences in arrangement of the experimental apparatus and instrumentation.

This work was conducted at the University of California under the sponsorship and with the financial assistance of the National Advisory Committee for Aeronautics.

REDUCTION OF DATA

Heat Transfer

Because the conditions for the tests of the heat exchangers were different in each case, it was necessary to adjust all results of measurement to a common basis before comparison could be attempted. The basis for comparison of the thermal outputs of the various heat exchangers was chosen at an exhaust-gas weight rate of 5000 pounds per hour, a ventilating-air weight rate of 3000 pounds per hour, and with an inlet temperature difference of 1550° F. The experimental data were usually interpolated (or extrapolated) to the desired weight rates of gas and air. The method of correction of the thermal output q_a of the heaters to the proper inlet temperature difference consisted in multiplying the interpolated (or extrapolated) value of the thermal output by the ratio of the desired inlet fluid temperature difference

(1550° F) to the measured inlet fluid temperature difference. This method of correction is based upon the equation, developed in reference 12,

$$q_a = K_a W_a c_{p_a} \left(\tau_{g_1} - \tau_{a_1}\right) \Phi \tag{1}$$

where

K_a	factor to account for heat losses to surroundings
W_a	weight rate of ventilating air
c_{p_a}	heat capacity of ventilating air
$\tau_{g_1} - \tau_{a_1}$	desired temperature difference of fluids at inlet
Φ	heater effectiveness

This last term, "heater effectiveness," is a function of the fluid weight rates and heat capacities, the over-all thermal conductance of the heater, and the geometrical type of flow. (Graphs of the heater effectiveness Φ are presented in reference 13 for parallel, counter, and cross flow of the fluids.) If the over-all thermal conductance and the heat capacities of the fluid are postulated to be independent of the fluid temperatures, then the effectiveness Φ is not a function of the inlet temperature difference of the fluids.[1] Consequently, for a given heater and fixed fluid weight rates, the relationship between the heat transferred and the inlet temperature difference is linear.

Pressure Drop

Only the isothermal pressure drops are presented in this report. These isothermal values correspond to the frictional pressure loss within the heat-exchanger - duct system because they are measurements of the isothermal static-pressure drop taken at stations of equal cross-sectional areas of flow.[2] The air-side pressure drops are plotted

[1]This postulate is only an approximation, but, as shown in appendix A of reference 6, the error committed by using invariable thermal properties was small even when the inlet temperature difference was changed by a factor of about 2.

[2]This was true of all exhaust-gas-side measuring stations, but on the ventilating-air side, two shrouds, those used with exchangers C and P, did not have equal cross-sectional areas at inlet and outlet. In the first case, of the two outlets present, only the cabin-air outlet differed in cross-sectional area. In each case the necessary corrections were calculated and added to the measured values.

for an air temperature of 100° F. The exhaust-gas-side pressure drops were corrected to a gas temperature of 1500° F. This correction was accomplished by multiplying the isothermal static-pressure drops by the ratio of the absolute temperatures to the 1.13 power. This ratio consists of two terms, $\left(\frac{T_{iso_2}}{T_{iso_1}}\right)^{1.00}$ and $\left(\frac{T_{iso_2}}{T_{iso_1}}\right)^{0.13}$. The first of these terms corrects for the variation of density with temperature, and the second one corrects for the variation of the friction factor with viscosity and consequently with temperature. The error involved in using this method for the correction of isothermal pressure-drop values from one fluid temperature to another lies in the fact that, whereas both the preceding terms are required for correction of the frictional pressure losses, only one of them, the term correcting for the variation of density with temperature, is valid for the correction of the expansion and contraction losses which occur within the heat exchanger. Hence, an error is introduced when these losses are also multiplied by the ratio of the absolute temperatures to the 0.13 power.

DESCRIPTION OF HEAT-EXCHANGER UNITS

The 16 heat exchangers discussed can be arranged into two distinct groups according to the type of flow (parallel and cross flow), and each group can be subdivided into smaller groups according to the type of construction. The subdivisions are (1) flute type, (2) plate type, (3) tube-bundle type, and (4) pin or fin type. For purposes of discussion each heat exchanger is designated by a letter of the alphabet and referred to by this letter throughout the report. Drawings and photographs of the heat exchangers, as well as sketches of the test setup used for each heat exchanger and performance curves for each heater, are shown in figures 1 to 64.

Parallel-Flow Heat Exchangers

Fluted type (heaters A, B, C, D, and E).- The five fluted heat exchangers shown in figures 1, 5, 9, 12, and 16 were all-prime-surface units with alternate air- and exhaust-gas-side ducts arranged circumferentially around a hollow cylindrical core. In one of these, exchanger E, the sides of the ducts were corrugated, though in other respects it differed very little from exchanger D. (See figs. 12 and 16.)

Plate type (heater F).- Though the flow characteristics of the plate-type exchanger F were more nearly those of cross flow at inlet and outlet, this exchanger is considered to be in the parallel-flow group because the flow characteristics in the main body of the heat exchanger were predominantly those of parallel flow. (See figs. 20 and 21.)

Cross-Flow Heat Exchangers

Tube-bundle type (heaters G and H).- The two heat exchangers of the tube-bundle type which were tested were all-prime-surface units. Heat exchanger G was a flattened-tube bundle with ventilating air flowing through the tubes and exhaust gas flowing over the staggered tubes. (See fig. 24.)

Heat exchanger H is a circular-tube bundle which was tested using two different flow distributions. (See fig. 28.)

Plate type (heaters I and J).- The two plate-type heat exchangers tested (see figs. 32 and 36) were all-prime-surface units with alternate passages for the ventilating air and the exhaust gas. Heat exchanger I was of flat-plate construction with beads and dimples to maintain the spacing between the various sections. Heat exchanger J consisted of alternate ventilating-air and exhaust-gas passages made of preformed sheets such that the exhaust-gas passages were diamond-shaped and the rectangular ventilating-air passages (cross flow) conformed to the contours of the exhaust-gas passages.

Pin or fin type (heaters K, L, M, N, O, and P).- The six pin- or fin-type heat exchangers which were tested are shown in figures 40, 44, 48, 52, 56, and 60. They were all the cylindrical-core type. Heat exchangers K and L had pin-type extended surfaces. The circular pins on exchanger K differed from those on exchanger L in that they were partially hollow. The number and spacing of the pins were likewise different. Exchanger M was a cast-aluminum unit with circumferential fins machined on the air side and with continuous longitudinal fins with tapered ends on the gas side. Exchangers N and O were constructed somewhat alike, but differed in the materials used; exchanger N was made entirely of aluminum, whereas exchanger O was built with copper fins on the air side and with stainless-steel fins on the gas side. The air-side fins were strip fins inserted longitudinally into the heater shell and twisted so that they were alined with the cross-flow air stream. The fins on the gas side were continuous, longitudinal fins with tapering ends. Heat exchanger P was a slotted-fin unit consisting of copper fins spot-welded to a stainless-steel shell. The air-side fins were angle sections which were slotted and bent to fit around the circumference of the shell. The gas-side fins were channel sections which were slotted at regular intervals. Two of the three ventilating-air shrouds used in the tests on this exchanger are shown, and the data obtained in using them are also presented. (See figs. 60 to 64.)

General Remarks

Heat exchangers A, B, and C were all the same type of construction, merely differing in the dimensions, particularly the length. The same shroud was used for the tests on exchangers A and B, but a different

shroud, an actual installation design, was used in the tests on heat exchanger C. As shown in figure 9, the inlet to the gas side of exchanger C was the main branch of an engine exhaust-collector section, the side branches being sealed off. The heat-transfer data for exchanger C are for flow through the "overboard" duct only, the cabin-air duct having been sealed off.

Heat exchangers D and E were of the same general type of construction except for the fact that exchanger E had corrugated walls for the passages. (See fig. 16.) The same shroud was used in the tests of the two exchangers

Heat exchanger H, the circular-tube-bundle type, was tested with two air shrouds of the same general dimensions which provided two different arrangements of the tubes in order to vary the flow characteristics. Both flow systems had staggered arrangements of the tubes, but the longitudinal and transverse spacings were not the same.

The flat-plate cross-flow heat exchanger I was another experimental design for an actual installation. As seen in figure 32, the air-side ducts were well vaned. Figures 32 and 34 show the two outlets on the exhaust-gas side. The data plotted are for flow through both outlets. Because the flow areas at the ventilating-air-side pressure measuring stations were not equal, static-pressure wall taps were not desirable and therefore the total pressures at these stations were measured by traversing with shielded total-pressure tubes.

The wave-plate heat exchanger J shown in figure 36 was provided with a shroud which had a vaned inlet duct elbow to distribute properly the ventilating air over the heat exchanger.

Heat exchangers K to P, all cross-flow, extended-surface units, were tested using a full cross-flow shroud, designated as UC-1. In the additional tests on heat exchanger P, which is a fin-type heat exchanger using the shroud designated as A-1, characteristics of diagonal or semi-cross flow of the ventilating air were produced. It should be stated, also, that heat exchanger O, the copper - stainless-steel fin type, had been tested using still another shroud before the tests using the UC-1 shroud were made and that during these first tests some of the brazing which connected the air-side fins to the heater shell melted and consequently impaired the thermal output of this heat exchanger in all subsequent tests. Because heat exchangers M and N were constructed of aluminum, it was deemed advisable to test them at an inlet temperature of about 1000° F rather than 1600° F. The results plotted in figures 51 and 55 show the heater outputs measured at the inlet temperature of 1000° F and also the calculated values of the output at an inlet gas temperature of 1600° F.

All predicted values of heater output are based upon an inlet temperature difference of the fluids of 1550° F (inlet temperature of exhaust gas, 1600° F; inlet temperature of ventilating air, 50° F).

DISCUSSION OF HEATER RESULTS

The greatest heater output, the lowest air-side pressure drop, and the next to lowest gas-side pressure drop were obtained with heat exchanger I. The great thermal output was due, in part, to the rather large area of heat transfer. Heat exchanger G, the flattened-tube-bundle unit, and heat exchanger J, the wave-plate unit, yielded the next highest thermal outputs, and, in view of their smaller size, were more effective on that basis. The isothermal pressure drops, however, were several times larger than those for heat exchanger I.

All the all-prime-surface heat exchangers except D and H (using the A-5 shroud) had thermal outputs greater than 200,000 Btu per hour, whereas only one of the extended-surface units, the cast-aluminum exchanger M, had a thermal output greater than 200,000 Btu per hour under the prescribed conditions. These conditions are actually artificial as far as exchanger M is concerned because the aluminum might not be able to withstand the high exhaust-gas temperatures and might melt. The outputs of the aluminum exchangers for an inlet temperature difference of 1550° F are presented in this report in order to permit comparison of heater types. It may be that neither this exchanger M nor the other aluminum unit, exchanger N, could be used directly in the exhaust-gas stream of aircraft engines, but they could be used as secondary heat exchangers for cabin-air heating where the hot fluid is the ventilating air from a primary exhaust-gas and air heat exchanger.

It is worthy of note, also, that exchanger K, the hollow-pin-type unit, yielded a thermal output of almost 75 percent of that of the solid-pin-type exchanger L though it weighed less and had a smaller number of pins than exchanger L.

For an exhaust-gas weight rate of 5000 pounds per hour, the exhaust-gas-side isothermal pressure drops (τ_g = 1500° F) varied from 3.17 inches of water for the flat-plate-type exchanger I to 42.7 inches of water for the flattened-tube-bundle-type exchanger G. Whereas most of the exchangers had pressure drops below 2 inches of mercury, three exchangers, F, G, and M (the flat-plate parallel-flow unit, the flattened-tube-bundle unit, and the cast-aluminum fin-type unit, respectively), had higher pressure drops. With respect to exchanger F, this high pressure drop would seem to be wholly due to the entrance and exit losses caused by the transition sections from circular duct to rectangular heater, since the pressure drops on the air side, where such transition sections are absent, were considerably lower. In heat exchanger G, the high pressure drop was probably due to the close spacing of the flattened tubes and could be lowered by changing the tube arrangement. For the case of exchanger M, the high pressure drop on the exhaust-gas side, as discussed in reference 7, is probably due in great part to the roughness of the as-cast lateral surfaces of the longitudinal fins on the exhaust-gas side.

Table I is included for purposes of comparison at an exhaust-gas weight rate of 5000 pounds per hour and a ventilating-air weight rate of 3000 pounds per hour. The use of the table is limited because it furnishes information on the individual heater performances under this one set of conditions only. For more information the graphs of the original report, referred to by reference number in the fourth row of table I, must be examined. The figures are grouped according to the heater designation. With the exception of heat exchangers C and P, there are four figures associated with each heat exchanger. These are:

(a) First figure: A semi-detailed drawing of the heat exchanger and the ventilating-air shroud (or shrouds, if the heater was tested using two different shrouds).

(b) Second figure: One or two photographs of the heat exchanger and, in figures 2, 6, and 61 (heat exchangers A, B, and P, respectively), a photograph of the heater test setup. (A photograph of heat exchanger C was not available.)

(c) Third figure: A diagrammatic sketch of the heat-exchanger test-setup with pertinent dimensions. Heat exchanger P was tested using two different shrouds, so that two sketches are necessary. (See figs. 62 and 63.)

(d) Fourth figure: The graphs of the performance curves of each heat exchanger are presented in this fourth figure. The abscissa for the weight rate of fluid is not designated as being for either the air or gas side because of the fact that the curves of performance on both sides are presented. The thermal-performance curves, plotted for an exhaust-gas weight rate of 5000 pounds per hour, are given as functions of the ventilating-air weight rate. In the case of heat exchanger P, this is the fifth figure.

DESCRIPTION OF INSTRUMENTATION

Temperature Measurements

The measurement of fluid temperatures, obtained on the heater test stand, usually was accomplished by using chromel-alumel traversing thermocouples. When measuring the temperature of hot exhaust gases, these thermocouples were shielded so as to minimize the heat loss by radiation from the thermocouple junction to the relatively cool duct wall. Shielding is necessary because this heat transfer by radiation causes the temperature recorded by the thermocouple to be inaccurate, often by as much as 150° to 200° F at temperatures near 1500° F. (See references 14 and 15.) The source of this error can be understood by inspection of the following heat balance on the thermocouple junction of an unshielded thermocouple:

Heat in by forced convection = Heat out by radiation to duct wall + Conduction along leads

$$f_c A_1(\tau - t_c) = \sigma F_{AE} A_1\left(T_c^4 - T_w^4\right) + kA_2\left(\frac{\partial t}{\partial x}\right)_{x=0} \tag{2}$$

where

f_c	unit thermal convective conductance over thermocouple junction
A_1	surface area through which heat is being transferred
τ	fluid temperature
k	thermal conductivity of metal in tube used to support thermocouple or thermal conductivity of the thermocouple leads
A_2	cross-sectional area of tube or of thermocouple leads
t_w	inner-wall temperature of pipe
T_w	absolute inner-wall temperature of pipe
t_c	temperature of thermocouple junction
T_c	absolute temperature of thermocouple junction
σ	Stefan-Boltzmann radiation constant
F_{AE}	factor which takes into account geometrical arrangements and emissivities of the radiating surfaces
x	distance from thermocouple junction along leads or along support tube

The factor F_{AE} is equal to ϵ_c, the emissivity of the thermocouple junction, for the case of an unshielded thermocouple junction placed in a pipe, because of the fact that the junction "sees" all the pipe and because only the emissivity of the smaller body is important when a small body is placed within a relatively large enclosure. The area A_1 for use in the radiation term of the equation need not be the same as the area A_1 for use in the convection term of the equation if there are re-entrant angles in the surface. In case there are such angles, the area to be used in the radiation term is approximated by using an effective "projected" area. The effective emissivity of such

a surface will be higher than the actual emissivity of the metal. For the unshielded thermocouple junction, where the conduction term is usually smaller than the radiation term and the heat-transfer areas for convection and radiation are the same, the heat-balance equation (2) can be simplified to:

$$f_c(\tau - t_c) = \sigma\epsilon_c\left(T_c^4 - T_w^4\right) \tag{3}$$

The thermocouple must measure the temperature of the fluid accurately; hence τ and t_c must be made to approach each other and, consequently, the heat transfer must approach zero. This can be accomplished for an unshielded thermocouple only by causing T_w to approach T_c, that is, to approach the absolute temperature of the fluid. The means available are insulation of the pipe and shielding of the thermocouple junction. Another means which is not always available, because the weight rate of fluid may be fixed, is to increase the flow thereby causing an increase in the wall temperature of the pipe with a consequent decrease in the radiation losses. Increasing the flow also causes an increase in the temperature of the thermocouple junction because of the decreased resistance to heat transfer of the fluid flowing over the junction. The readings of a thermocouple are therefore more accurate at the higher weight rates. Insulation of the pipe is not a convenient method because the amount of insulation required to increase the relatively low pipe-wall temperature to a point where the radiation term would become small is large in terms of space and weight when the temperature of the fluid is in the region of 1000° F. Because of the ease of surface oxidation of most metals at high temperatures, polishing of the surfaces in order to reduce the emissivity and in this way to reduce the radiant transfer of heat, is not a practicable procedure. The aforementioned methods are not usually satisfactory, so that recourse must be had to the use of shields to reduce the heat transfer by radiation. This method gives the desired results for two reasons: First, considering radiant heat transfer only, the introduction of n shields between a radiating body and its surroundings will decrease the heat transfer by a factor of $\frac{1}{n + 1}$; and second, when such a system of shields is placed in a hot gas stream the tendency will be for all the shields to attain the temperature of the gas stream because of the heat transferred by convection. A description of the design of shields and a fuller discussion of the theory underlying their use is presented in reference 14.

On the ventilating-air side of the test apparatus, these traversing thermocouples were not shielded because calculation showed that the errors introduced by radiation from the thermocouple to the cooler pipe wall were only about 1 percent of the temperature rise of the ventilating air as it passed through the heat exchanger because of the lower values of absolute temperature involved.

The measurement of fluid temperatures in heat-exchanger tests has as its object the obtaining of the proper "mixed-mean" temperature of the fluid flowing at a section. This mean temperature can be obtained by traversing with a thermocouple, by using "averaging" networks of thermocouples - both series and parallel - by using mixing devices, or by using combinations of these techniques.

Use of the first method implies that the temperature distribution is the same along any diameter. This is not always the case and, consequently, two or more traverses along different diameters may be necessary in order to obtain a more representative value of the temperature. A better method consists in employing devices to mix the fluid before a traverse is made.

When multiple temperature measurements are to be used to obtain a mixed-mean temperature of a fluid, the following considerations must be taken into account.

The total enthalpy H_T (measured above zero temperature) of a fluid of heat capacity c_p, weight density γ, velocity u, and temperature τ flowing in a duct is given by

$$H_T = \int_A u c_p \gamma \tau \, dA$$

where u, c_p, γ, and τ are taken at a differential area dA and then summed up over the total area A of the duct.

The mixed-mean temperature τ_m may be defined by[3]

$$\tau_m = \frac{\int_A u c_p \gamma \tau \, dA}{\int_A u c_p \gamma \, dA} \tag{4}$$

Because c_p and γ are functions of temperature and may vary across a duct section, and because u varies according to the flow characteristics, these variables must also be measured at the same points where the temperature is measured in order to obtain a true mixed-mean temperature. The integration can be accomplished graphically.

---

[3]The mixed-mean temperature τ_m corresponds to the temperature which would be obtained if a representative sample of the fluid flowing were adiabatically mixed to a uniform temperature before a measurement of the temperature was undertaken.

If c_p and γ are not functions of temperature (or if the temperature gradient in the fluid is small) these terms may be taken out of the integral so that

$$\tau_m = \frac{\int_A u\tau \, dA}{\int_A u \, dA}$$

In this laboratory the temperature measurements are usually made over small areas $A_1, A_2 \cdot \cdot \cdot A_n$ such that $u_1A_1 = u_2A_2 = \cdot \cdot \cdot u_nA_n$. If the integrals are first replaced by a summation of the mean values over finite areas, the equation then can be simplified as follows:

$$\left.\begin{aligned} \tau_m &= \frac{u_1A_1\tau_1 + u_2A_2\tau_2 + \cdot \cdot \cdot u_nA_n\tau_n}{u_1A_1 + u_2A_2 + \cdot \cdot \cdot u_nA_n} \\ &= \frac{(u_1A_1)(\tau_1 + \tau_2 + \cdot \cdot \cdot \tau_n)}{n(u_1A_1)} \\ &= \frac{(\tau_1 + \tau_2 + \cdot \cdot \cdot \tau_n)}{n} \end{aligned}\right\} \qquad (5)$$

Thus the arithmetic average of these specified temperature measurements may be taken as the mixed-mean temperature. This technique requires a knowledge of the velocity distribution in a duct which is a function of the Reynolds modulus R.

At a particular value of the Reynolds modulus, zones are defined such that the product of velocity and intercepted area in one zone is equal to that in any other zone. Because the distribution of velocity across a duct section is a function of the Reynolds modulus, the location of these zones is variable. If the temperature in each small zone does not vary greatly, then a measurement of the temperature at the midpoint of the zone may be taken as the mixed-mean temperature of that zone. If the temperatures do vary greatly in these zones, then a more exact location of the proper point for temperature measurement in each zone requires some knowledge of the temperature distribution. For a value of R = 90,000 in a circular duct the points for a ten-point temperature traverse are

$$\frac{r}{r_o} = 0.21,\ 0.51,\ 0.67,\ 0.80,\ \text{and } 0.92$$

where r_o is the radius of the pipe and r is the radial distance to the point. These points are at the midpoints of the ten zones of equal uA.

The use of averaging networks of thermocouples consists in locating the thermocouples at certain points in a section of a fluid stream and recording either the arithmetic average value directly or the sum of several thermocouple readings, from which the arithmetic average may be obtained by dividing the sum by the number of thermocouples. This method considerably simplifies the obtaining of the mixed-mean temperature, but some practical difficulties exist. If the thermocouples are connected in parallel, with equal electrical resistances of the individual leads, then the desired average temperature is obtained, provided that all the thermocouples are functioning. There are difficulties involved when a thermocouple is no longer functioning, for then the accuracy of the "average" reading cannot be certain unless the network is easily accessible for frequent inspection. Obtaining leads of equal resistance for each thermocouple, a necessary requirement, is sometimes difficult because the resistance of the leads is a function of temperature. The series system of connection also has some disadvantages. If one of the thermocouples becomes faulty the entire network is rendered unusable. Also, the fact that the thermocouples are connected in series means that if a larger number of thermocouples are used, the range of the usual potentiometer may be exceeded at moderate temperatures and consequently it may not be possible to employ a simple null method of measurement. If a null method is not used, then the measurement of current or voltage is a function of the electrical resistance of the thermocouple system which is in turn a function of temperature. Thus a calibration is required for a large temperature range.

Mixing devices are used to mix the fluids so that a more uniform distribution of temperature is obtained. A device for mixing exhaust gases which was used in these laboratories with satisfactory results is shown in reference 1, where the results obtained with one or two other types are also discussed briefly. Orifices are generally used with equally satisfactory results for the mixing of the ventilating air at outlet to increase the accuracy of the temperature traverses. The efficacy of various types of this device, as noted by different experimenters, is listed in reference 16.

The fluctuation of the fluid temperature was not a factor in the tests performed on the large test stand, but may be a small factor in flight tests in which the temperature of the exhaust gases varies with time. Because of the thermal capacitance of thermocouple leads, however, and the high frequency of the gas temperature cycle, the temperature recorded by thermocouples in such a gas stream is a time mean of the fluctuations.

Surface-temperature measurements were obtained in some tests by using chromel-alumel thermocouples welded to the surfaces of which temperatures were desired. Other methods of attachment which are in use are (1) peening of the thermocouple junctions in specially prepared holes and (2) fastening the junction to the metal by placing it under a rivet head or by fastening the thermocouple wires to the rivet. Calculation of the error in surface-temperature measurement by thermocouples because of thermal losses from the thermocouple leads is made possible through use of the methods presented in reference 17. These methods permit the estimation of the effect on this error of the variation of the size of the lead wires, the thermal conductivity of the leads, the thermal conductivity, and the thickness of the surface of which the temperature is to be measured, as well as several other physical variables.

These thermal losses in the leads may be decreased by flattening the leads and laying them along the surface for a short distance so that this section of the leads is in good thermal (but not electrical) contact with the surface. This procedure decreases the thermal gradients in the leads which control the heat losses from the leads for a short distance from the junction. Another method of achieving the same result consists in making a groove in the surface and imbedding the leads in this groove.

Radiometers similar to those described in references 18, 19, and 20 have been used to measure surface temperatures as low as 300° F. These low temperatures were measured by means of a radiometer of the design described in reference 18. The theory for this design, which was used for the measurement of surface temperatures in turbosuperchargers, is also discussed in reference 18. Other radiation pyrometers of improved design are reported in references 19 and 20.

The use of lacquers, pellets, and crayons for the evaluation of the maximum temperature attained by a surface is a method of measurement which is also worthy of attention. The lacquers and pellets have a range of temperature from about 125° to about 1600° F, whereas the crayons have a temperature range of about 125° to about 700° F. At the lower temperatures the selection is available for about every 25° F, but at the higher temperatures the selection is more limited and the lacquers are available only at intervals of 50° F or more.

Fluid Metering

The theory and the practical application of all types of fluid meters are extensively discussed in the report by the A.S.M.E. (See reference 21.) In this laboratory the meters used have been exclusively of the "head" class, in that they are dependent upon a change of the fluid head as an indication of the fluid rate.

The weight rates of fluid through the heat exchangers were measured using calibrated square-edged orifice plates the coefficients of which corresponded to the standard values given in reference 22. The orifices are calibrated when in their operating location in the 8-inch round ducts of the test stand, by comparing the flow rates measured with these orifices and those calculated from traverses with a pitot-static tube of standard design. (See reference 21.) The pressure-tap locations were those for radius taps because the differential head obtained with pipe taps is slightly smaller than that obtained with the radius taps. Other types of tap (flange, vena contracta, etc.) are used, but they are more difficult to locate accurately than are the radius taps. If the small differential head is not a factor, then the pipe taps are probably more desirable because they do not have to be located so accurately to correspond with the "standard" coefficients given in reference 21.

Venturi meters and nozzles cause less over-all pressure loss than orifices and would therefore be more desirable when high weight rates of fluid are to be attained. Other low-pressure-drop metering procedures are:

(1) Use of a section of calibrated pipe

(2) Measurement of the velocity of the fluid with a pitot-static tube.

The first method involves the measurement of the frictional pressure loss within a section of pipe at known fluid rates such that the pipe is calibrated for all future use, except for occasional rechecks to make certain that the roughness of the pipe (due to rusting, etc.) has not caused a change in the calibration. The second method, based upon the use of a pitot-static tube for measurement of the velocity of the fluid at a fixed point, depends upon the placing of this pitot-static tube either at the position where it will measure a velocity corresponding to the average velocity in the section or where it will measure the maximum velocity in the section. Because of the fact that the radial location of the velocity corresponding to the average velocity changes with the Reynolds number and because a slight variation of the pitot tube from this point means a relatively great change in the velocity measured (the point is usually located on a portion of the velocity-distribution curve where the gradient is very large), it is again necessary to calibrate the readings against known fluid rates. Calibration is also necessary when the pitot-static tube is placed at the center of the pipe to measure the maximum velocity because of the fact that the ratio of the average velocity to the maximum velocity varies as the Reynolds modulus is varied. Of course, traverses with a pitot-static tube are also means of obtaining a flow rate, the ten-point method being the most commonly used system for the placement of the pitot-static tube.

Pulsations in the flow which originate at the blower were not apparent at the orifices at low weight rates, but when the maximum flow was approached some fluctuation was present, even as far as the heat exchanger, since the pressure-drop manometer readings were not steady. At these high rates, however, the fluctuation range was only a small percentage of the value to be measured. Two devices for the measurement of pulsating flows are described and discussed in reference 23, and a general discussion of the errors inherent in the use of square-edged orifices and other instruments for measurement of pulsating flows is given in references 24 to 27. Reference 23 also contains a chart which permits determination of the range of the pulsation error included in the readings of orifice meters if the readings obtained with a mechanical pulsameter, one of the devices described in the article, are available.

The flow rates are metered before the fluids pass through the respective sides of the heat exchanger because this obviates the difficulty of metering high-temperature fluids, a distinct disadvantage in the case of the hot exhaust gases which are frequently at temperatures of 1400° F on leaving the heat exchanger. On the other hand, metering the fluid before it enters the heater section has disadvantages in that the presence of leaks at the entrance to the heater will mean that the determination of the amount of fluid flowing through the heater is in error. Because all leaks in the test-setup connections are prevented, if possible, and because the effect of most leaks is negligible, it was felt that the advantages of metering the fluid before it enters the heater outweighed the disadvantages of so doing. Metering the fluids before they enter the heat exchanger required the separate metering of the natural gas and combustion air and the subsequent addition of these rates to obtain the weight-rate of the exhaust gases through the heat exchanger.

Pressure Drop

In order to determine the pressure-drop characteristics of a heat-exchanger system the following magnitudes may be measured:

(1) Total pressure

(2) Velocity pressure

(3) Static pressure

Various instruments used for these measurements are described in this section.

The fundamental pressure-drop measurement which should be used to evaluate the performance of a heater system is the isothermal total-pressure drop. This term represents the irrecoverable losses due to skin friction, expansion and contraction losses, and so forth, and is

also referred to here as the frictional pressure loss. Pressure drops due to acceleration of the fluid are recoverable either by mechanical means (diffusers, etc.) or by thermal means (cooling of the fluid).

In the case of isothermal flow a measurement of the total-pressure drop across a system is sufficient to determine this frictional pressure loss. In the special case where the cross-sectional areas for flow are equal and the velocity distributions are equal at the upstream and downstream measuring stations, a measurement of the static-pressure drop is sufficient.

For a nonisothermal-flow system the measurement of the total-pressure drop is not sufficient to evaluate this frictional pressure loss, and thus additional calculations are required.

Of course the frictional pressure loss is not the only pressure measurement desired in the analysis of a heater. For instance, for mechanical or structural reasons it may be necessary to know the value of the static pressure at a certain point in the exchanger system. For analytical design purposes, however, the frictional pressure loss is important because it is useful in estimating the flow of fluid through the heater and thus fixing the rates of heat transfer obtainable. This term is easily measured under isothermal conditions and also can be estimated from known values of friction factors and head-loss coefficients.

In the following text the instruments and fittings used to measure the previously mentioned pressures or pressure drops will be discussed first, and then the significance of these measurements with respect to the relations between the frictional pressure loss and the total pressure, velocity pressure, and static pressure will be shown by means of equations.

Discussion of instruments.- Static pressures, if constant over the measuring section (far from bends, etc.) can be measured most simply through the use of properly installed wall taps. In all the tests reported here, these wall taps were used to measure the static-pressure drops. The taps usually consisted of a 1/32- to 1/16-inch hole drilled through the pipe wall after a suitable fitting for the manometer leads had been installed on the outside of the pipe. The inner pipe surface near the static hole must, of course, be clean and free from burrs, and so forth. In a few cases, not reported here, special "round-head" taps (see following sketch) were inserted through the pipe wall to measure the static pressure.

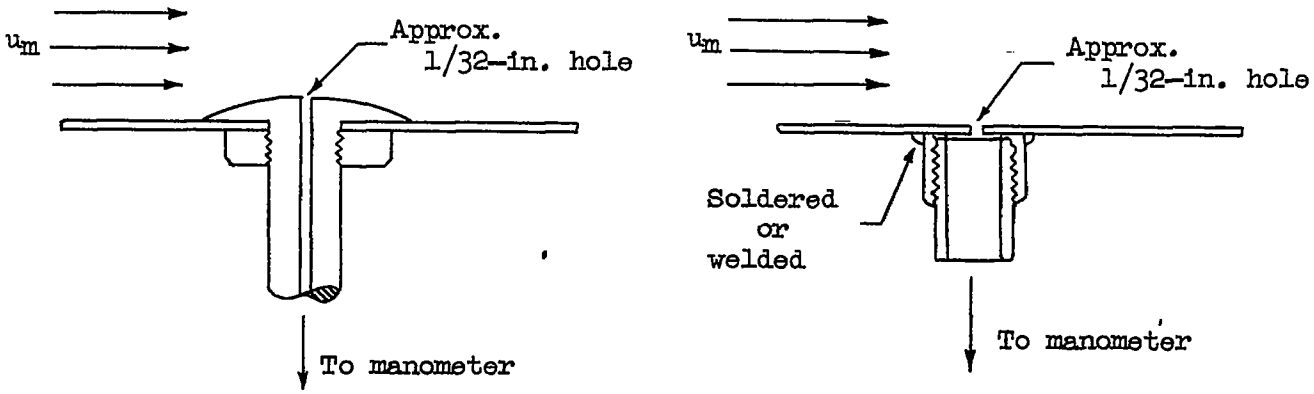

Round-head taps

Wall taps

These round-head taps were satisfactory at low fluid velocities but yielded low values of static pressure at high velocities because of the distribution of static pressure over the surface of the round head.

If the static pressure is not uniform across the duct section, it becomes necessary to use a traversing tube to measure the static-pressure distribution. These tubes are satisfactory if properly directed in the fluid stream. If the static pressure varies because of cross-flow components of velocity, however, the proper orientation of these tubes in the fluid stream is difficult. Static tubes are very useful when the walls of the duct are in such condition that wall taps are difficult to install.

Velocity pressures and total pressures were measured with traversing tubes. The velocity pressures were measured with standard pitot-static tubes only, but the total pressures were measured with two types of pitot tube. The ordinary pitot tube was used for some of the earlier measurements, but the more recent measurements of the total pressure have been

carried out by making traverses with shielded total-head tubes. These tubes have a venturi section located over the inlet of the total-head tube and are very insensitive to the direction of flow of the fluid with respect to the axis of the total-head tube. The angle between the axis of the tube and the flow direction can become as high as about 60° to 80° before a noticeable change occurs in the reading obtained with the tube. Such tubes are nonetheless sensitive to changes in the magnitude of the total pressure. Some of these tubes have been made of stainless steel and were satisfactorily used in the tests on heat exchanger I to measure the total pressure in the hot exhaust gases.

Discussion of pressure-drop equations.- For isothermal flow the frictional pressure loss is determined from the measurements of the total pressure at given sections because the total pressure is a measure of the mean mechanical energy of the fluid at those given sections. This energy consists of the potential energy, measured by the static pressure, and of kinetic energy, measured by the velocity pressure. The mean static heads $\frac{P}{\gamma}$ and the mean velocity heads $\frac{u_m^2}{2g}$ represent the ratio of the respective potential and kinetic energies of the fluid passing a given section in unit time to the weight of fluid passing the section in the same unit time. (See reference 28.) The mean static pressure P and the mean velocity pressure $\frac{\rho u_m^2}{2}$ may be thought of as the ratio of the energy of the fluid passing a given section in unit time to the volume of fluid passing that section in the same unit time. The kinetic energy of the fluid passing a given section in unit time is then equal to one-half the product of the mass rate of the fluid and the square of the velocity of the fluid, as follows:

$$\frac{1}{2}\int_0^m dm\ u^2 = \frac{1}{2}\int_0^{r_o}\left(\frac{u\gamma 2\pi r\ dr}{g}\right)u^2 = \pi\int_0^{r_o}\frac{\gamma}{g}u^3 r\ dr$$

where

dm	mass rate of fluid flowing in differential annulus
u	velocity of fluid in annulus
γ	weight density of fluid
r	radial distance from center of circular duct to annulus
r_o	radius of duct

dr differential thickness of annulus (symmetrical flow is postulated)

g gravitational force per unit of mass

If the kinetic energy of the fluid passing a given section in unit time is divided by the volumetric rate of the fluid $\left(\frac{W}{3600\gamma}\right)$, the result then represents the velocity pressure. By letting the static pressure represent the potential energy, the over-all energy loss of a fluid flowing from one section of a duct to another can be expressed by the following equation:

$$\Delta F_{a-b} = (P_a - P_b) + \left[\frac{\int_0^{r_a} \pi\frac{\gamma}{g}u_a{}^3 r\ dr - \int_0^{r_b} \pi\frac{\gamma}{g}u_b{}^3 r\ dr}{\left(\frac{W}{3600\gamma}\right)}\right]$$

which can be simplified to

$$\Delta F_{a-b} = (P_a - P_b) + \frac{3600\pi\gamma^2}{gW}\left(\int_0^{r_a} u_a{}^3 r\ dr - \int_0^{r_b} u_b{}^3 r\ dr\right) \qquad (6)$$

where ΔF_{a-b} is the frictional loss from section a to section b, that is, the irrecoverable loss of energy.

Under certain conditions, equation (6) can be simplified:

(a) If the areas at the two sections are not equal, but the velocity distributions are the same (or approximately the same), then equation (6) reduces to:

$$\Delta F_{a-b} = (P_a - P_b) + (q_a - q_b) = (P_a + q_a) - (P_b + q_b) = \Delta P_{total} \qquad (7)$$

where q_a and q_b are the velocity pressures $\frac{\rho u_m{}^2}{2}$ at the two sections, respectively. (The term u_m is the mean velocity at each cross section.) It can be seen from the form of the equation that for this case the isothermal frictional pressure loss can be obtained by measuring the difference in the total pressures at the sections under consideration. It should be noted here that some caution is necessary when using results

of a total-pressure traverse to determine this frictional loss because, as is evident from equation (6), the total pressure is a function of the cube of the local velocity, but the values obtained from measurements with a total-pressure tube are functions of the square of this velocity. A precise determination of the total pressure of a stream from traverse data can be made only by reference to equation (6). The local velocity must be determined (by making, for example, both total- and static-pressure measurements at the same point) and the integrals on the right-hand side of equation (6) must be evaluated graphically. It can be said, however, that in most cases the total pressure determined in this manner does not differ greatly from that obtained by taking a simple arithmetic average of the data from a traverse with a total-pressure tube. Some experiments performed in this laboratory indicate that the errors are about 7 percent or less.

(b) If the areas at sections a and b are equal and if the velocity distributions are the same (or approximately the same), then equation (6) reduces to

$$\Delta F_{a-b} = (P_a + q_a) - (P_b + q_a) = P_a - P_b = \Delta P_{static} \tag{8}$$

that is, the isothermal frictional pressure loss is equal to the difference in static pressures at stations a and b. For this case, then, the static-pressure drop as measured by wall taps or static-tube traverses, and so forth is sufficient to obtain the isothermal frictional loss.

For the case of nonisothermal flow the frictional pressure drop can be determined from the following expression[4] (reference 13):

$$\Delta F_{a-b}\left(\frac{T_{av}}{T_{iso}}\right)^{0.13}\left(\frac{\rho_{iso}}{\rho_{av}}\right) = (P_a + q_a) - (P_b + q_b) - (q_{hb} - q_{ha}) \tag{9}$$

---

[4]The multipliers $\left(\frac{T_{av}}{T_{iso}}\right)^{0.13}$ and $\frac{\rho_{iso}}{\rho_{av}}$ are used to correct the isothermal value of ΔF_{a-b} to another temperature T_{av} and density ρ_{av}. Thus the term on the left-hand side of equation (9) is the isothermal frictional pressure loss at T_{av} and ρ_{av}.

where

$(P_a + q_a)$, $(P_b + q_b)$ total pressures at measuring sections a and b

q_{ha}, q_{hb} velocity pressures at entrance and exit of heat exchanger (of constant cross-sectional area), respectively

ρ_{iso}, ρ_{av} average densities within system for isothermal and nonisothermal flow conditions, respectively

From equation (9) it can be seen that the total-pressure drop between the pressure measuring stations is not equal to the frictional pressure loss in the case of nonisothermal flow but differs from it by an amount corresponding to the thermal acceleration (or deceleration) of the fluid within the heat exchanger $(q_{hb} - q_{ha})$. The frictional pressure loss can not be regained by use of mechanical devices, but as shown in reference 13, this loss (and more) can be regained by thermal means. Consequently, it is usually considered as part of the pumping work which must be done upon the fluid to force it through the heat exchanger and duct system.

If the areas at the pressure measuring stations are equal, then equation (9) reduces to the form:

$$\Delta F_{a-b}\left(\frac{T_{av}}{T_{iso}}\right)^{0.13}\left(\frac{\rho_{iso}}{\rho_{av}}\right) = (P_a - P_b) + q_a\left(1 - \frac{T_b}{T_a}\right) - (q_{hb} - q_{ha}) \qquad (10)$$

The magnitudes of the frictional pressure loss are determined from laboratory measurements in the following manner: Either the static-pressure drop $(P_a - P_b)$ or the total-pressure drop $(P_a + q_a) - (P_b + q_b)$ is measured. The term $(q_{hb} - q_{ha})$, the change in velocity pressure due to heating or cooling (change in fluid density) through the heater section (for constant cross-sectional area within the heater), is calculated. These measurements and calculations are then used in equations (9) or (10) to calculate $\Delta F_{a-b}\left(\frac{T_{av}}{T_{iso}}\right)^{0.13}\left(\frac{\rho_{iso}}{\rho_{av}}\right)$. Of course if the measurements consist of only the static-pressure drop $(P_a - P_b)$, then q_a and q_b must be calculated to obtain $(P_a + q_a) - (P_b + q_b)$. In most cases, for nonisothermal flow the measurements of total-pressure drops are not of much more use than measurements of static-pressure drops because additional calculations are necessary in either case in order to obtain ΔF_{a-b}. It may be stated again that static-pressure drops are usually easier to obtain, because traversing of the stream is not required, provided that the static pressure is uniform at the measuring stations.

The frictional pressure loss $\Delta F_{a-b}\left(\frac{T_{av}}{T_{iso}}\right)^{0.13}\left(\frac{\rho_{iso}}{\rho_{av}}\right)$ may be defined from equation (9) as the total-pressure drop which would occur if the fluid passed through the heater system at constant temperature T_{av} (that is, isothermal flow) and constant density ρ_{av}.

It should be noted that the pressure-drop values shown graphically in this report are values of $\Delta F_{a-b}\left(\frac{T_{av}}{T_{iso}}\right)^{0.13}\left(\frac{\rho_{iso}}{\rho_{av}}\right)$ because the data are given for isothermal flow (for air at 100° F and exhaust gas at 1500° F), and all static-pressure-drop measurements have been corrected to equal areas, if necessary (that is, calculated to be total-pressure drops).

Additional theory and derivation of these equations are given in references 13 and 29. Discussion of the significance and limitations of use of the term $\left(\frac{T_{av}}{T_{iso}}\right)^{0.13}\frac{\rho_{iso}}{\rho_{av}}$ is given in the section REDUCTION OF DATA, Pressure Drop.

Department of Engineering
University of California
Berkeley, Calif., October 30, 1944

REFERENCES

1. Boelter, L. M. K., Miller, M. A., Sharp, W. H., Morrin, E. H., Iversen, H. W., and Mason, W. E.: An Investigation of Aircraft Heaters. IX - Measured and Predicted Performance of Two Exhaust Gas-Air Heat Exchangers and an Apparatus for Evaluating Exhaust Gas-Air Heat Exchangers. NACA ARR, March 1943.

2. Boelter, L. M. K., Dennison, H. G., Guibert, A. G., and Morrin, E. H.: An Investigation of Aircraft Heaters. X - Measured and Predicted Performance of a Fluted-Type Exhaust Gas and Air Heat Exchanger. NACA ARR, March 1943.

3. Boelter, L. M. K., Miller, M. A., Sharp, W. H., and Morrin, E. H.: An Investigation of Aircraft Heaters. XI - Measured and Predicted Performance of a Slotted-Fin Exhaust Gas and Air Heat Exchanger. NACA ARR No. 3D16, 1943.

4. Boelter, L. M. K., Dennison, H. G., Guibert, A. G., and Morrin, E. H.: An Investigation of Aircraft Heaters. XII - Performance of a Formed-Plate Crossflow Exhaust Gas and Air Heat Exchanger. NACA ARR No. 3E10, 1943.

5. Boelter, L. M. K., Guibert, A. G., Miller, M. A., and Morrin, E. H.: An Investigation of Aircraft Heaters. XIII - Performance of Corrugated and Noncorrugated Fluted Type Exhaust Gas-Air Heat Exchangers. NACA ARR No. 3H26, 1943.

6. Boelter, L. M. K., Guibert, A. G., Rademacher, J. M., and Sloggy, L. J. B.: An Investigation of Aircraft Heaters. XIX - Performance of Two Finned-Type Crossflow Exhaust Gas and Air Heat Exchangers. NACA ARR No. 4H21, 1944.

7. Boelter, L. M. K., Guibert, A. G., Rademacher, J. M., Romie, F. E., and Sanders, V. D.: An Investigation of Aircraft Heaters. XX - Measured and Predicted Performance of a Finned-Type Cast-Aluminum Crossflow Exhaust Gas and Air Heat Exchanger. NACA ARR No. 5A08, 1945.

8. Boelter, L. M. K., Guibert, A. G., Rademacher, J. M., Romie, F. E., Sanders, V. D., and Sloggy, L. J. B.: An Investigation of Aircraft Heaters. XXI - Measured and Predicted Performance of a Flattened-Tube Type Crossflow Exhaust Gas and Air Heat Exchanger. NACA ARR No. 5A10, 1945.

9. Boelter, L. M. K., Guibert, A. G., Rademacher, J. M., and Romie, F. E.: An Investigation of Aircraft Heaters. XXII - Measured and Predicted Performance of a Fluted-Type Exhaust Gas and Air Heat Exchanger. NACA ARR No. 5A11, 1945.

10. Boelter, L. M. K., Guibert, A. G., Rademacher, J. M., and Sanders, V. D.: An Investigation of Aircraft Heaters. XXIII - Measured and Predicted Performance of a Flat-Plate Type Exhaust Gas and Air Heat Exchanger. NACA ARR No. 5A12, 1945.

11. Jackson, Richard, and Hillendahl, Wesley H.: Flight Tests of Several Exhaust-Gas-to-Air Heat Exchangers. NACA ARR No. 4C14, 1944.

12. Martinelli, R. C., Morrin, E. H., and Boelter, L. M. K.: An Investigation of Aircraft Heaters. VI - Heat Transfer Equations for the Single Pass Longitudinal Exchanger. NACA ARR, Dec. 1942.

13. Boelter, L. M. K., Martinelli, R. C., Romie, F. E., and Morrin, E. H.: An Investigation of Aircraft Heaters. XVIII - A Design Manual for Exhaust Gas and Air Heat Exchangers. NACA ARR No. 5A06, 1945.

14. King, W. J.: Measurement of High Temperatures in High-Velocity Gas Streams. Trans. A.S.M.E., vol. 65, no. 5, July 1943, pp. 421-428; discussion, pp. 428-431.

15. Kepner, R. A.: Exhaust Gas Generators and Model 900-A Exhaust-Gas Heat Exchanger No. 105. Rep. No. 628, Stewart-Warner Corp., May 1943.

16. A.S.M.E. Heat Transfer Div.: Measurement of the Average Temperature of Stratified Fluid Streams. Rep. of Committee on Heat Transfer Testing Technique, Dec. 1943.

17. Boelter, L. M. K., Romie, F. E., Guibert, A. G., and Miller, M. A.: An Investigation of Aircraft Heaters. XXVIII - Equations for Steady-State Temperature Distribution Caused by Thermal Sources in Flat Plates Applied to Calculation of Thermocouple Errors, Heat-Meter Corrections, and Heat Transfer by Pin-Fin Plates. NACA TN No. 1452, 1948.

18. Head, V. P.: Radiation Pyrometry in Turbosupercharger Testing. Trans. A.S.M.E., vol. 66, no. 4, May 1944, pp. 265-269.

19. Harrison, T. R., and Wannamaker, W. H.: An Improved Radiation Pyrometer. Temperature - Its Measurement and Control in Science and Industry. Am. Inst. Phys., Rheinhold Pub. Corp. (New York), 1941, pp. 1206-1224; also, Rev. Sci. Instr., vol. 12, no. 1, Jan. 1941, pp. 20-32.

20. Boelter, L. M. K., Bromberg, R., Gier, J. T., and Dempster, E. R.: An Investigation of Aircraft Heaters. XXV - Use of the Thermopile Radiometer. NACA ARR No. 5A13, 1945.

21. Anon.: Fluid Meters - Their Theory and Application. Rep. of A.S.M.E. Special Res. Committee on Fluid Meters. Fourth ed., A.S.M.E. (New York), 1937.

22. A.S.M.E. Power Test Codes: Information on Instruments and Apparatus. Pt. 5, Measurement of Quantity of Materials; ch. 4, Flow Measurement by Means of Standardized Nozzles and Orifice Plates, 1940.

23. Beitler, S. R., Lindahl, E. J., and McNichols, H. B.: Developments in the Measuring of Pulsating Flows with Inferential-Head Meters. Trans. A.S.M.E., vol. 65, no. 4, May 1943, pp. 353-356.

24. Hodgson, J. L.: The Orifice as a Basis of Flow Measurement. Selected Eng. Paper No. 31, The Institution of Civil Engineers (London), 1925.

25. Beitler, S. R.: The Effect of Pulsations on Orifice Meters. Trans. A.S.M.E., vol. 61, no. 4, May 1939, pp. 309-312; discussion, pp. 312-314.

26. Judd, Horace, and Pheley, Donal B.: Effect of Pulsations on Flow of Gases. Trans. A.S.M.E., vol. 44, no. 1869, 1922, pp. 853-902; discussion, pp. 902-918.

27. Bailey, Neil P.: Pulsating Air Velocity Measurement. Trans. A.S.M.E., vol. 61, no. 4, May 1939, pp. 301-306; discussion, pp. 306-308.

28. Dodge, Russell A., and Thompson, Milton J.: Fluid Mechanics. McGraw-Hill Book Co., Inc., 1937, ch. IX.

29. Boelter, L. M. K., Morrin, E. H., Martinelli, R. C., and Poppendiek, H. F.: An Investigation of Aircraft Heaters. XIV - An Air and Heat Flow Analysis of a Ram-Operated Heater and Duct System. NACA ARR No. 4C01, 1944.

TABLE I.- COMPARISON OF HEAT-EXCHANGER PERFORMANCE

	Parallel flow						Cross flow									
Heat exchanger	A	B	C	D	E	F	G	H		I	J	K	L	M	N	O	P	
AAL designation[a]	12	29	-----	10	----------	-----	34	39		-------	11	4	----	----	----	----	----------	
Shroud	A-2	A-2	B-3	A-4	A-4	G-1	UC-3	A-5	A-6	-------	Tr-1	UC-1	UC-1	UC-1	UC-1	UC-1	A-1	UC-1
Reference	1	2	9	5	5	10	8	----------		-------	4	------	----	7	6	6	3	
Type	Flute	Flute	Flute	Flute	Corrugated flute	Flat plate	Flat-tube bundle	Round-tube bundle		Flat plate	Wave plate	Hollow pin	Pin	Fin	Fin	Fin	Fin	
Weight rate of gas, W_g, lb/hr	5000	5000	5000	5000	5000	5000	5000	5000		5000	5000	5000	5000	5000	5000	5000	5000	
Inlet gas temperature, τ_{g_1}, °F	1600	1600	1600	1600	1600	1600	1600	1600		1600	1600	1600	1600	1600	1600	1600	1600	
[b]$\Delta P_g''$, in. H_2O	5.00	3.67	4.61	2.71	7.24	31.1	42.7	10.1		[c]A-3.17 B-2.90	14.1	2.44	9.45	37.9	19.6	12.7	5.51	
Weight rate of air, W_a, lb/hr	3000	3000	3000	3000	3000	3000	3000	3000		3000	3000	3000	3000	3000	3000	3000	3000	
Inlet air temperature, τ_{a_1}, °F	50	50	50	50	50	50	50	50		50	50	50	50	50	50	50	50	
[d]$\Delta P_a''$, in. H_2O	5.78	5.05	[e]3.10	7.45	12.5	1.50	5.46	2.52	2.68	0.34	3.5	2.92	3.89	2.18	1.87	1.84	3.62	1.95
Thermal output, q_a, kBtu/hr — Measured	271	220	288	159	214	330	386	191	216	416	326	74.0	96.8	232	113	126	164	166
Thermal output, q_a, kBtu/hr — Predicted	225	201	229	127	197	261	421	202	205	411	283	------	81.2	228	108	120	----	----
Heat-transfer area, A, sq ft — Gas side	17.9	11.4	13.5	7.19	6.50	20.4	19.4	9.76		63.0	19.2	------	----	----	----	----	----	----
Heat-transfer area, A, sq ft — Air side	17.9	11.4	16.0	7.19	6.50	20.4	17.3	10.3		64.0	19.2	------	----	----	----	----	----	----
Weight of heat exchanger, Wt, lb	38.2	22.5	34	19.5	18	27	[f]38	30		97	33	13	25	31	10	24.5	32.5	
[g]q_a/A, (kBtu/hr)/sq ft	15	19	18	22	33	16	22	19	21	6.5	17	------	----	----	----	----	----	----
q_a/Wt, (kBtu/hr)/lb	7.1	9.8	8.5	8.2	12	12	10	6	7	4	10	6	4	8	11	5	5	5
$q_a/\Delta P_a''$, (kBtu/hr)/in. H_2O	47	44	93	21	17	220	70	76	81	1220	93	25	25	106	60	69	45	85

[a]AAL designation refers to numbers assigned these heat exchangers in reference 11.

[b]Isothermal frictional pressure drop across the exhaust-gas side of the heat exchanger and ducts (τ_g = 1500° F).

[c]Exhaust gas flowed out through outlet A and outlet B. (See fig. 32.)

[d]Isothermal frictional pressure drop across the ventilating-air side of the heat exchanger and ducts (τ_a = 100° F).

[e]Ventilating air flowed out through the cabin duct. (See fig. 9.)

[f]Weight of heater includes weight of a short section of pipe added to the gas side.

[g]A is the air-side heat-transfer area.

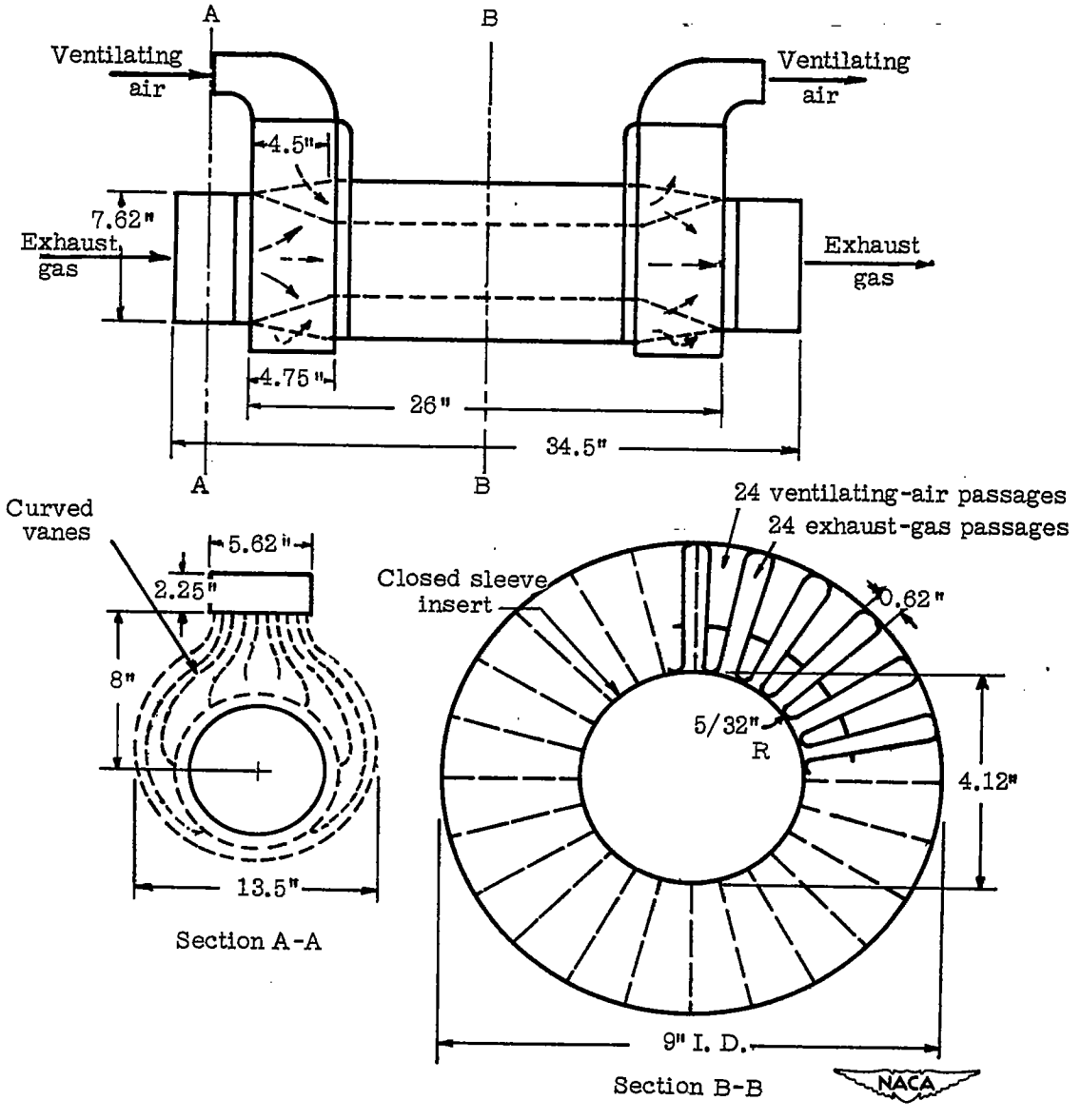

Figure 1.- Schematic diagram of heat exchanger A and air shroud. Weight of heat exchanger, 38.25 pounds; weight of air shroud, 10.5 pounds.

Section B-B	Air side	Gas side
Cross-sectional area, sq ft	0.172	0.270
Heat-transfer area, sq ft	17.9	17.9

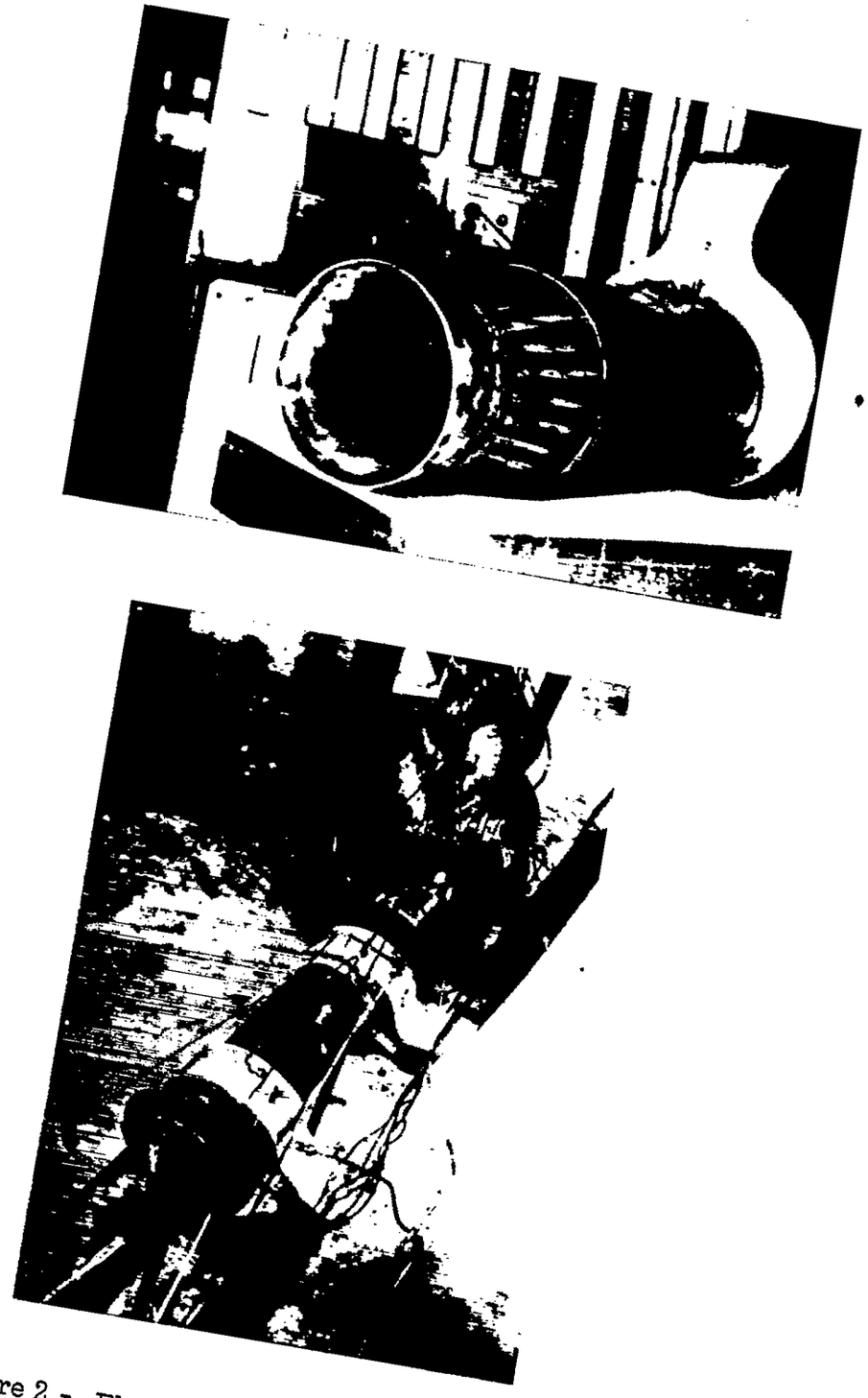

Figure 2.- Fluted heat exchanger A and test setup.

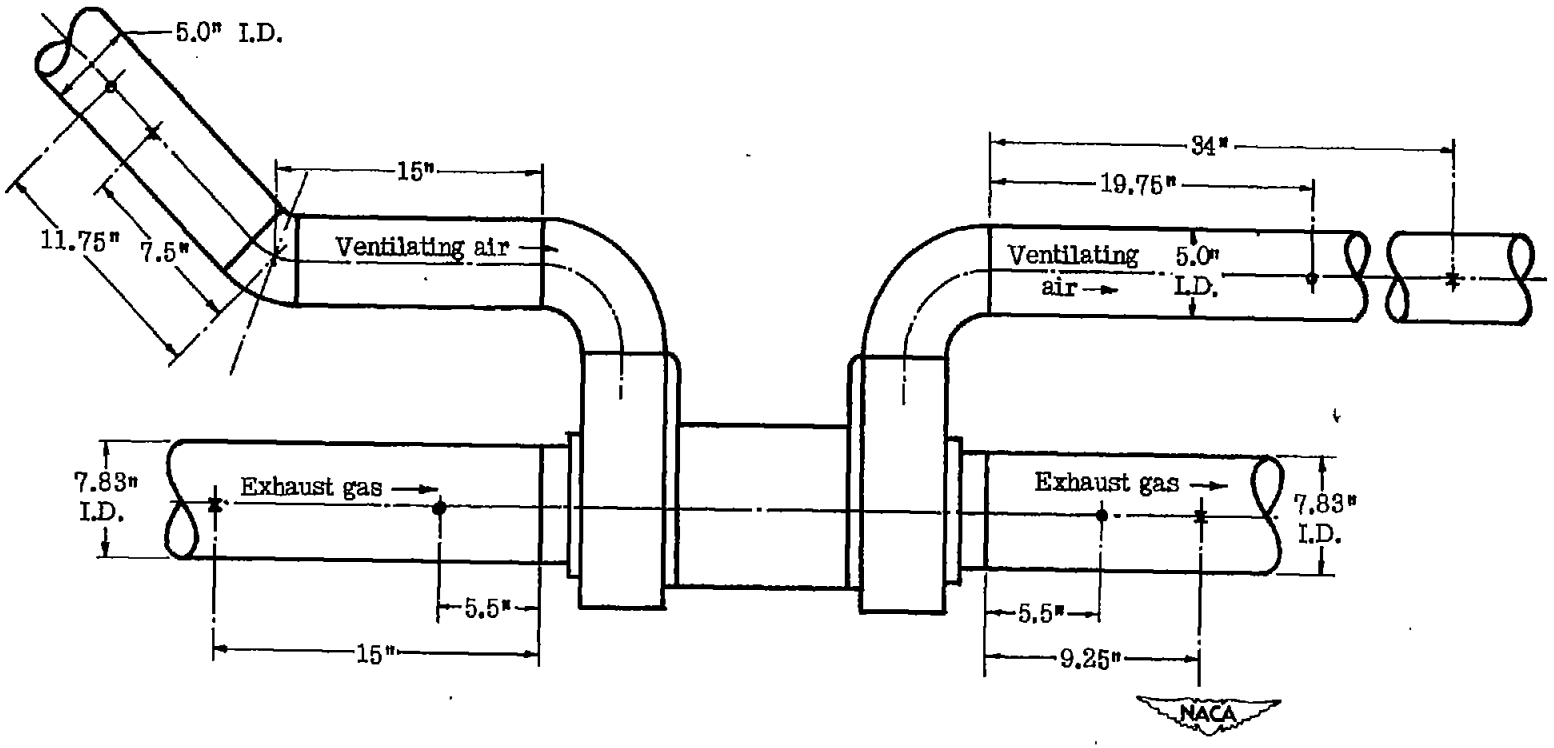

•o Static-pressure tap

x Temperature traverse

Figure 3.- Schematic diagram of test setup of heat exchanger A and air shroud, showing location of static-pressure and temperature measuring stations.

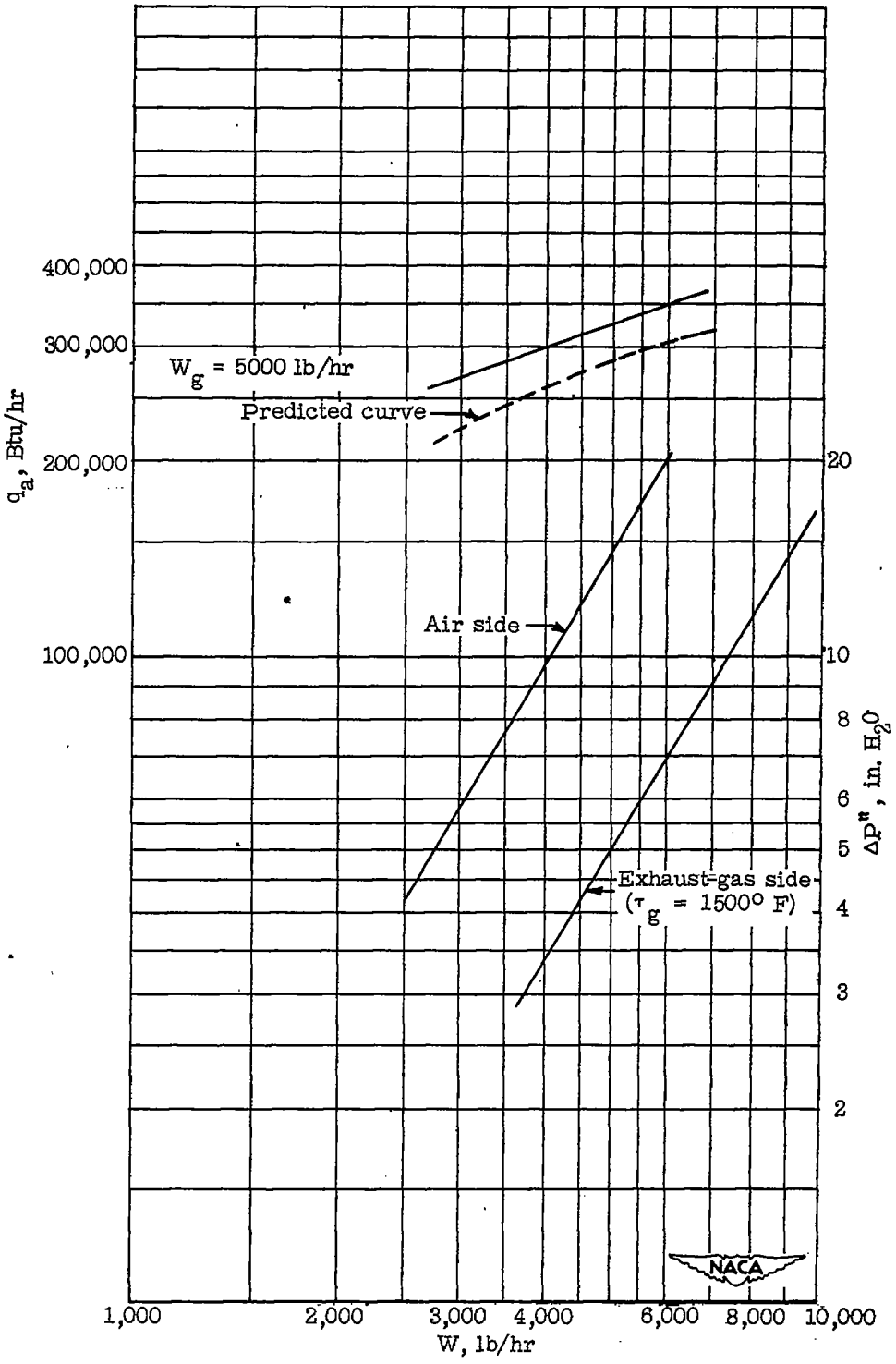

Figure 4.- Thermal output and isothermal frictional pressure drops of fluted heat exchanger A.

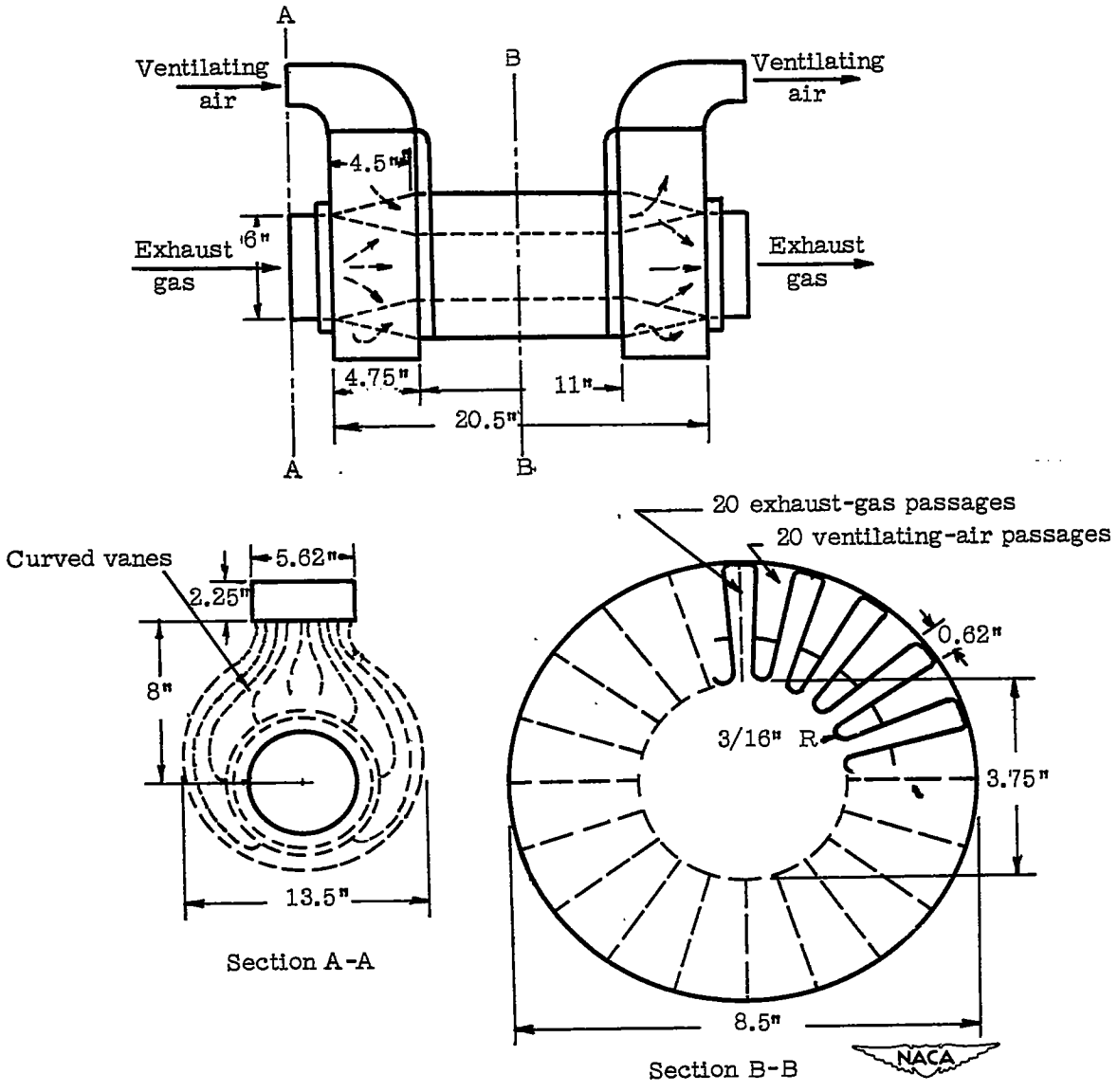

Figure 5.- Schematic diagram of heat exchanger B and air shroud. Weight of heat exchanger, 22.5 pounds; weight of air shroud, 10.5 pounds.

Section B-B	Air side	Gas side
Cross-sectional area, sq ft	0.180	0.214
Heat-transfer area, sq ft	11.4	11.4

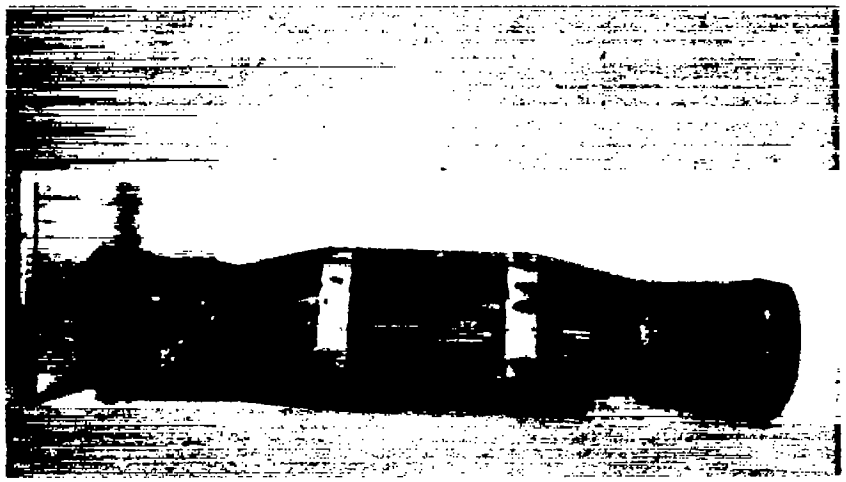

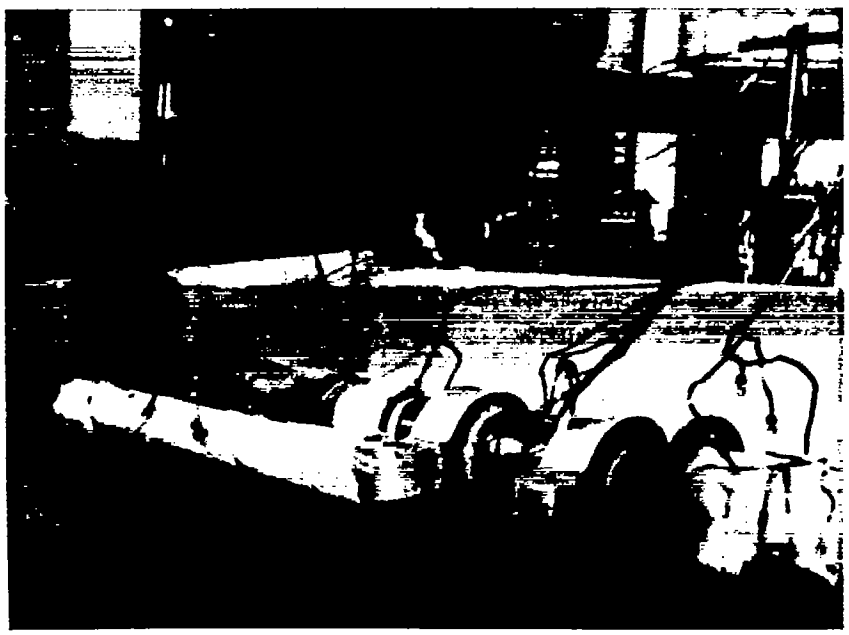

Figure 6.- Fluted heat exchanger B and test setup.

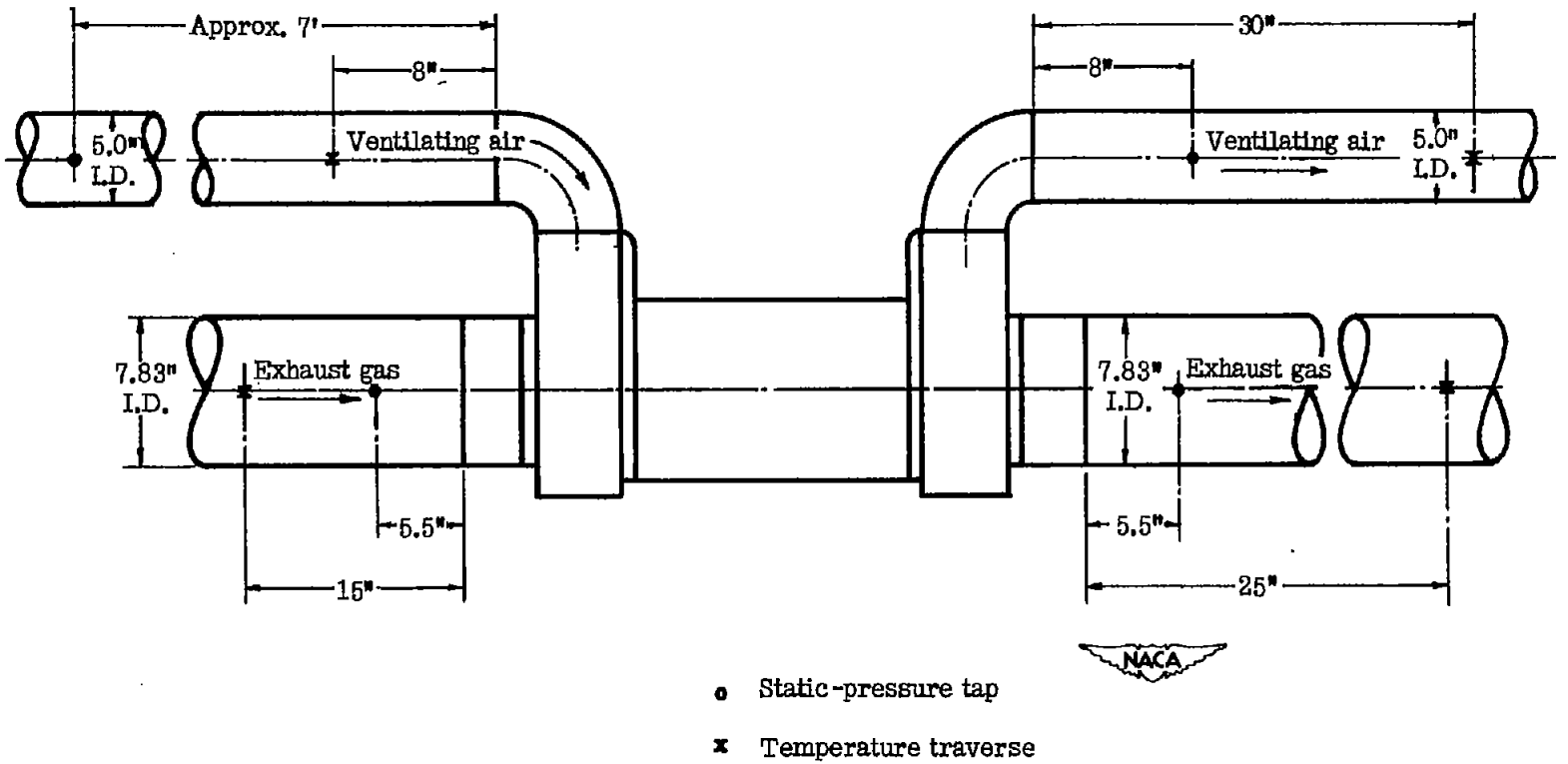

Figure 7.- Schematic diagram of test setup of heat exchanger B and air shroud, showing location of static-pressure and temperature measuring stations.

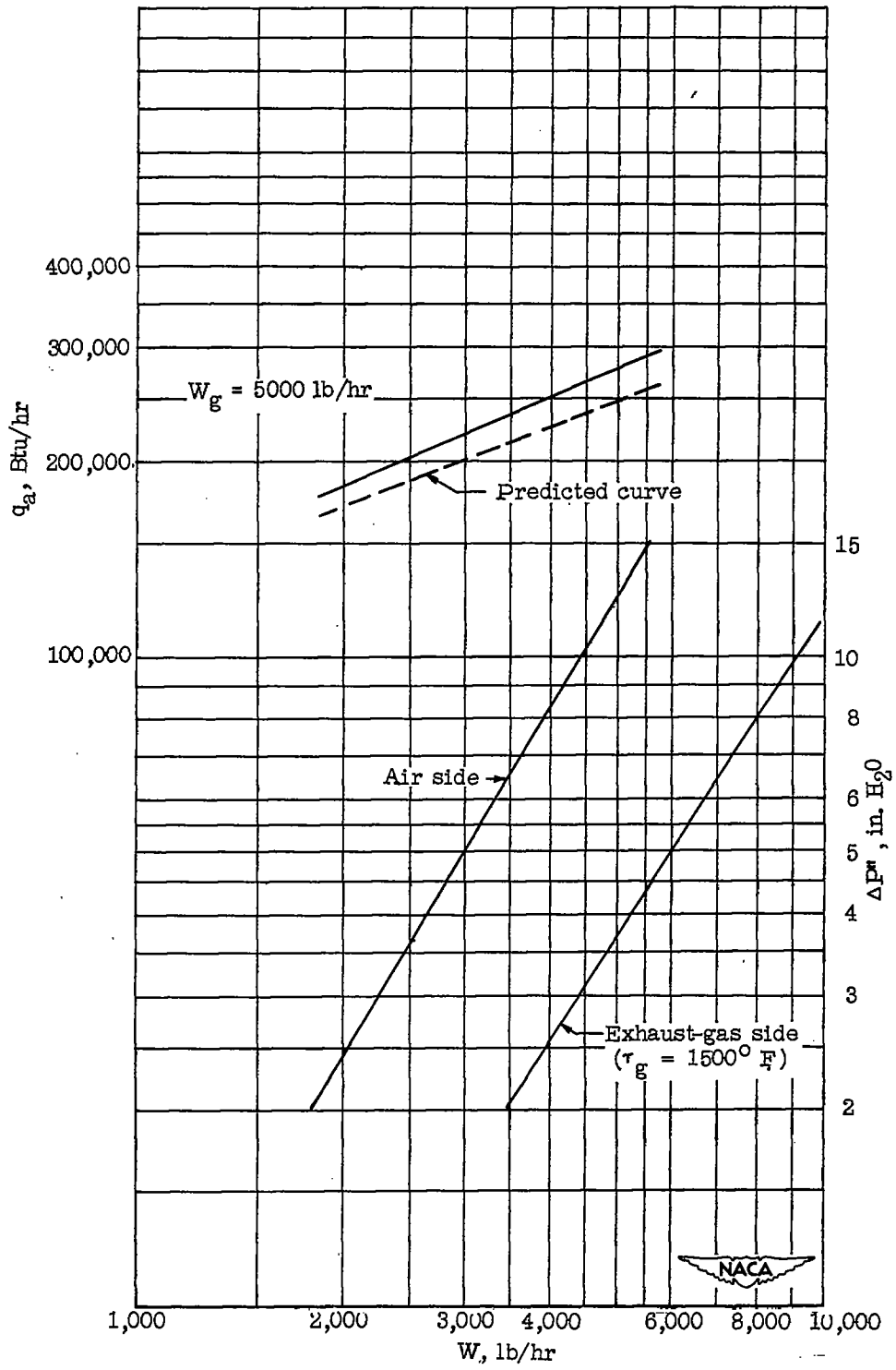

Figure 8.- Thermal output and isothermal frictional pressure drops of fluted heat exchanger B.

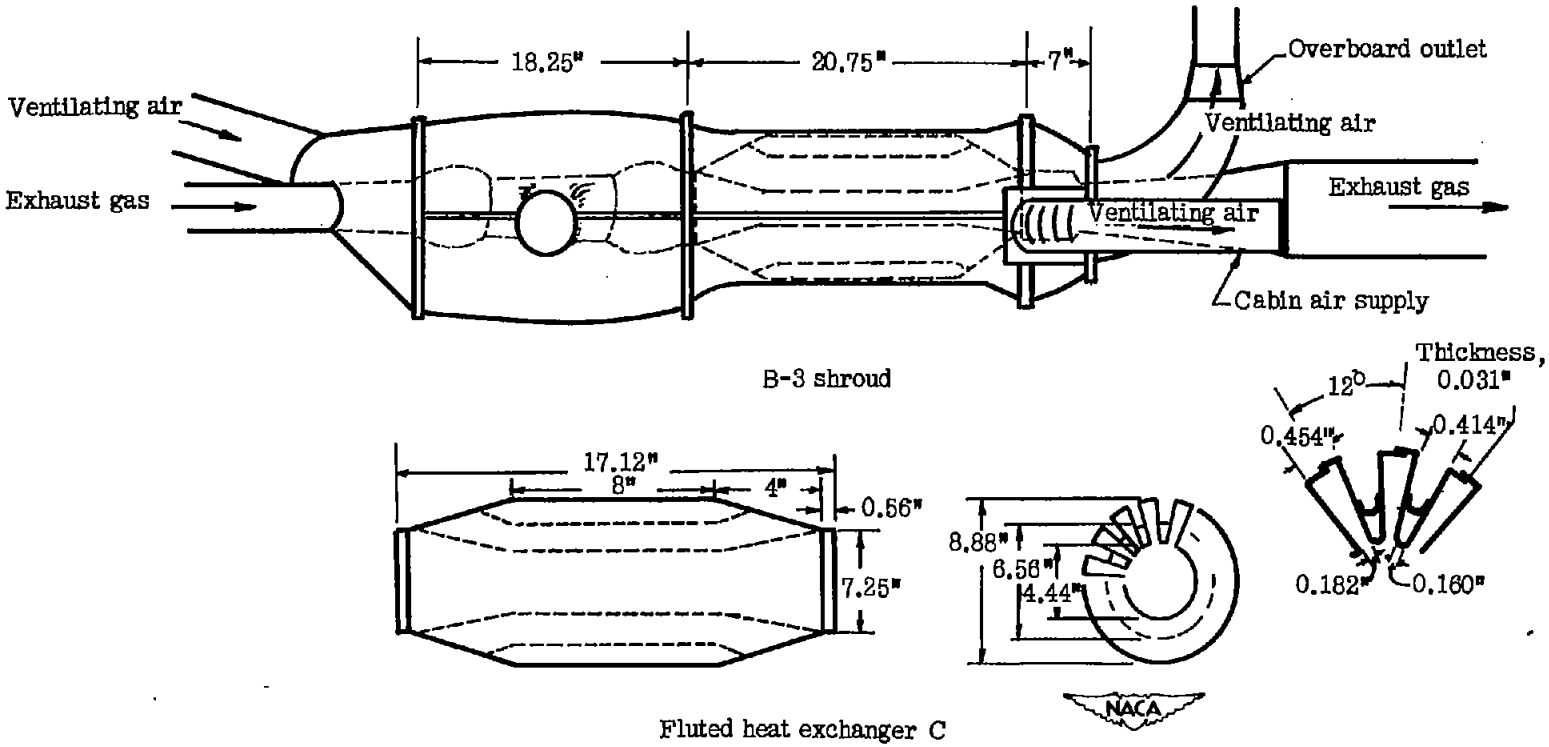

Figure 9.- Schematic diagram of heat exchanger C and air shroud. Weight of heat exchanger, 34 pounds.

	Approach section (Weighted mean values)		Heat-exchanger section (Weighted mean values)		Exit section (Weighted mean values)	
	Air side	Gas side	Air side	Gas side	Air side	Gas side
Cross-sectional area, sq ft	0.254	0.127	0.202	0.265	0.400	0.230
Heat-transfer area, sq ft	3.87	3.87	16.0	13.5	3.12	3.12

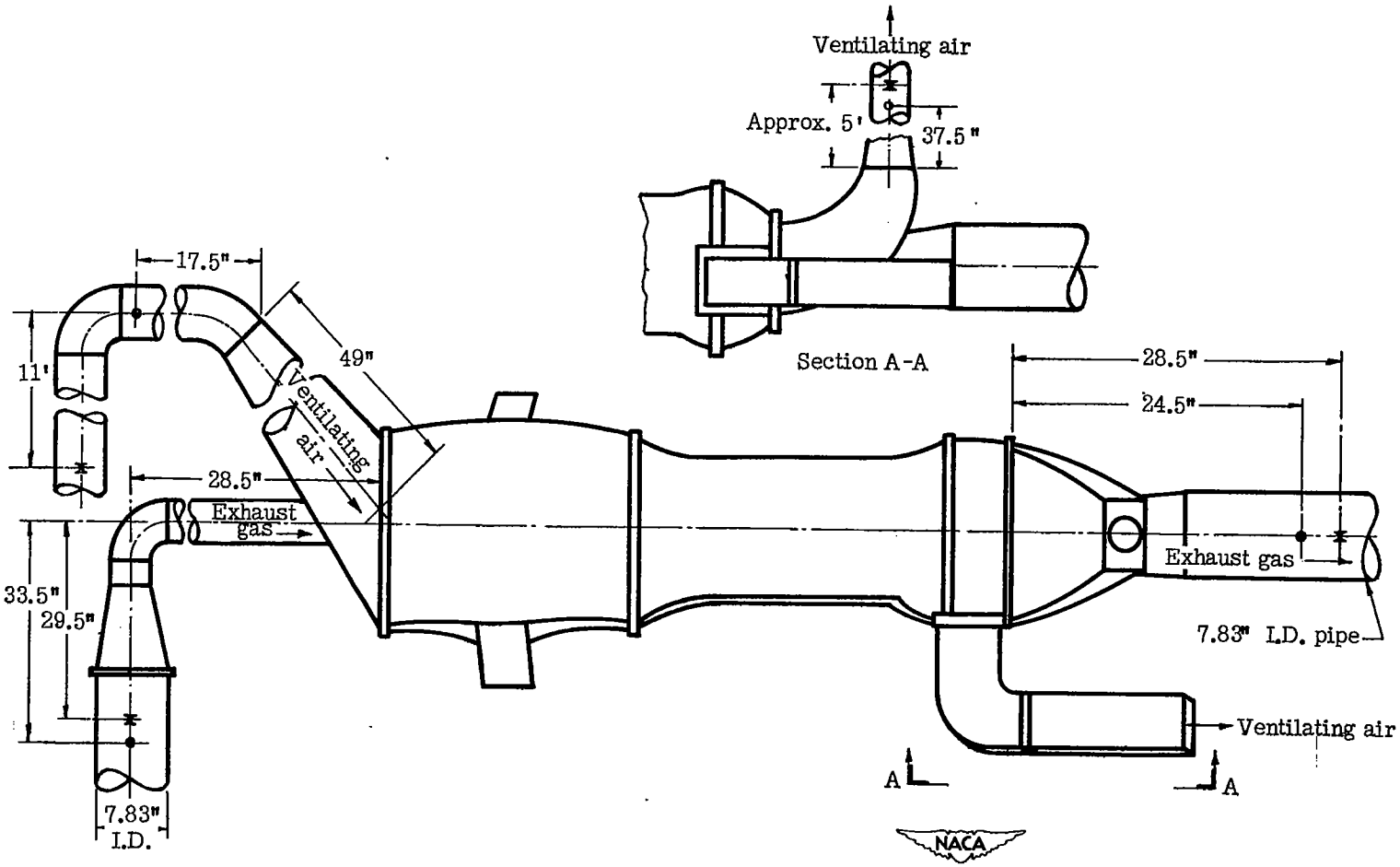

o Static-pressure tap

x Temperature traverse

Figure 10.- Schematic diagram of test setup of heat exchanger C, showing location of static-pressure and temperature measuring stations.

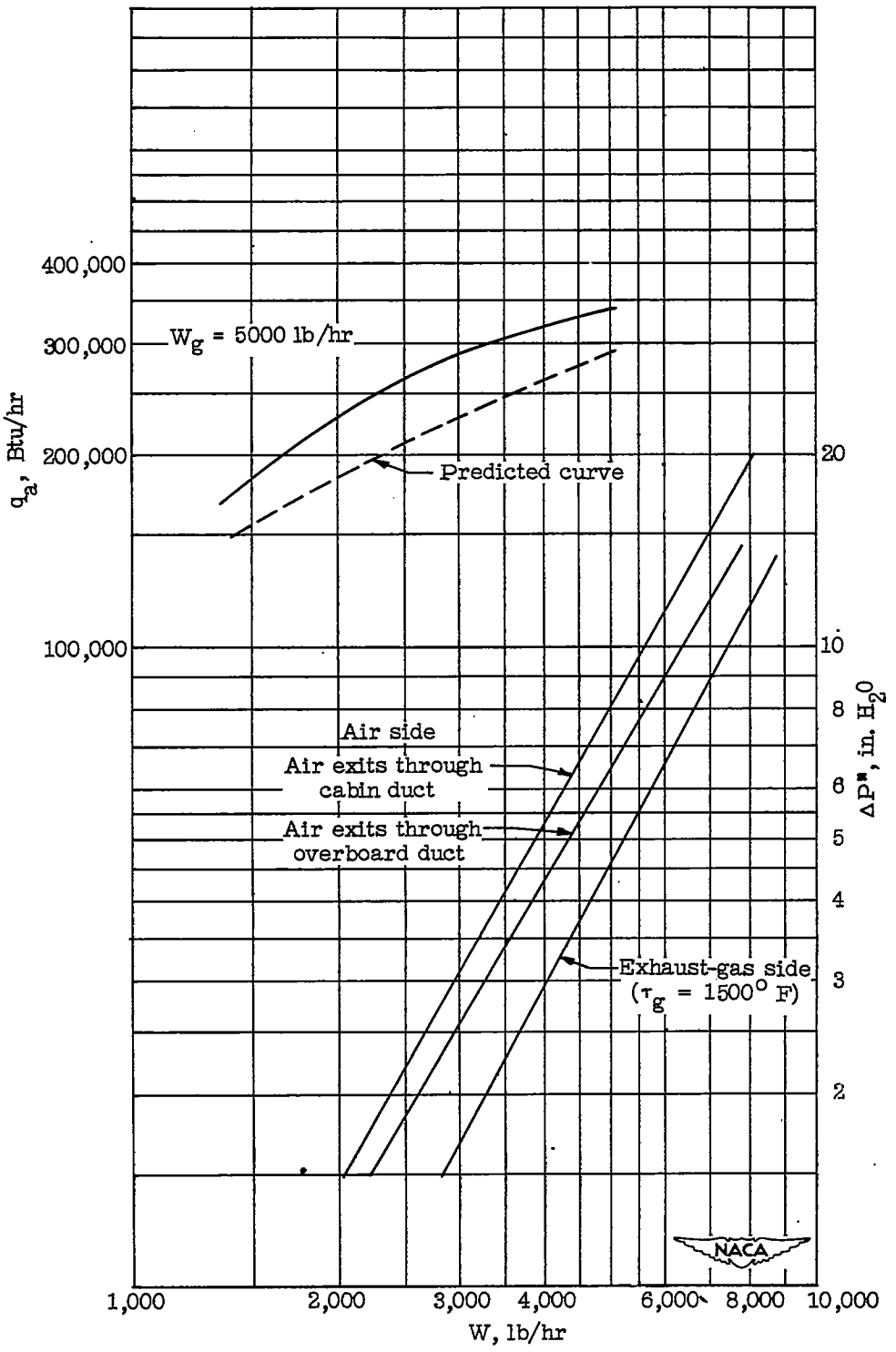

Figure 11.- Thermal output and isothermal frictional pressure drops of fluted heat exchanger C.

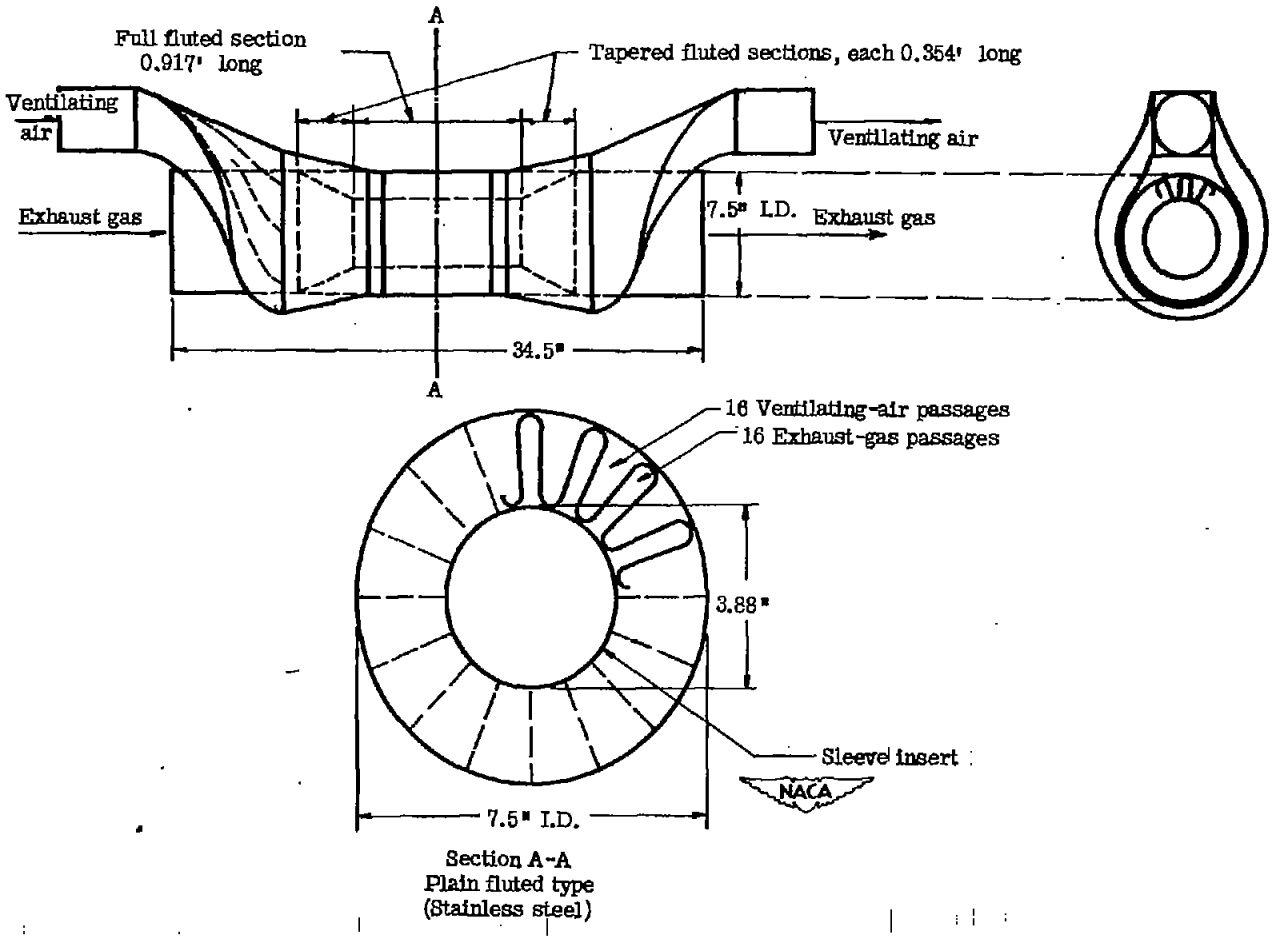

Figure 12.- Schematic diagram of heat exchanger D and air shroud. Weight of heat exchanger, 19.5 pounds; weight of air shroud, 8.5 pounds.

Section A-A	Air side	Gas side
Cross-sectional area, sq ft	0.112	0.194
Heat-transfer area, sq ft	7.19	7.19

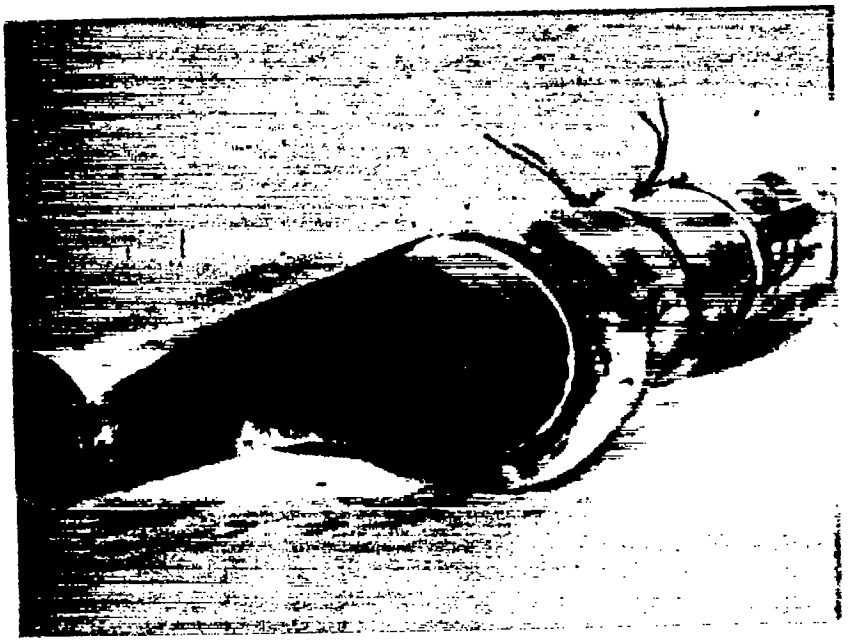

Figure 13.- Fluted heat exchanger D using A-4 shroud.

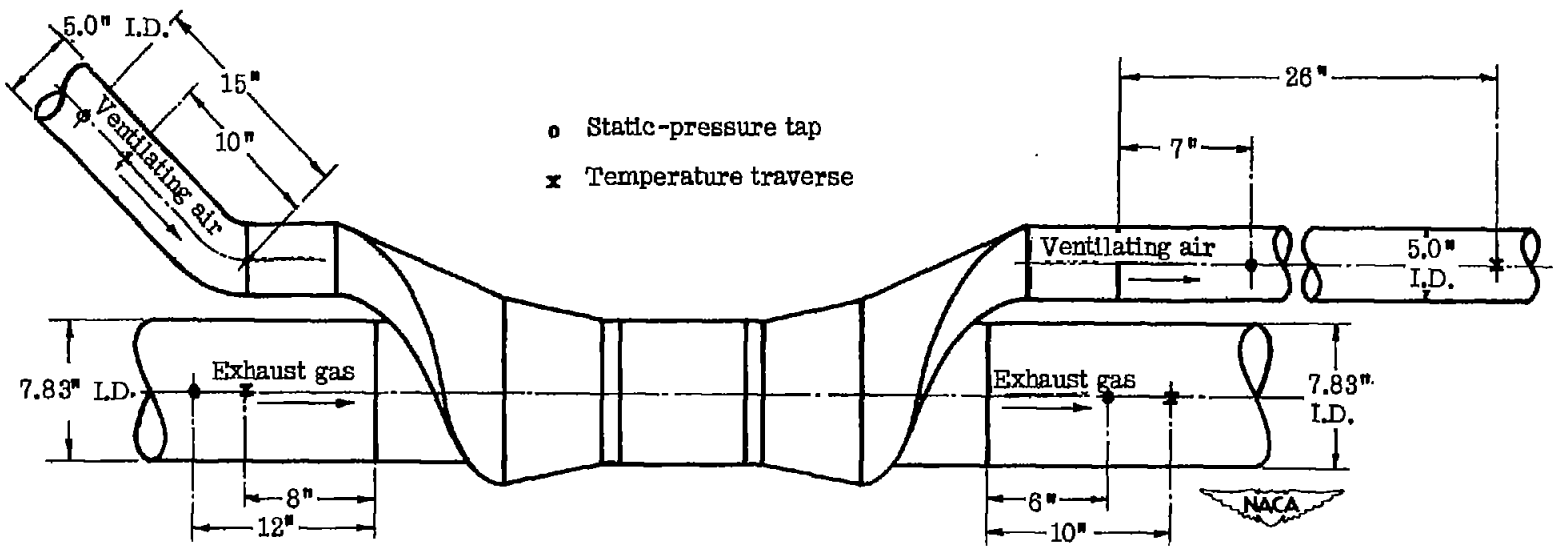

Figure 14.- Schematic diagram of test setup of heat exchanger D and air shroud, showing location of static-pressure and temperature measuring stations.

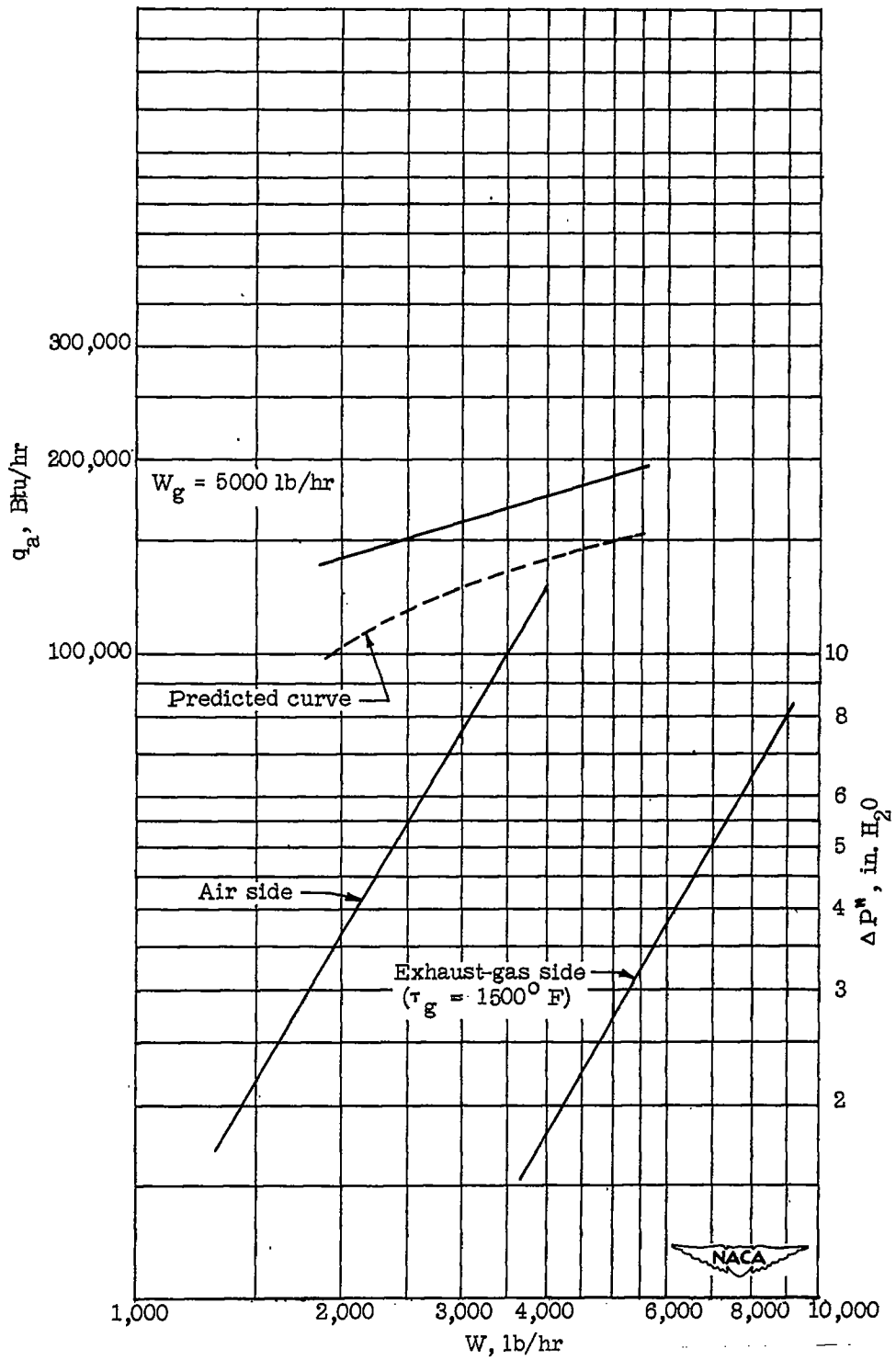

Figure 15.- Thermal output and isothermal frictional pressure drops of fluted heat exchanger D.

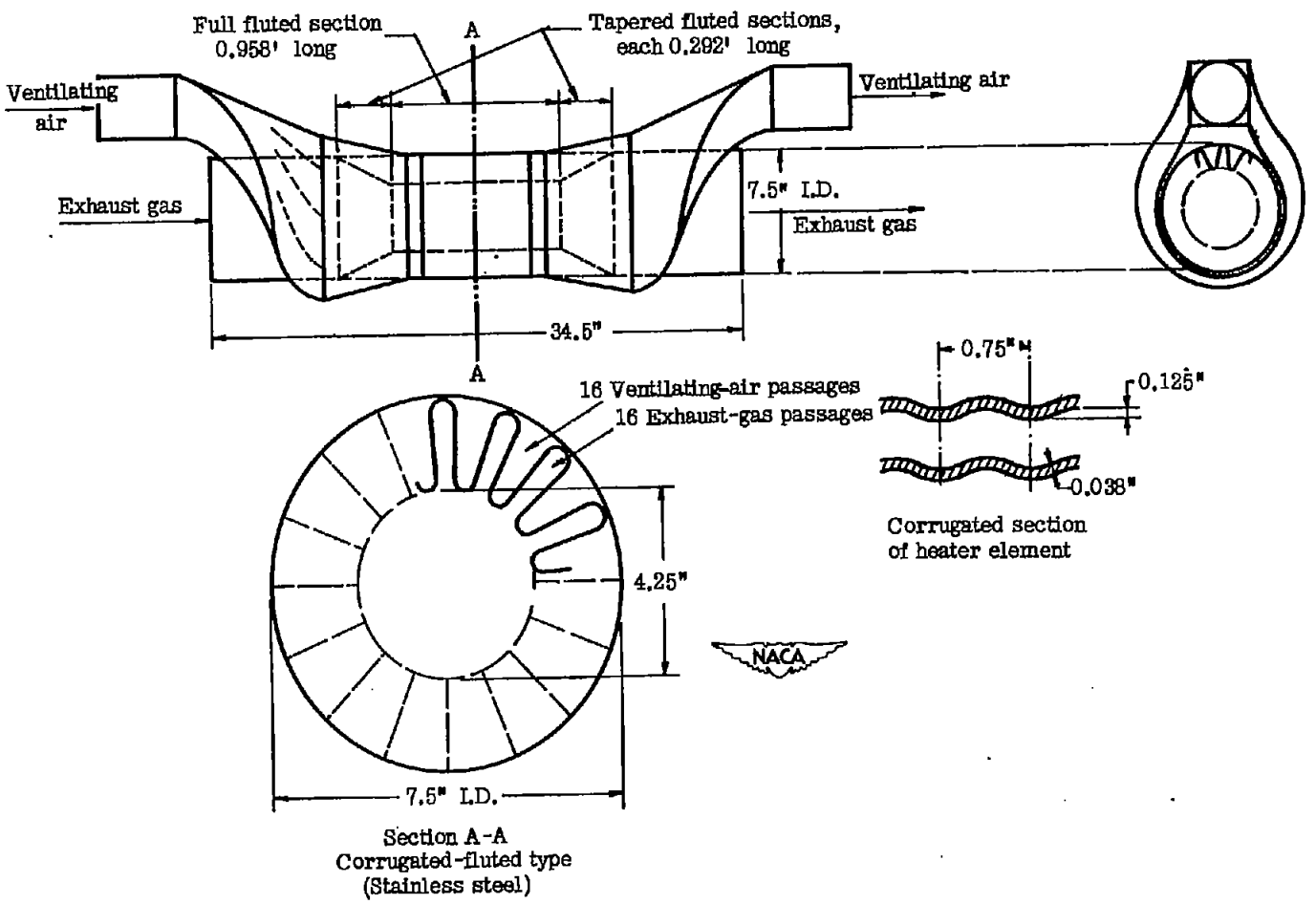

Figure 16.- Schematic diagram of heat exchanger E and air shroud. Weight of heat exchanger, 18.0 pounds; weight of air shroud, 8.5 pounds.

Section A-A	Air side	Gas side
Cross-sectional area, sq ft	0.104	0.187
Heat-transfer area, sq ft	6.50	6.50

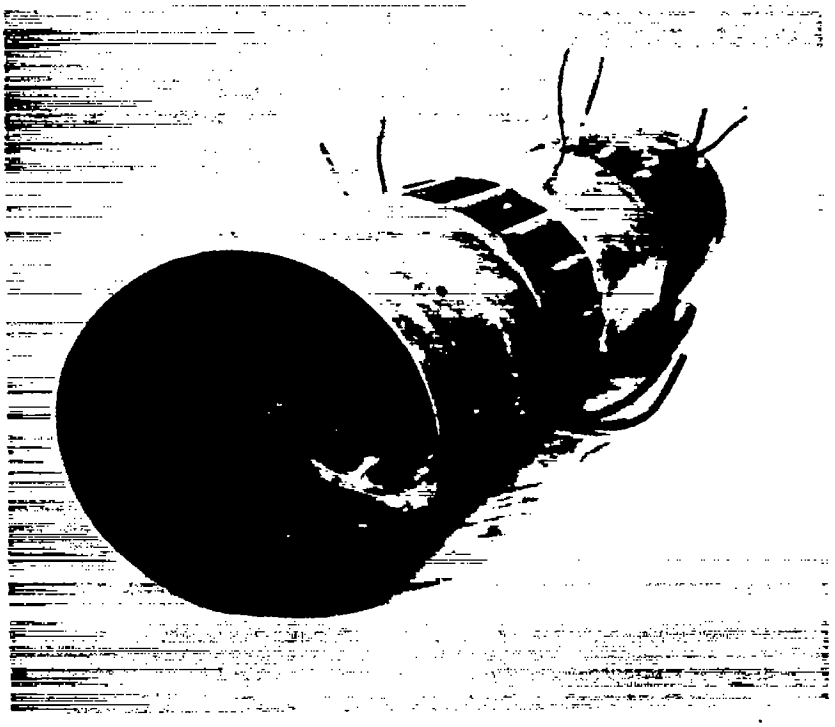

Figure 17.- Corrugated-fluted heat exchanger E.

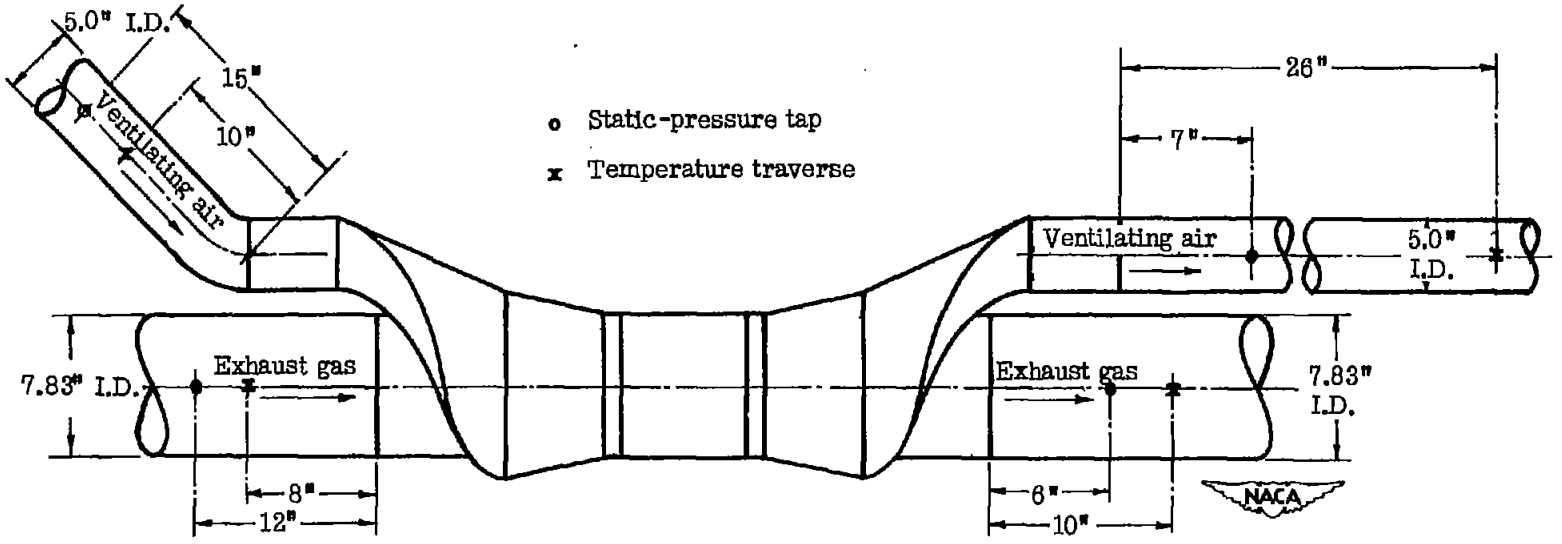

Figure 18.- Schematic diagram of test setup of heat exchanger E and air shroud, showing location of static-pressure and temperature measuring stations.

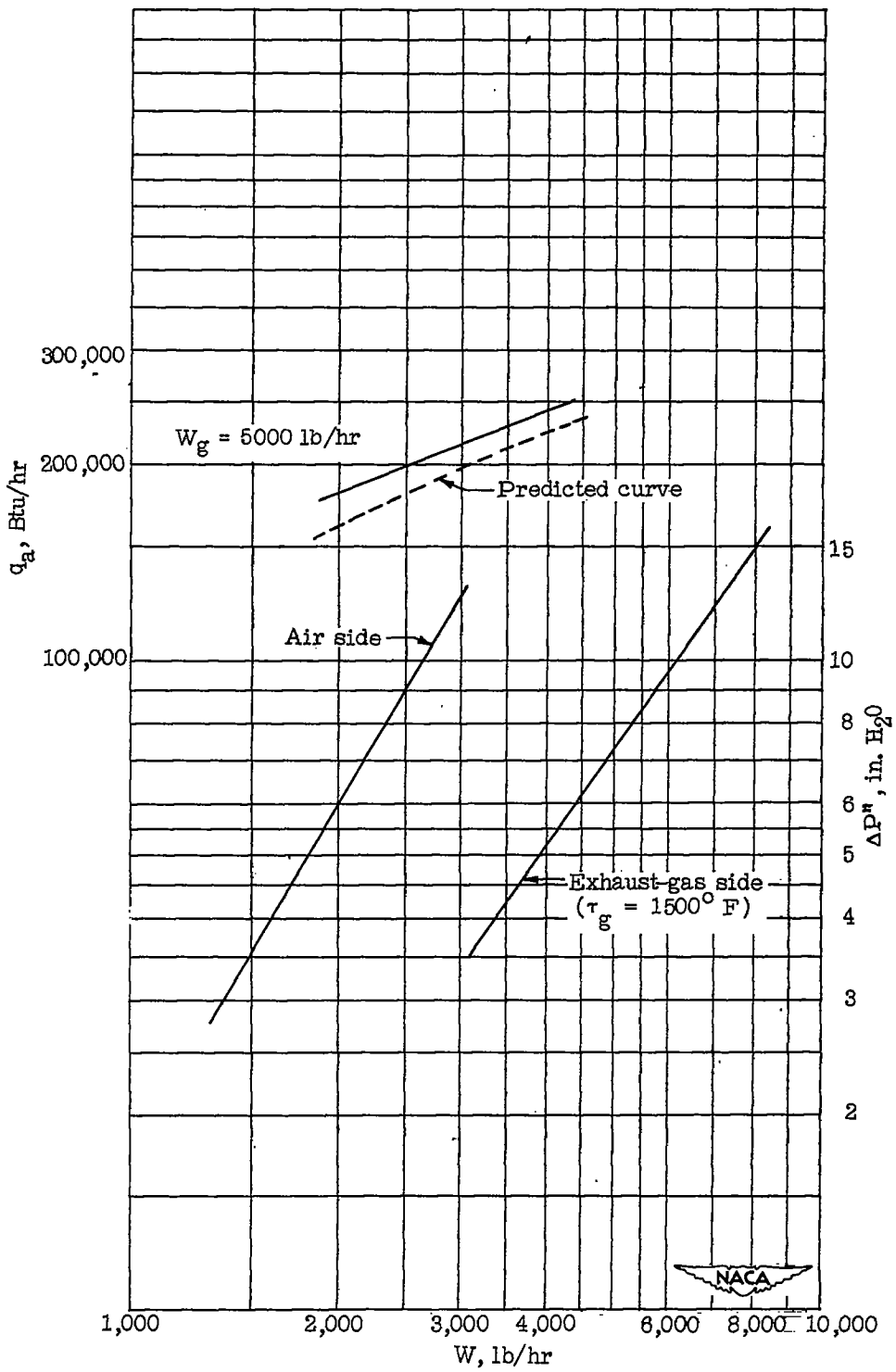

Figure 19.- Thermal output and isothermal frictional pressure drops of corrugated-fluted heat exchanger E.

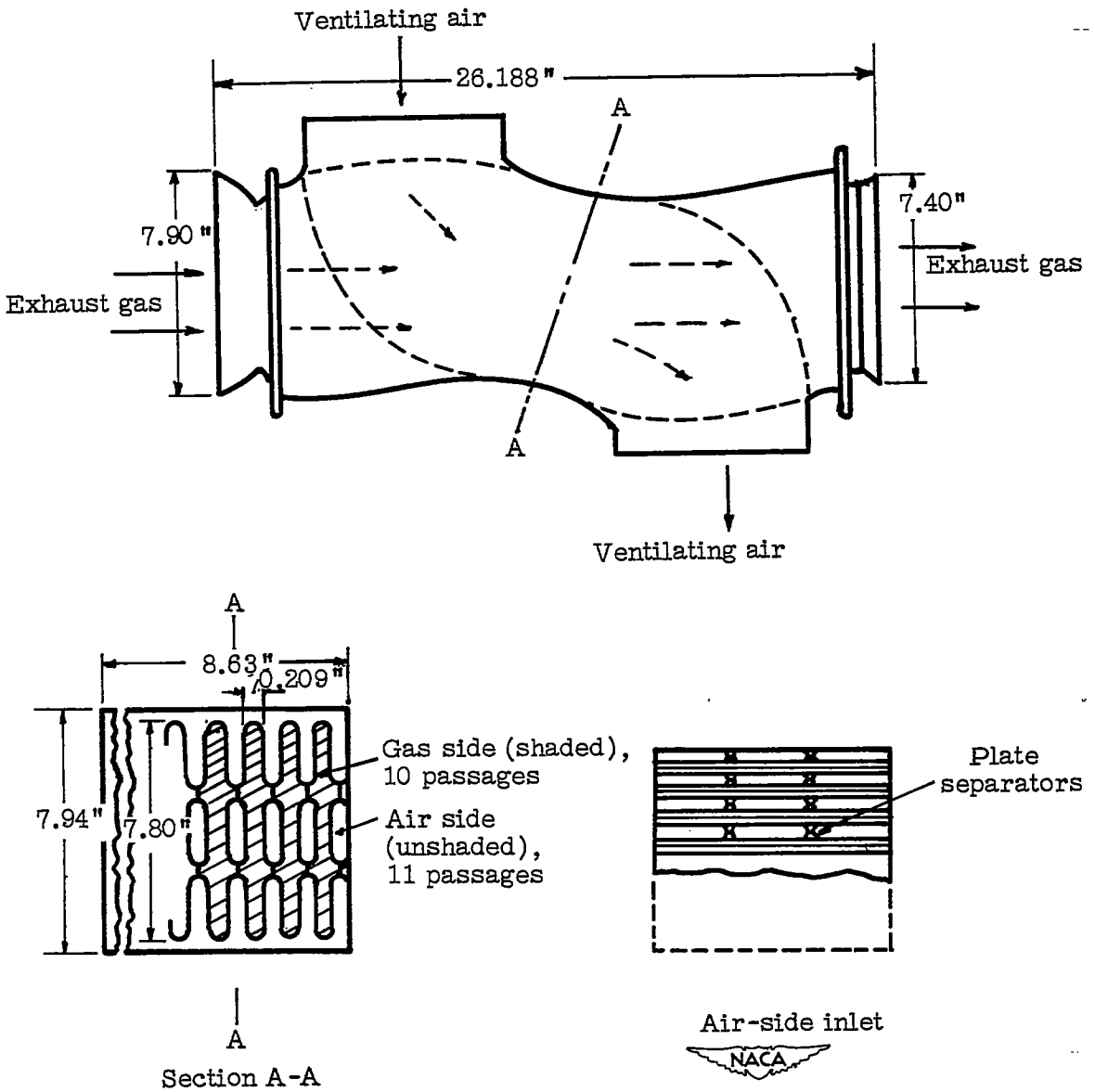

Figure 20.- Schematic diagram of heat exchanger F. Weight of heat exchanger, 27 pounds.

Section A-A	Air side	Gas side
Cross-sectional area, sq ft	0.222	0.199
Heat-transfer area, sq ft	20.4	20.4

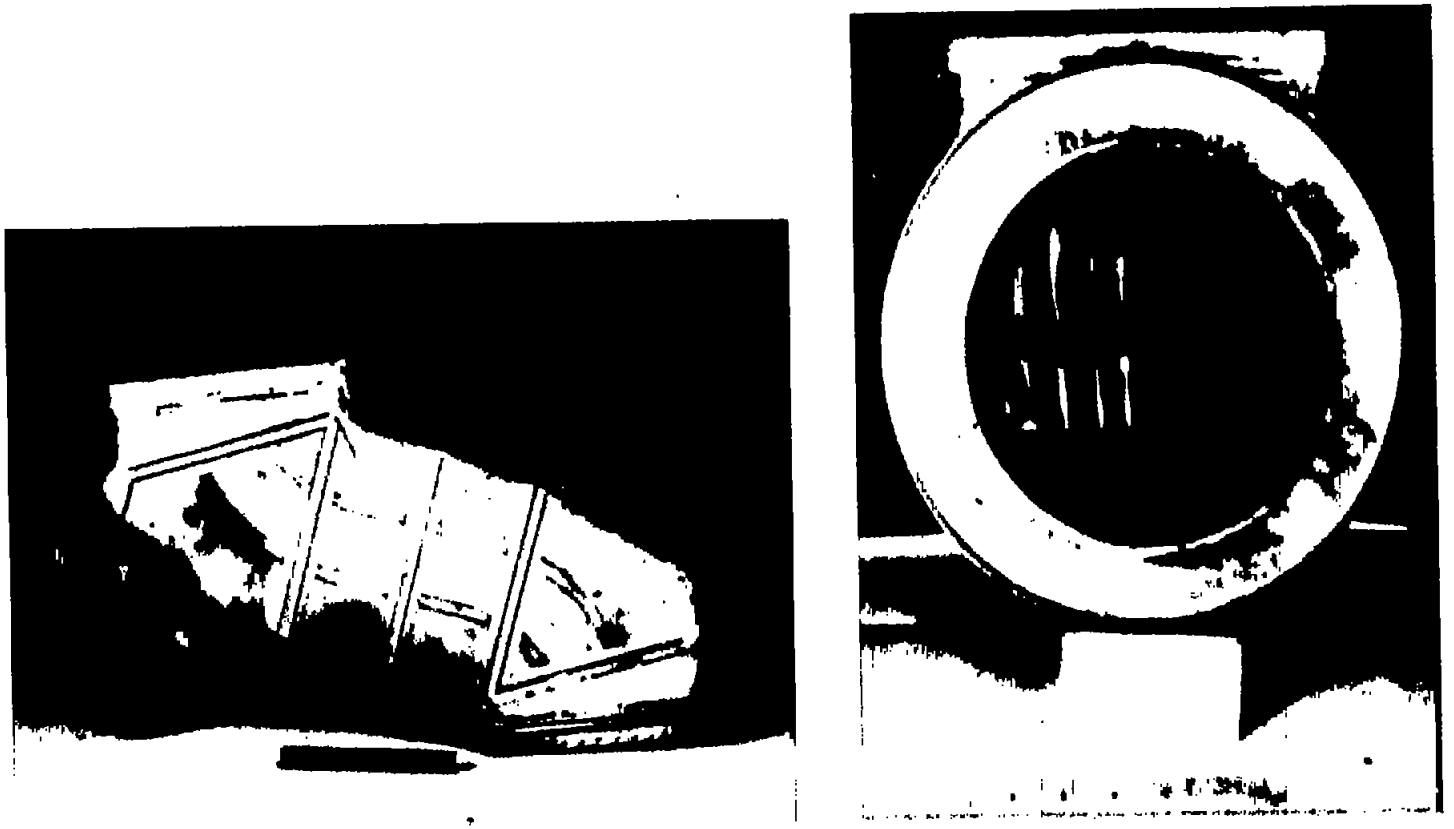

Figure 21.- Flat-plate heat exchanger F. (Photograph at right is that of exhaust-gas inlet.)

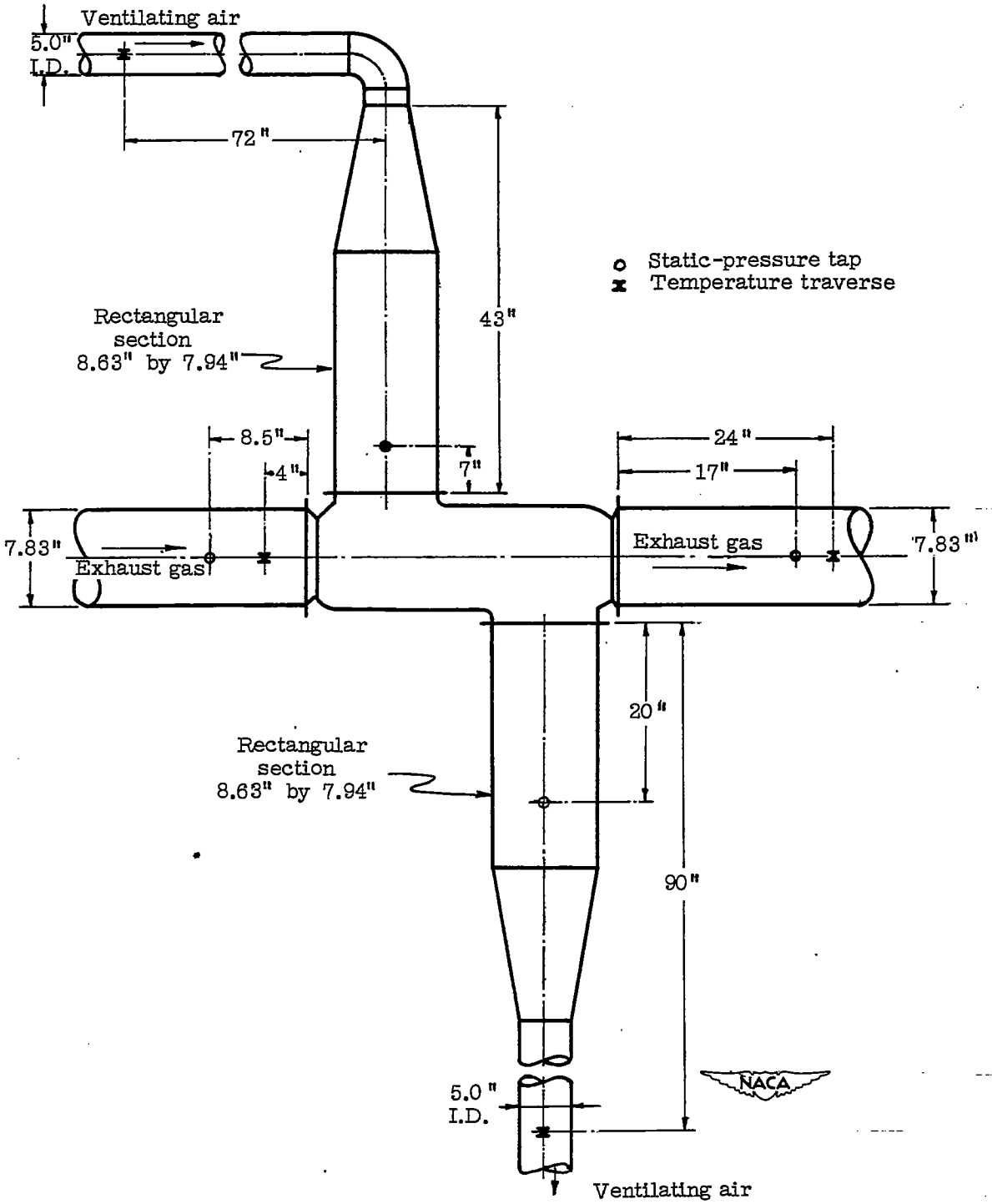

Figure 22.- Schematic diagram of test setup of heat exchanger F, showing location of static-pressure and temperature measuring stations.

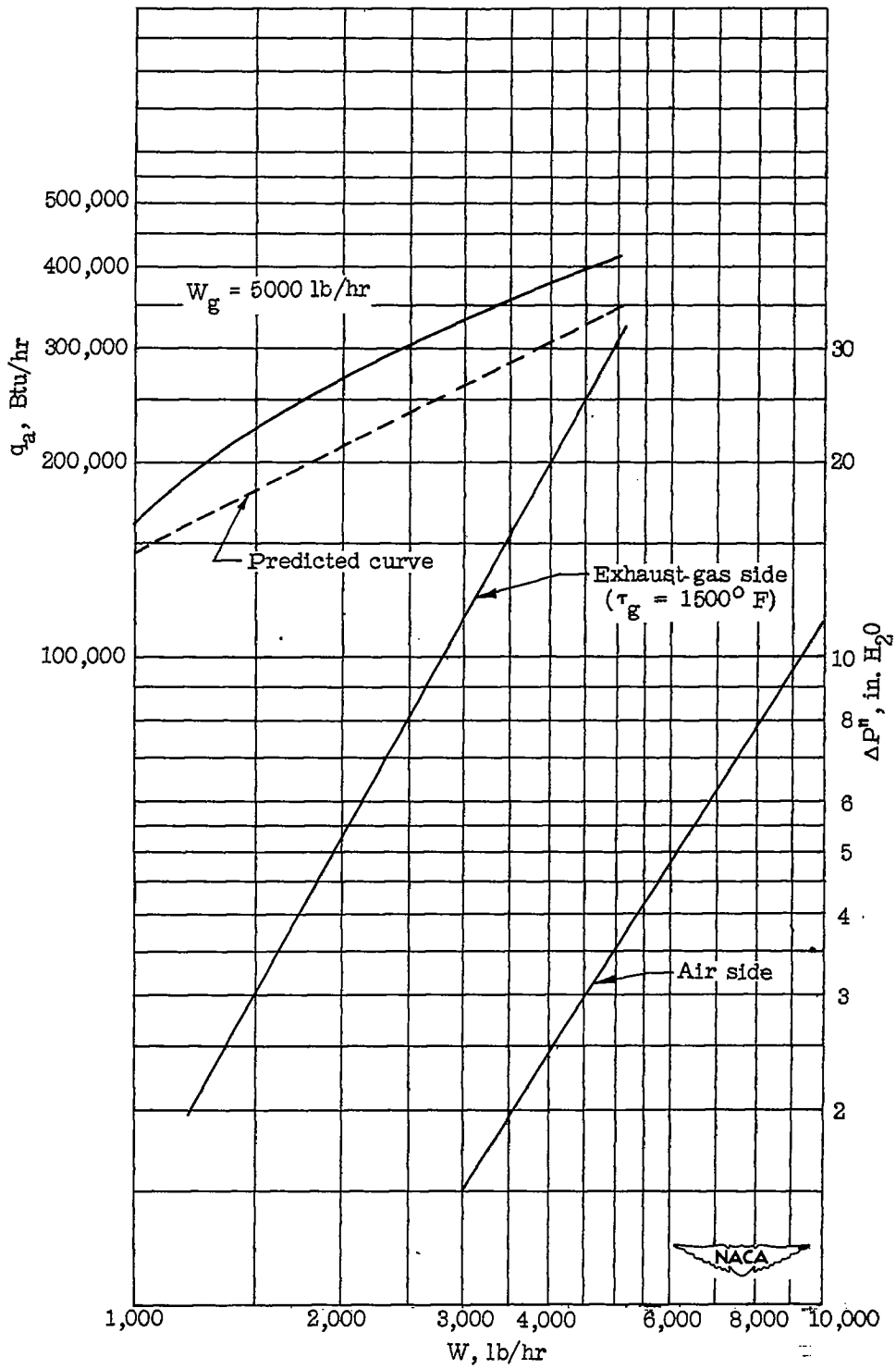

Figure 23.- Thermal-output and isothermal frictional pressure drops of flat-plate heat exchanger F.

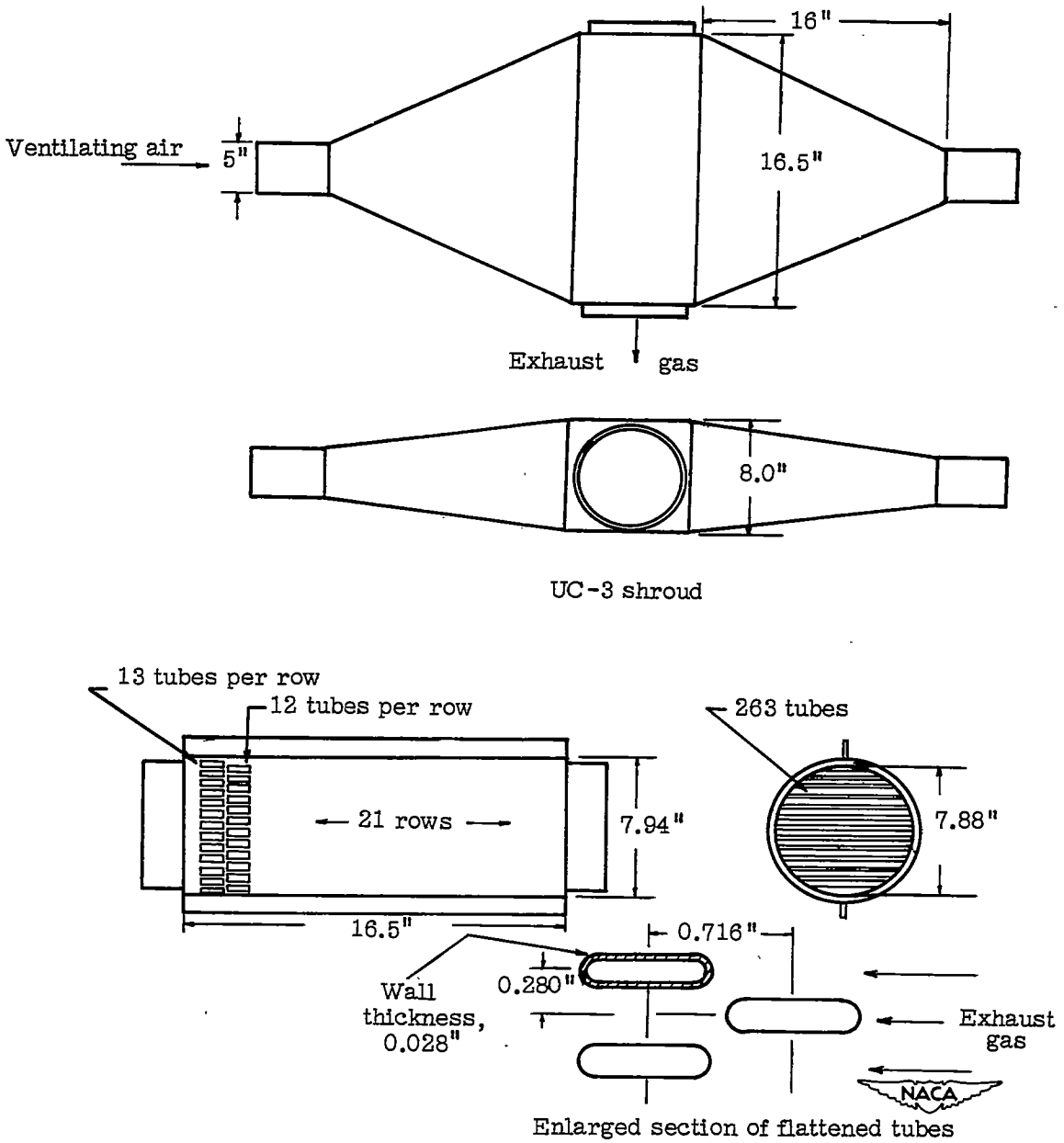

Figure 24.- Schematic diagram of flattened-tube heat exchanger G and UC-3 shroud. Weight of heat exchanger, 38 pounds.

	Air side	Gas side	
		Flat-plate portion	Cylindrical portion
Cross-sectional area (total), sq ft	0.145	0.229	0.195
Heat-transfer area (total), sq ft	17.3	12.2	7.20

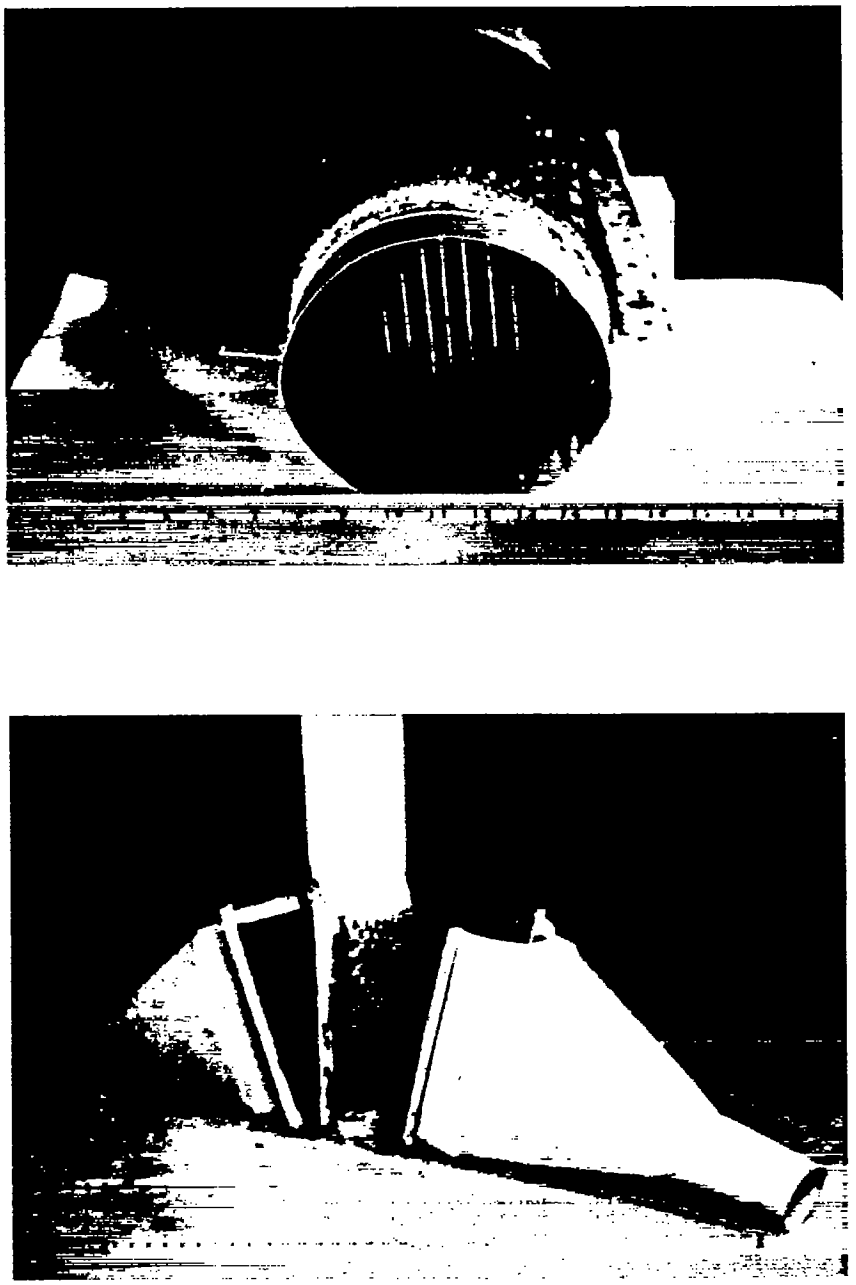

Figure 25.- Flattened-tube-bundle heat exchanger G and UC-3 shroud.

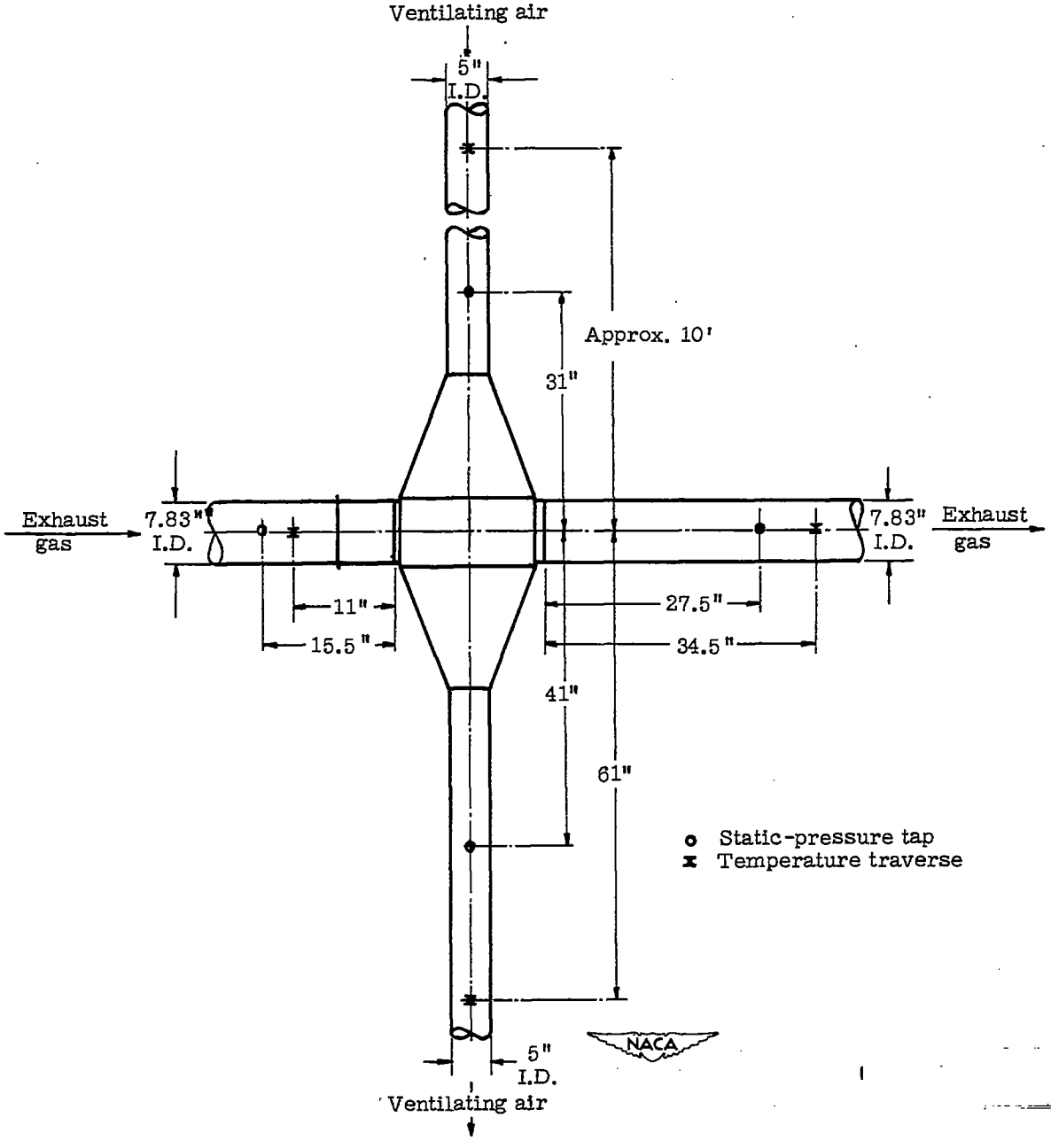

Figure 26.- Schematic diagram of test setup of heat exchanger G and air shroud, showing location of static-pressure and temperature measuring stations.

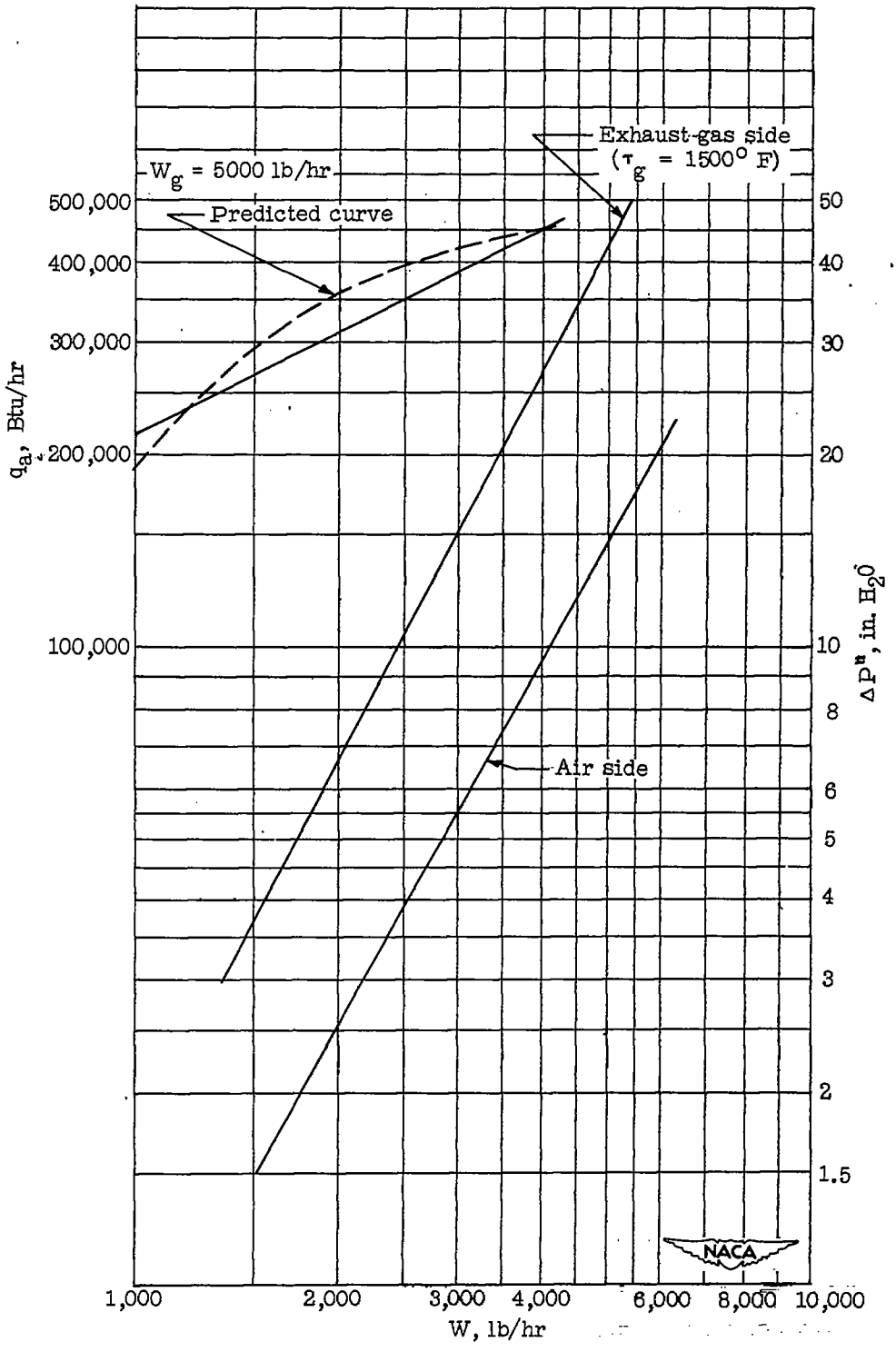

Figure 27.- Thermal output and isothermal frictional pressure drops of flattened-tube-bundle heat exchanger G.

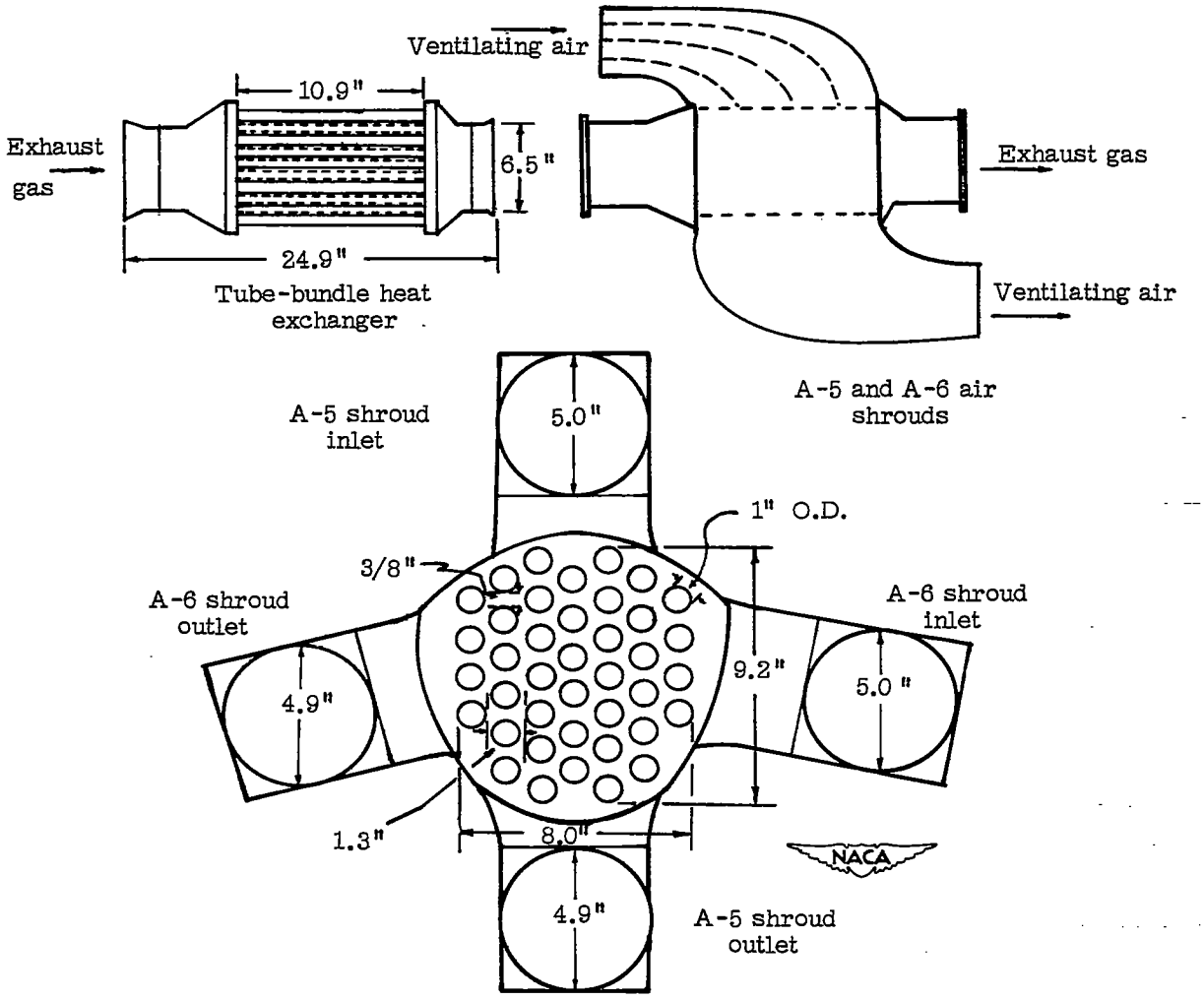

Figure 28.- Schematic diagram of tube-bundle heat exchanger H and A-5 and A-6 air shrouds. Weight of heat exchanger, 30.0 pounds.

	Air side		Gas side
	A-5	A-6	
Minimum free cross-sectional area, sq ft	0.321	0.272	0.192
Heat-transfer area, sq ft	10.3	10.3	9.76

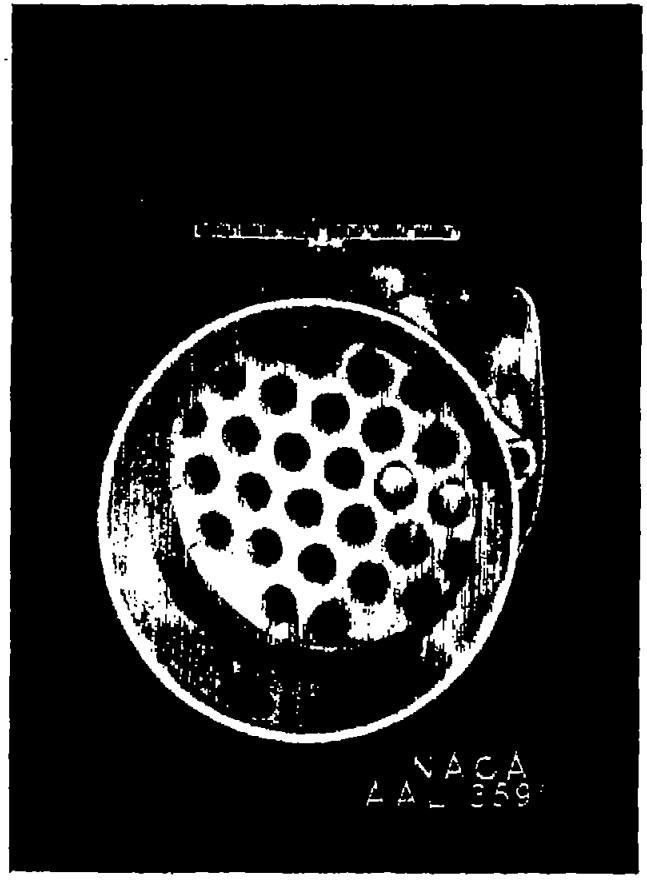

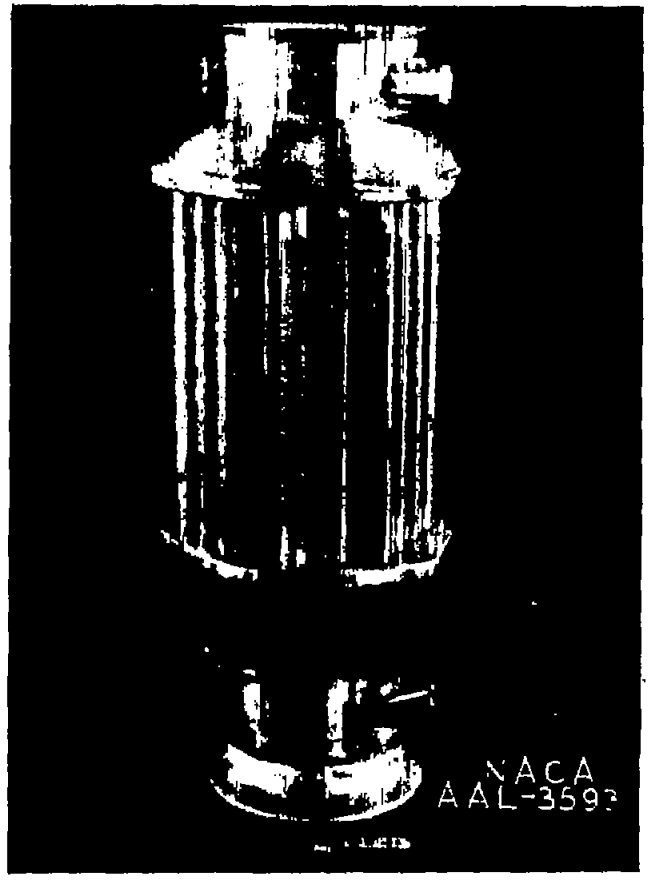

Figure 29.- Circular-tube-bundle heat exchanger H.

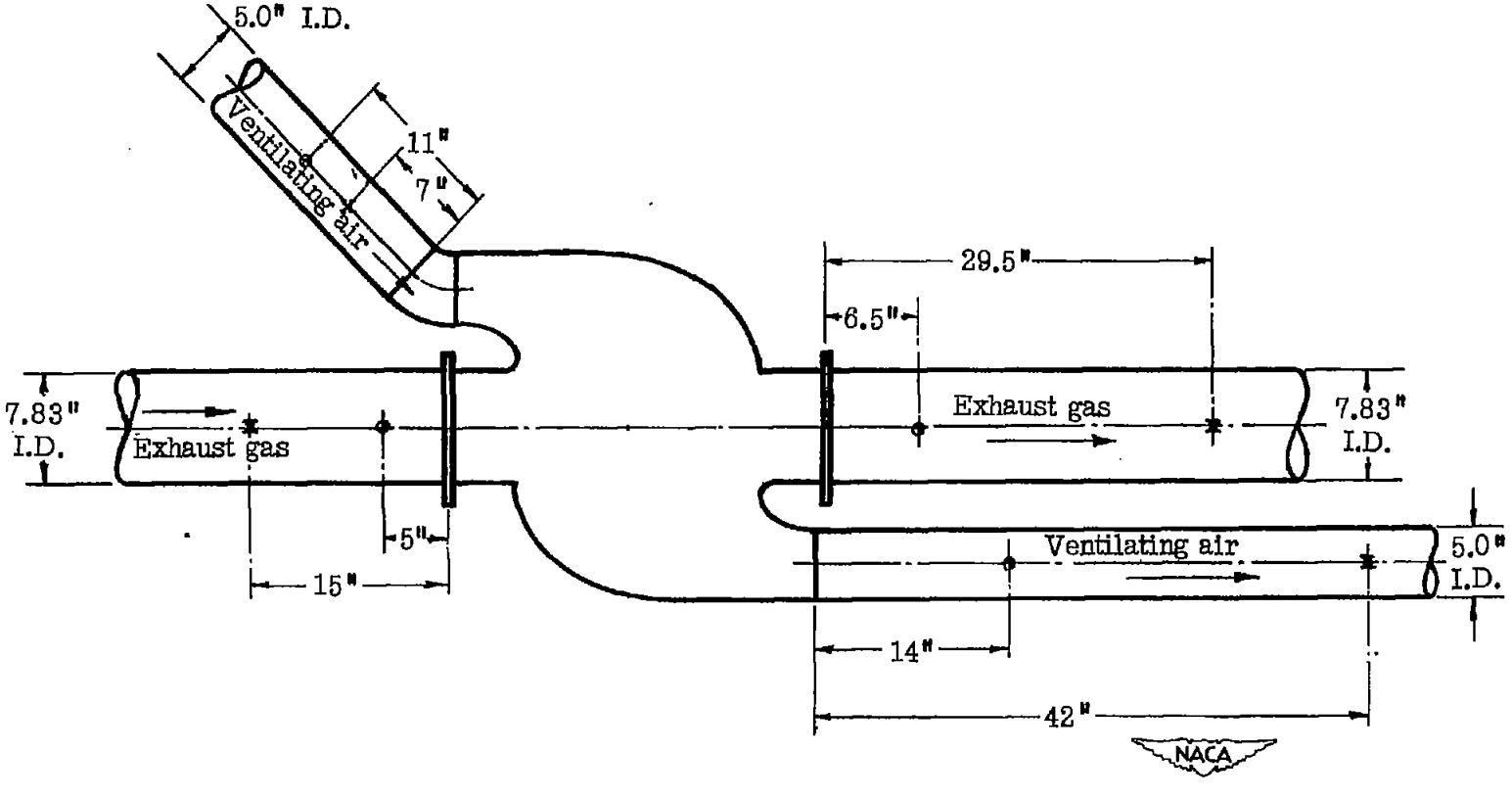

o Static-pressure tap

x Temperature traverse

Figure 30.- Schematic diagram of test setup of heat exchanger H and air shroud, showing location of static-pressure and temperature measuring stations.

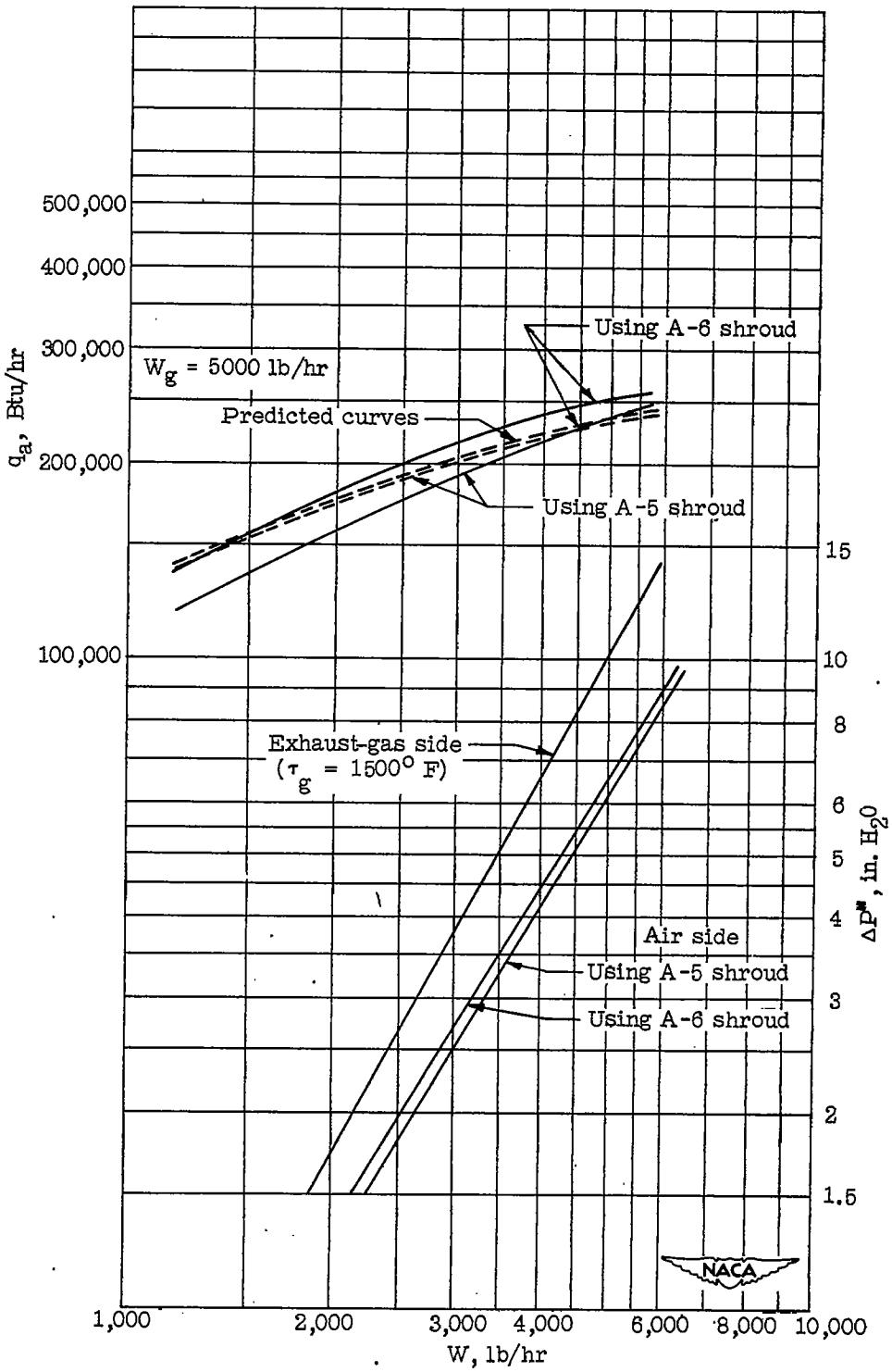

Figure 31.- Thermal output and isothermal frictional pressure drops of circular-tube-bundle heat exchanger H using A-5 and A-6 air shrouds.

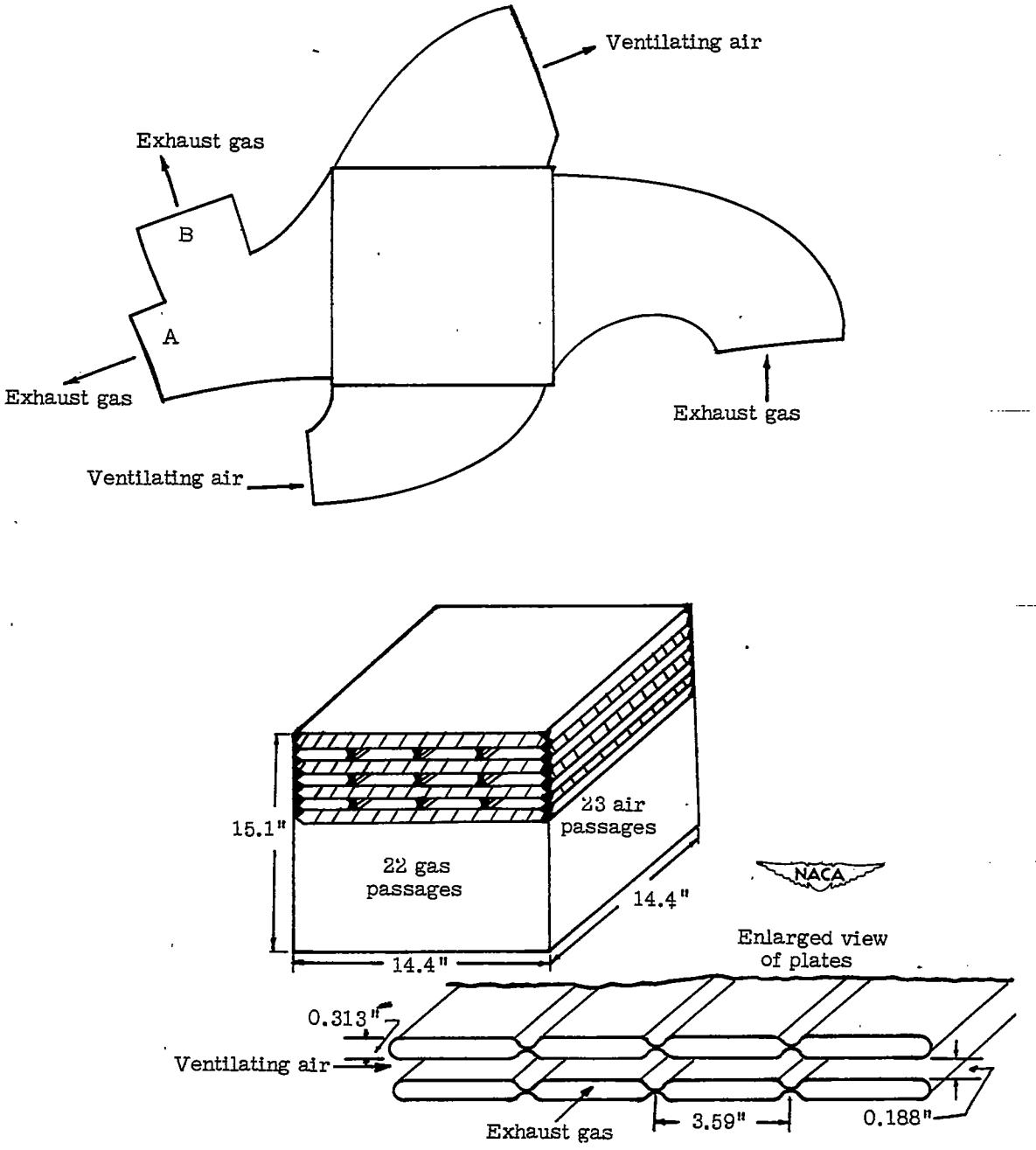

Figure 32.- Schematic diagram of heat exchanger I and ducts. Weight of heat exchanger, 97 pounds.

	Air side	Gas side
Cross-sectional area, sq ft	0.430	0.618
Heat-transfer area, sq ft	64.0	63.0

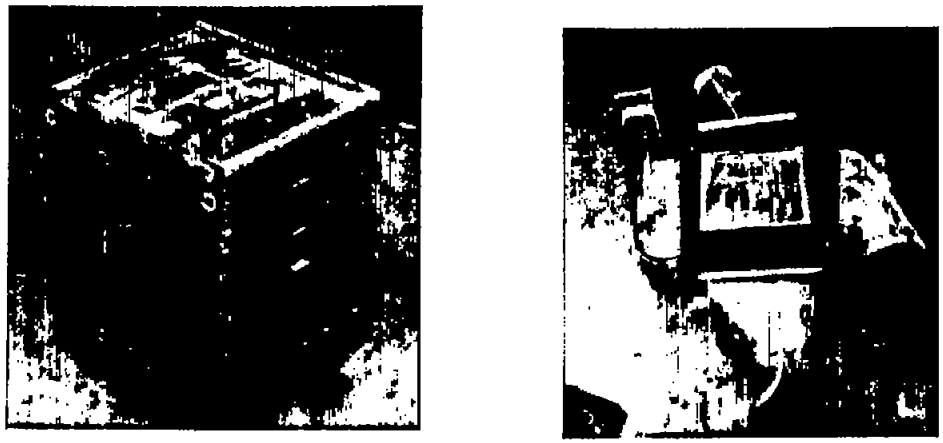

Figure 33.- Flat-plate heat exchanger I and (on right) disassembled heater and headers.

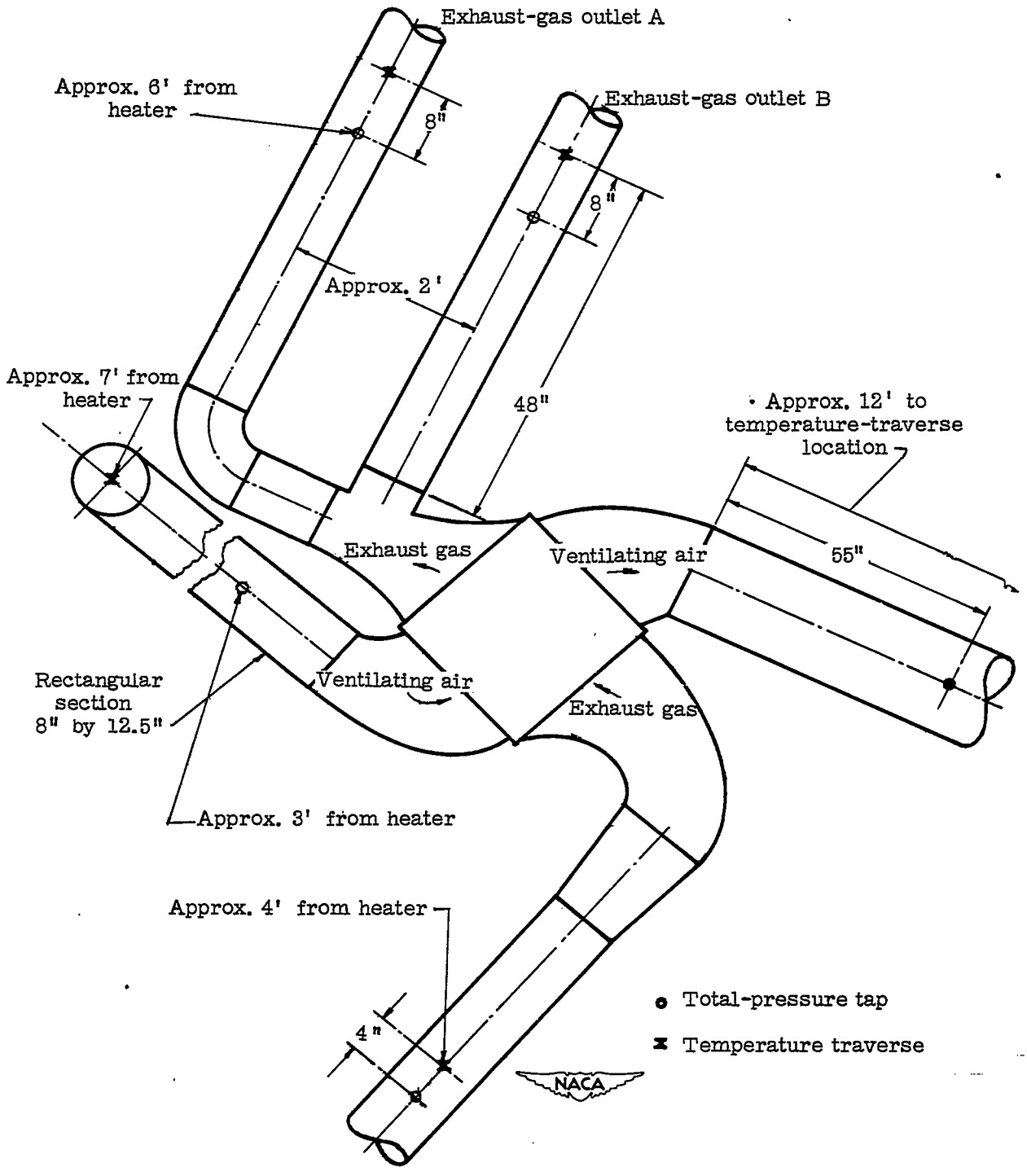

Figure 34.- Schematic diagram of test setup of heat exchanger I, showing location of total-pressure and temperature measuring stations.

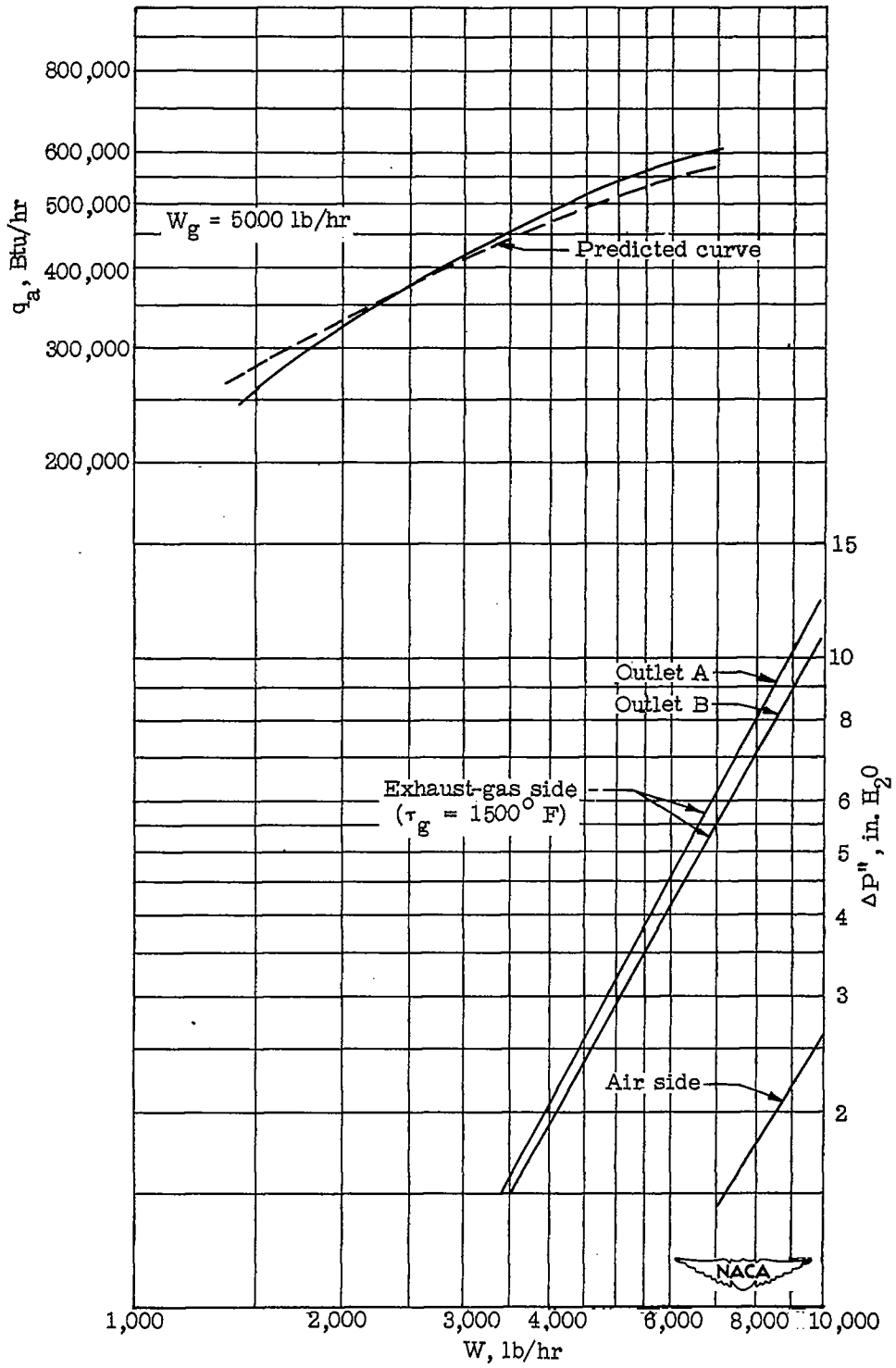

Figure 35.- Thermal output and isothermal frictional pressure drops of flat-plate heat exchanger I.

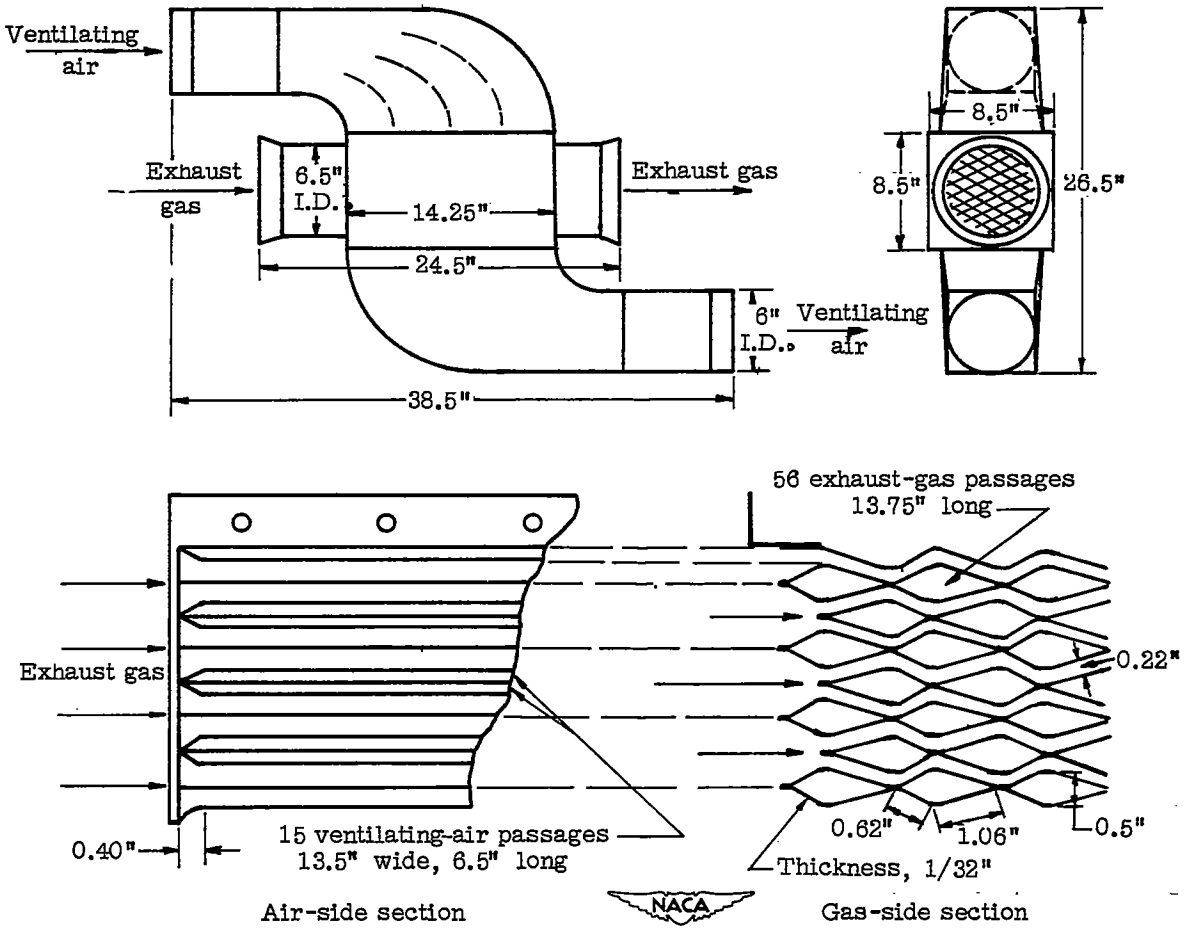

Figure 36.- Schematic diagram of heat exchanger J and air shroud. Weight of heat exchanger, 33 pounds; weight of air shroud, 12 pounds.

	Air side	Gas side
Cross-sectional area, sq ft	0.216	0.152
Heat-transfer area, sq ft	19.2	19.2

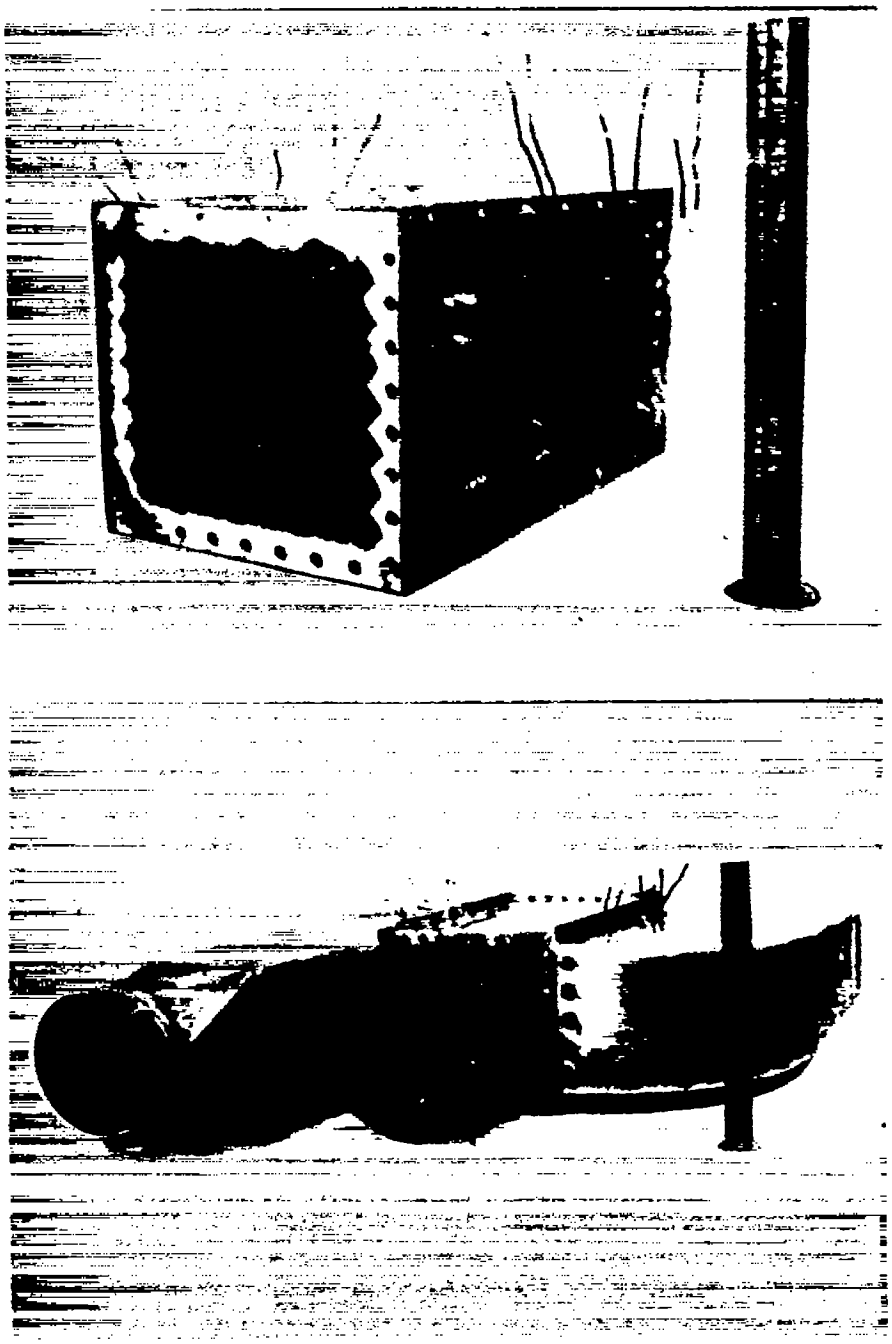

Figure 37.- Wave-plate heat exchanger J using Tr-1 shroud.

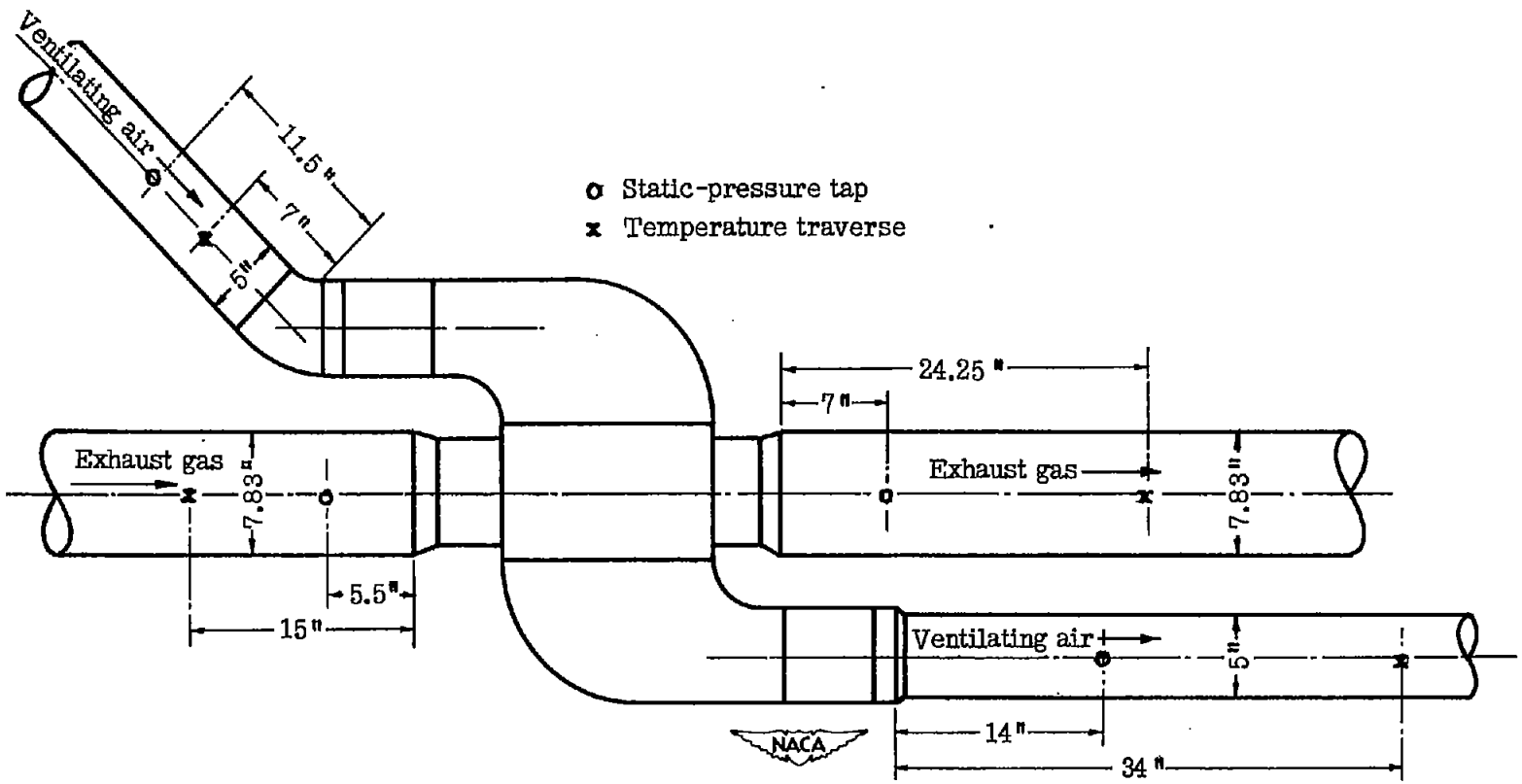

Figure 38.- Schematic diagram of test setup of heat exchanger J and air shroud, showing location of static-pressure and temperature measuring stations.

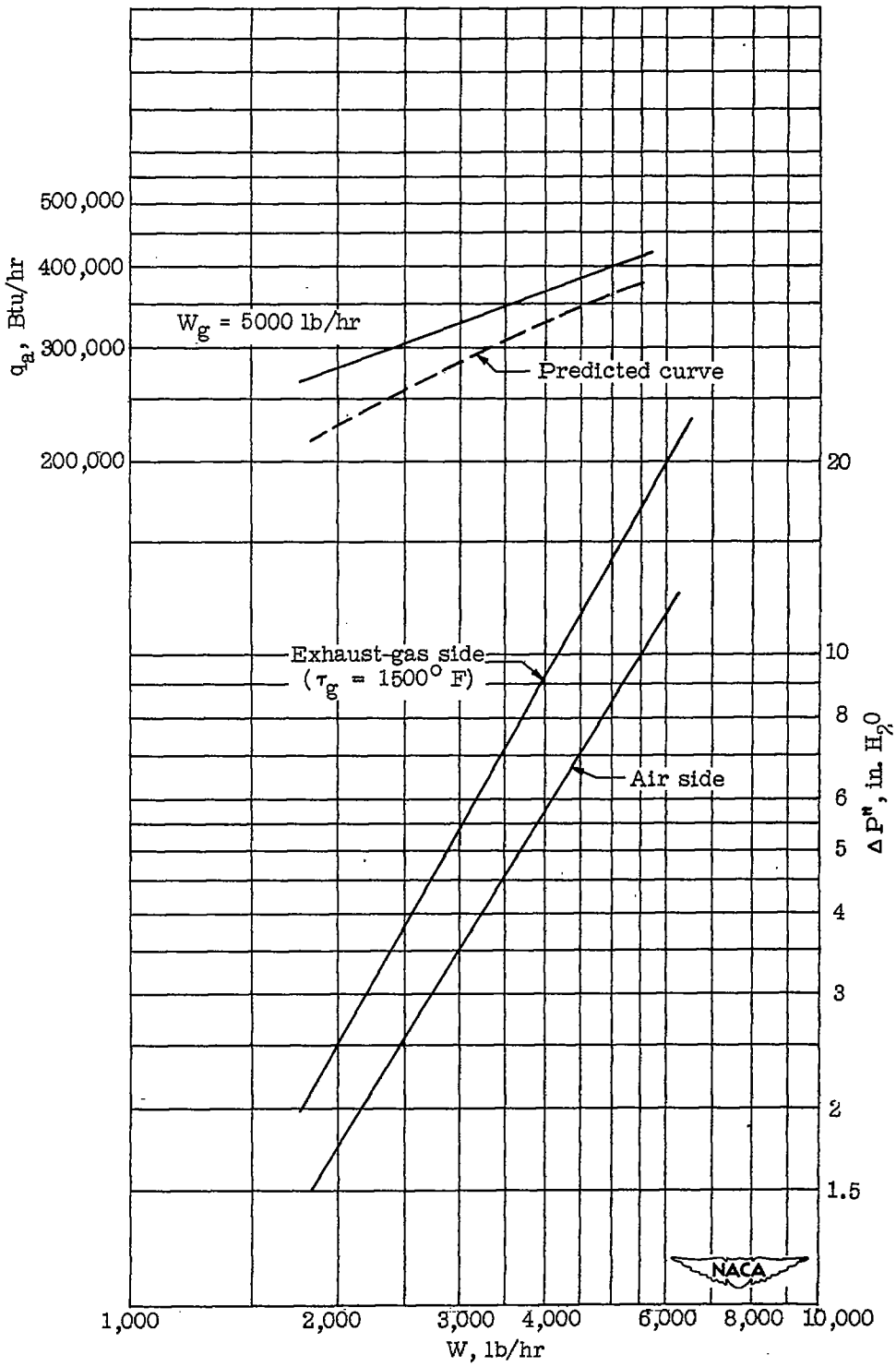

Figure 39.- Thermal output and isothermal frictional pressure drops of wave-plate heat exchanger J.

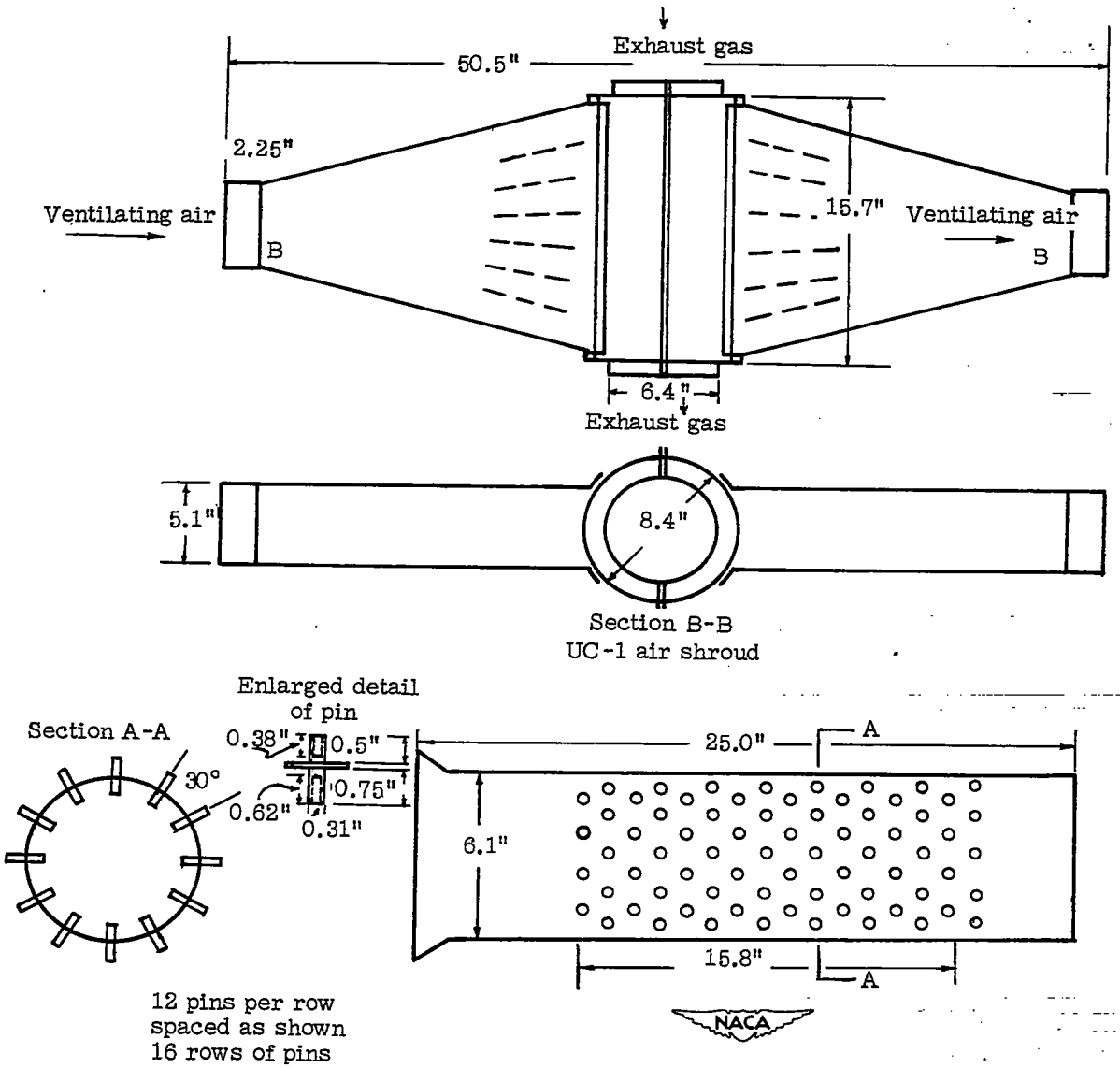

Figure 40.- Schematic diagram of hollow-pin-fin heat exchanger K and air shroud. Weight of heat exchanger, 13 pounds.

Section A-A	Air side	Gas side
Minimum cross-sectional area, sq ft	0.193	0.213

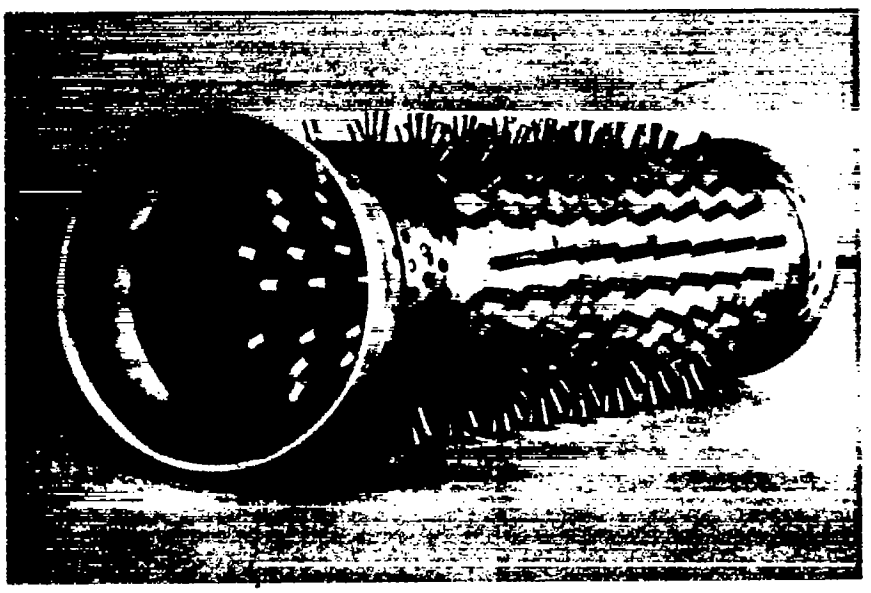

Figure 41.- Hollow-pin heat exchanger K.

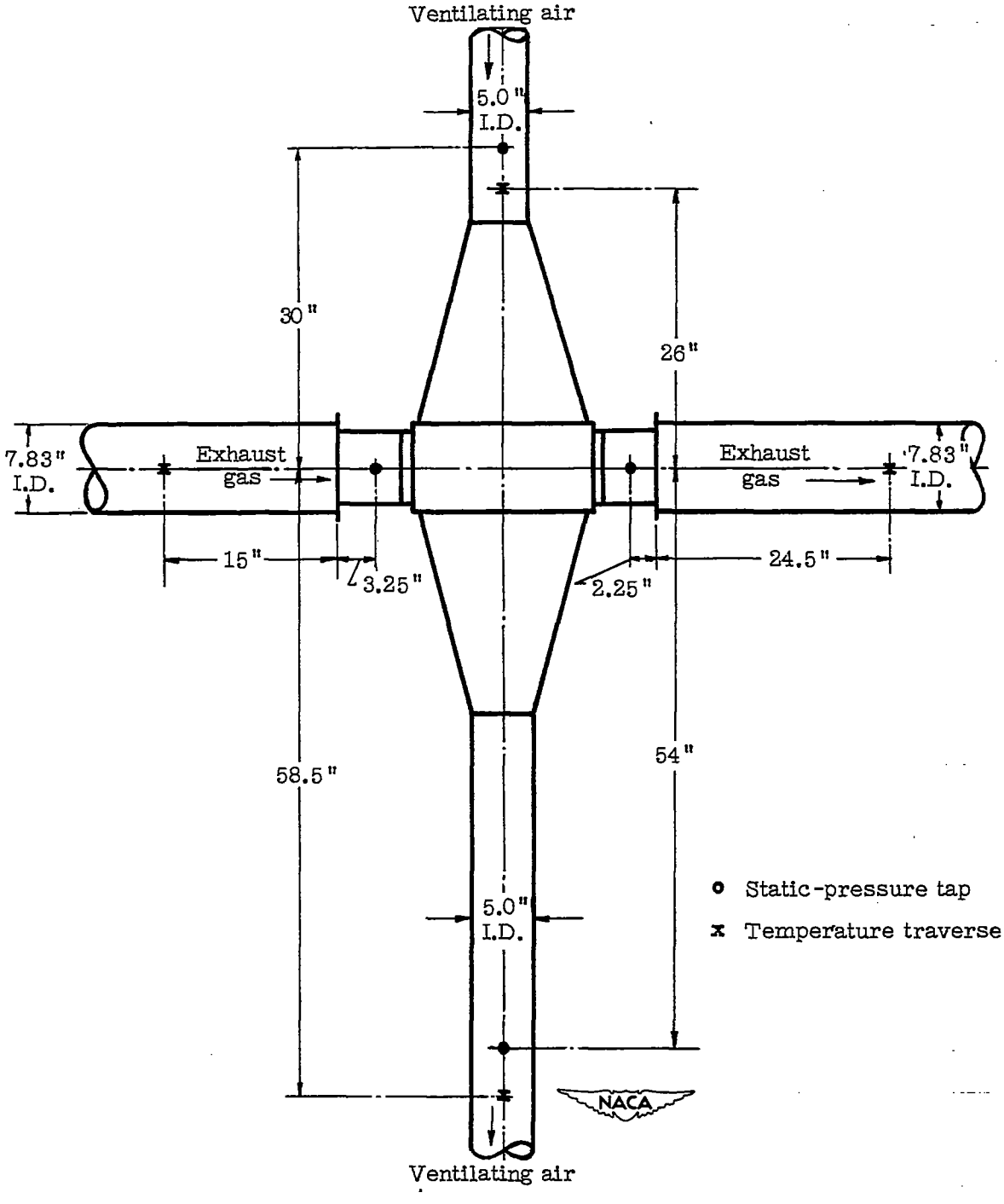

Figure 42.- Schematic diagram of test setup of heat exchanger K and air shroud, showing location of static-pressure and temperature measuring stations.

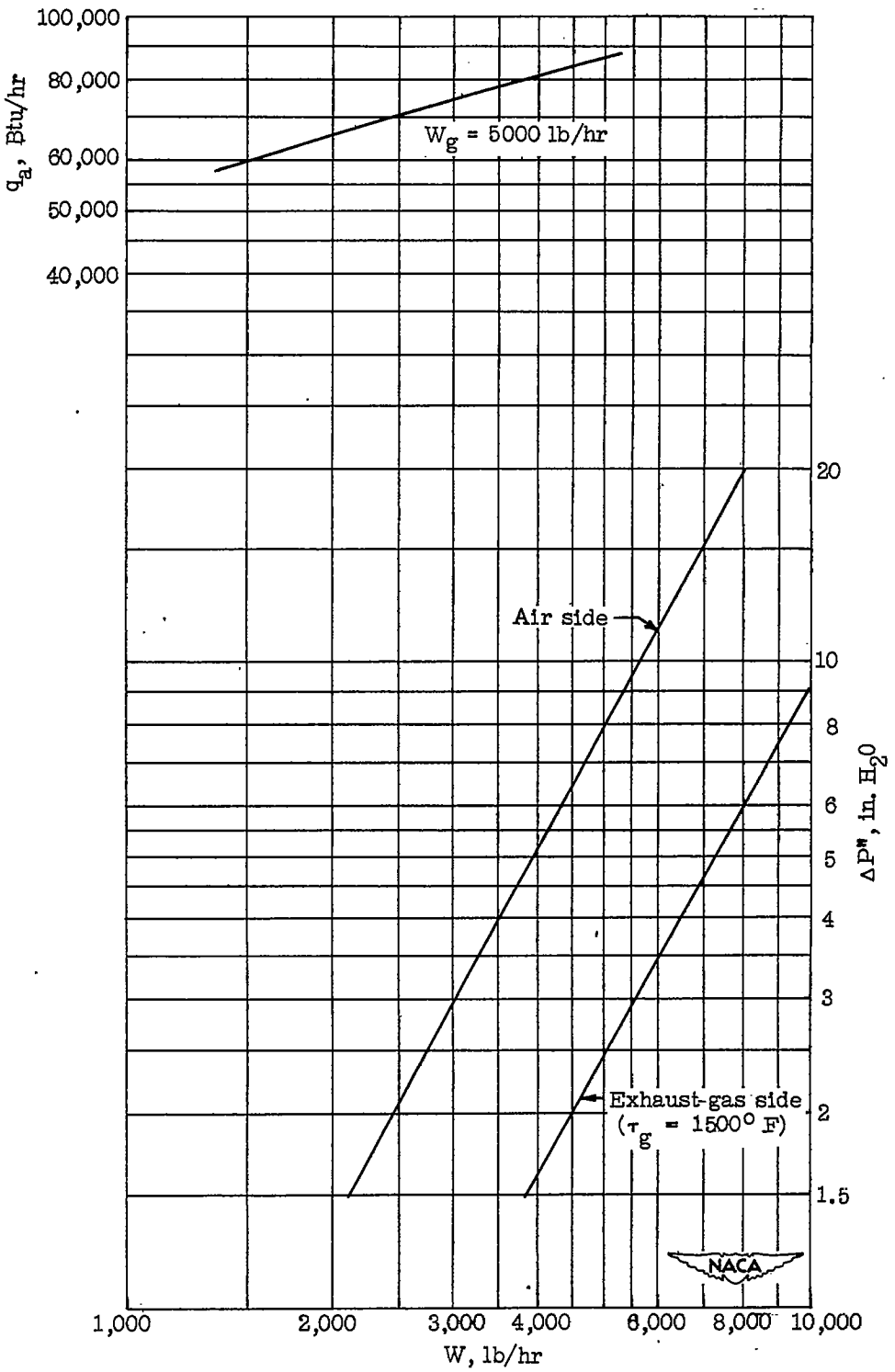

Figure 43.- Thermal output and isothermal frictional pressure drops of hollow-pin heat exchanger K.

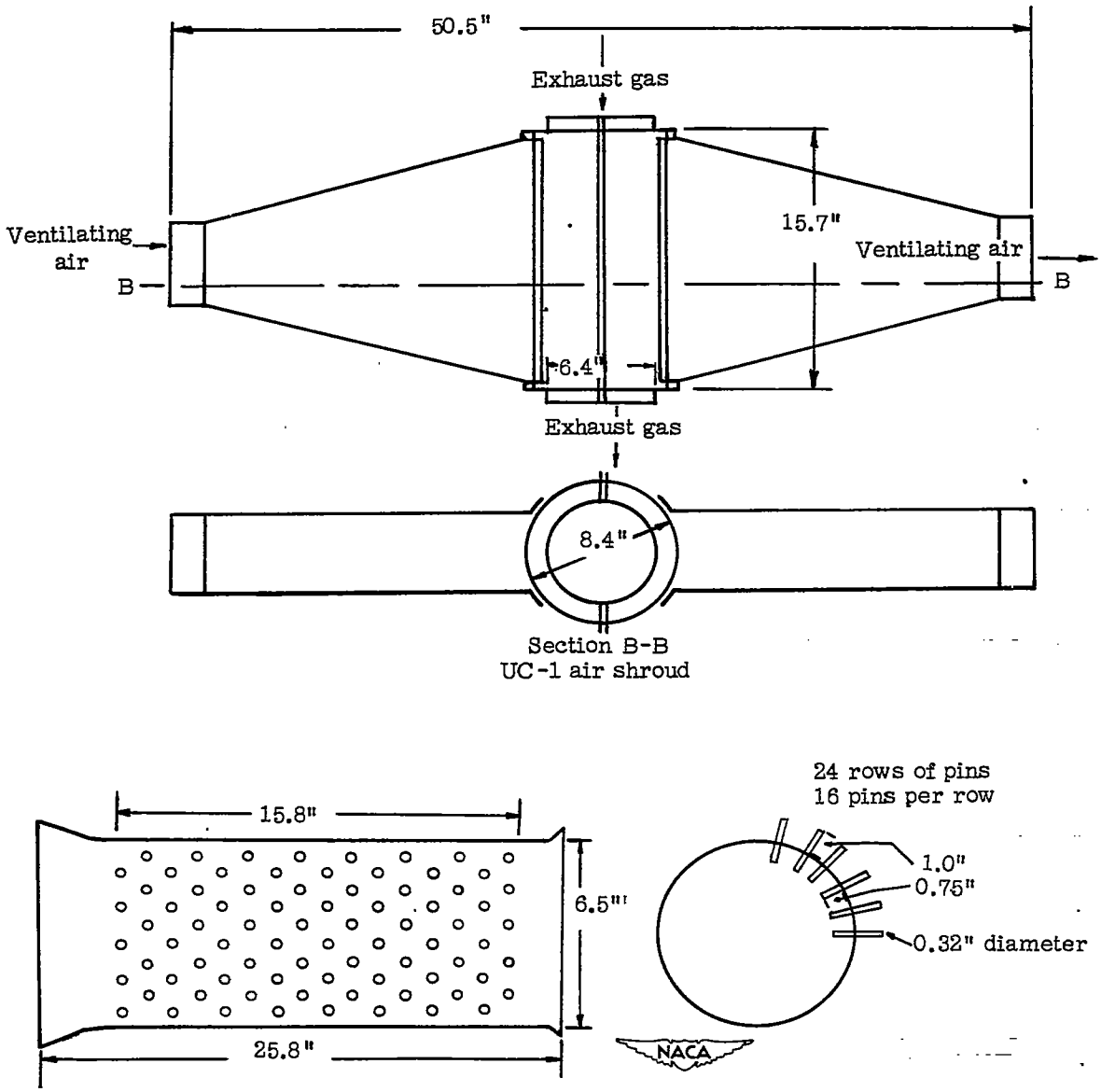

Figure 44.- Schematic diagram of heat exchanger L and air shroud. Weight of heat exchanger, 25 pounds.

	Air side	Gas side
Minimum cross-sectional area, sq ft	0.184	0.191

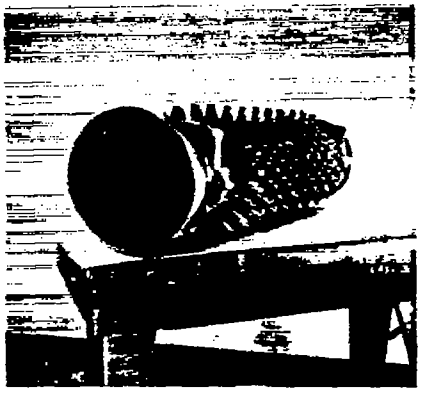

Figure 45.- Pin heat exchanger L.

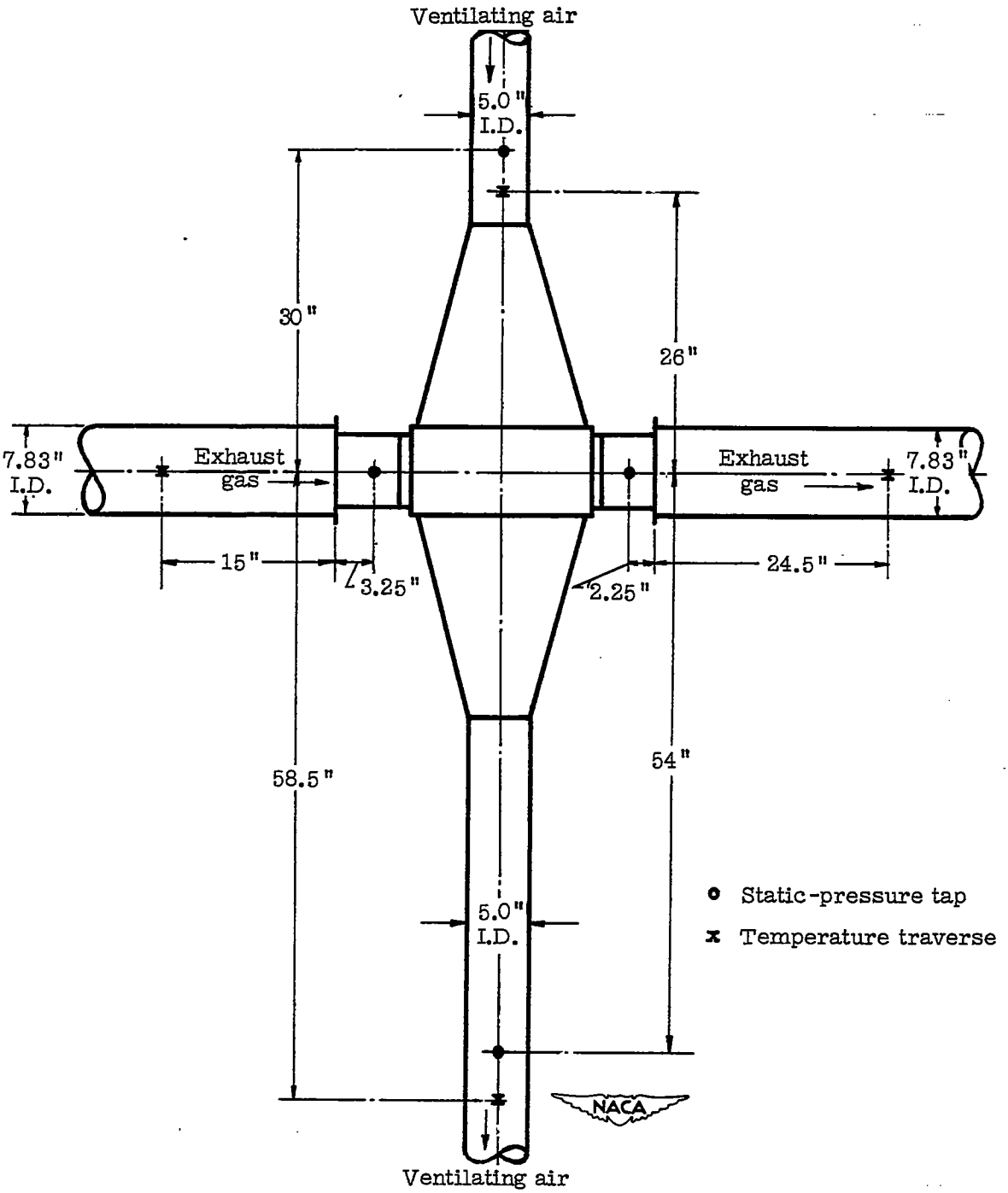

Figure 46.- Schematic diagram of test setup of heat exchanger L and air shroud, showing location of static-pressure and temperature measuring stations.

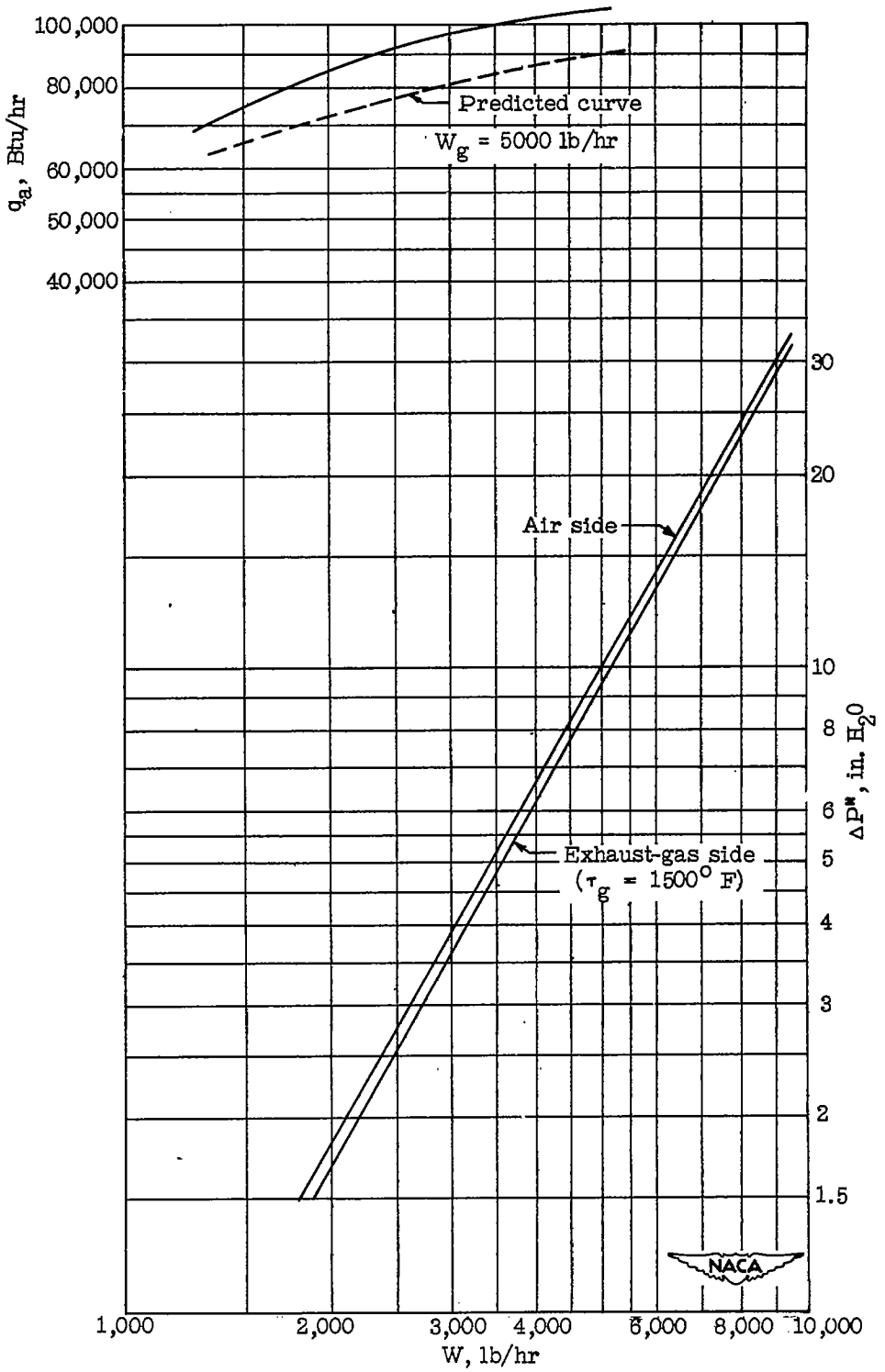

Figure 47.- Thermal output and isothermal frictional pressure drops of pin heat exchanger L.

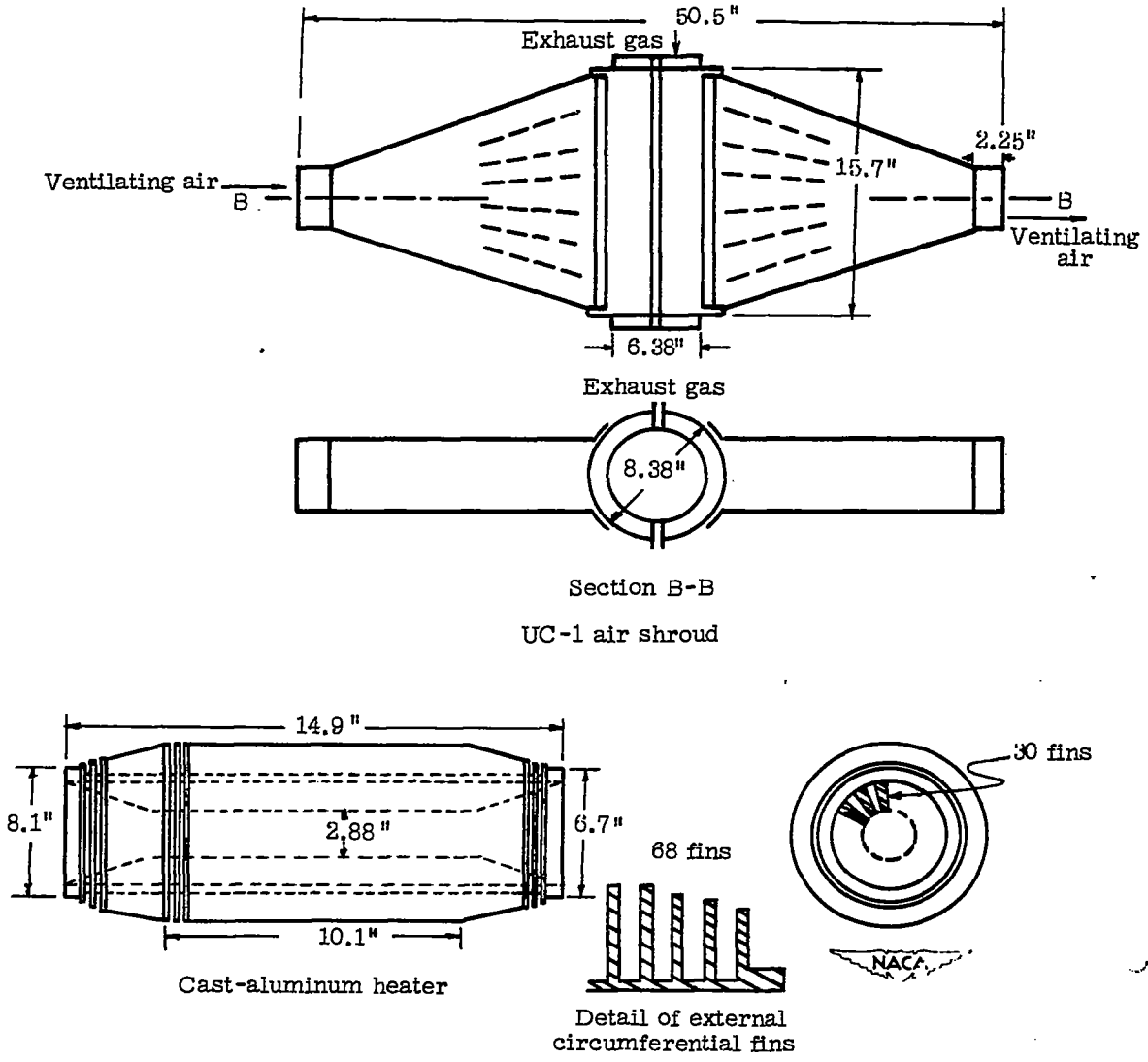

Figure 48.- Schematic diagram of cast-aluminum heat exchanger M and air shroud. Weight of heat exchanger, 31.0 pounds.

	Air side	Gas side
Cross-sectional area, sq ft	0.170	0.111

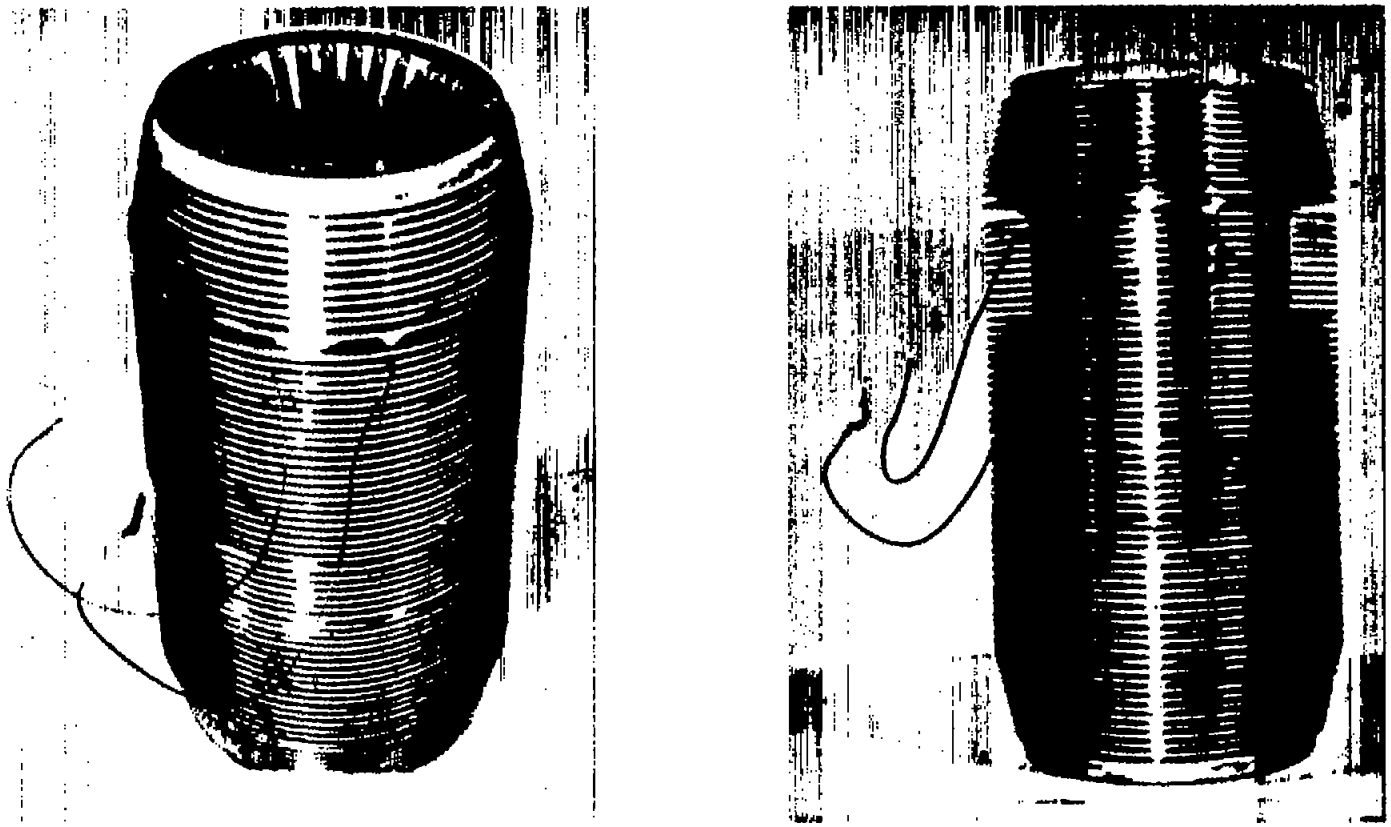

Figure 49.- Cast-aluminum fin heat exchanger M.

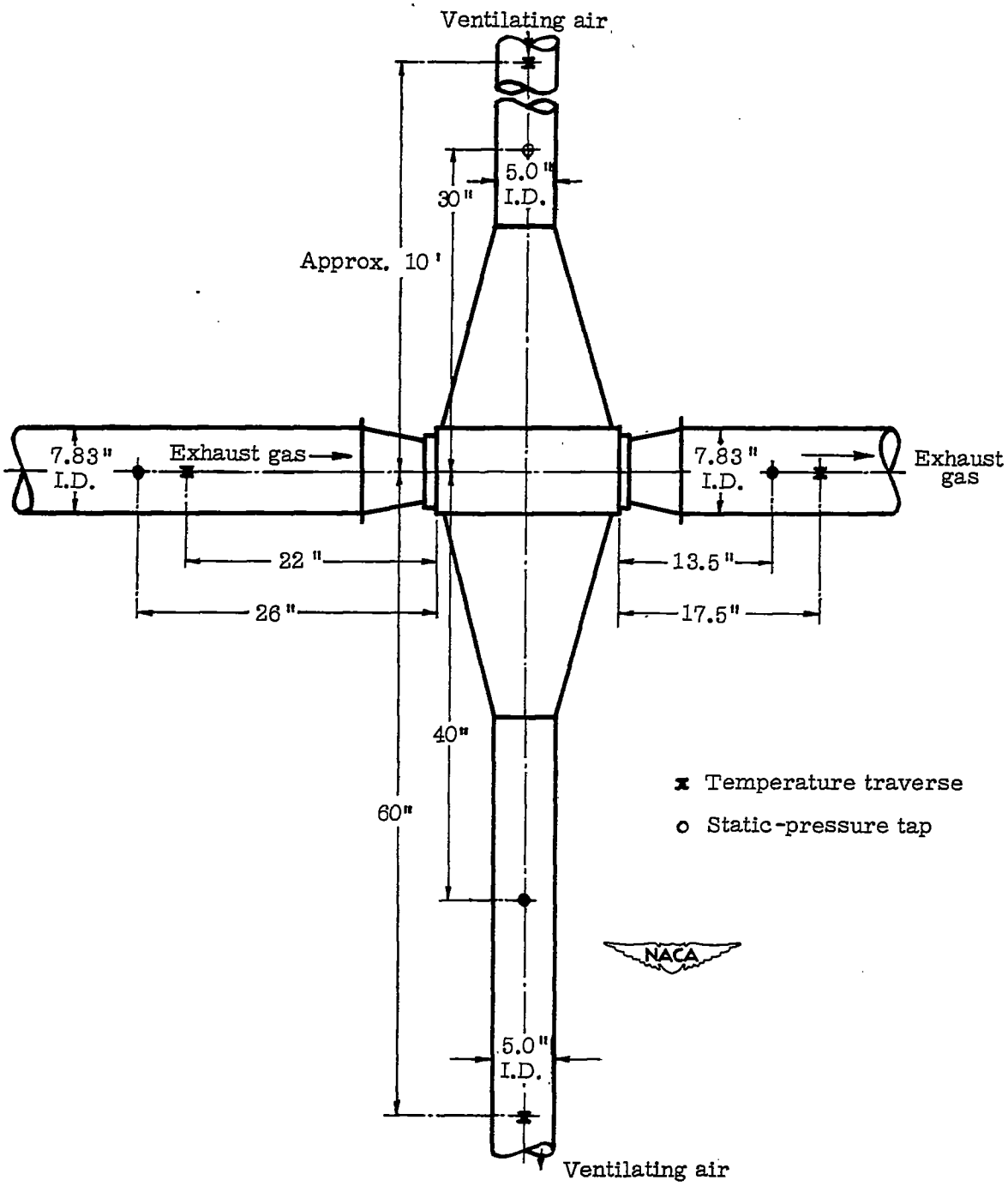

Figure 50.- Schematic diagram of test setup of heat exchanger M and air shroud, showing location of static-pressure and temperature measuring stations.

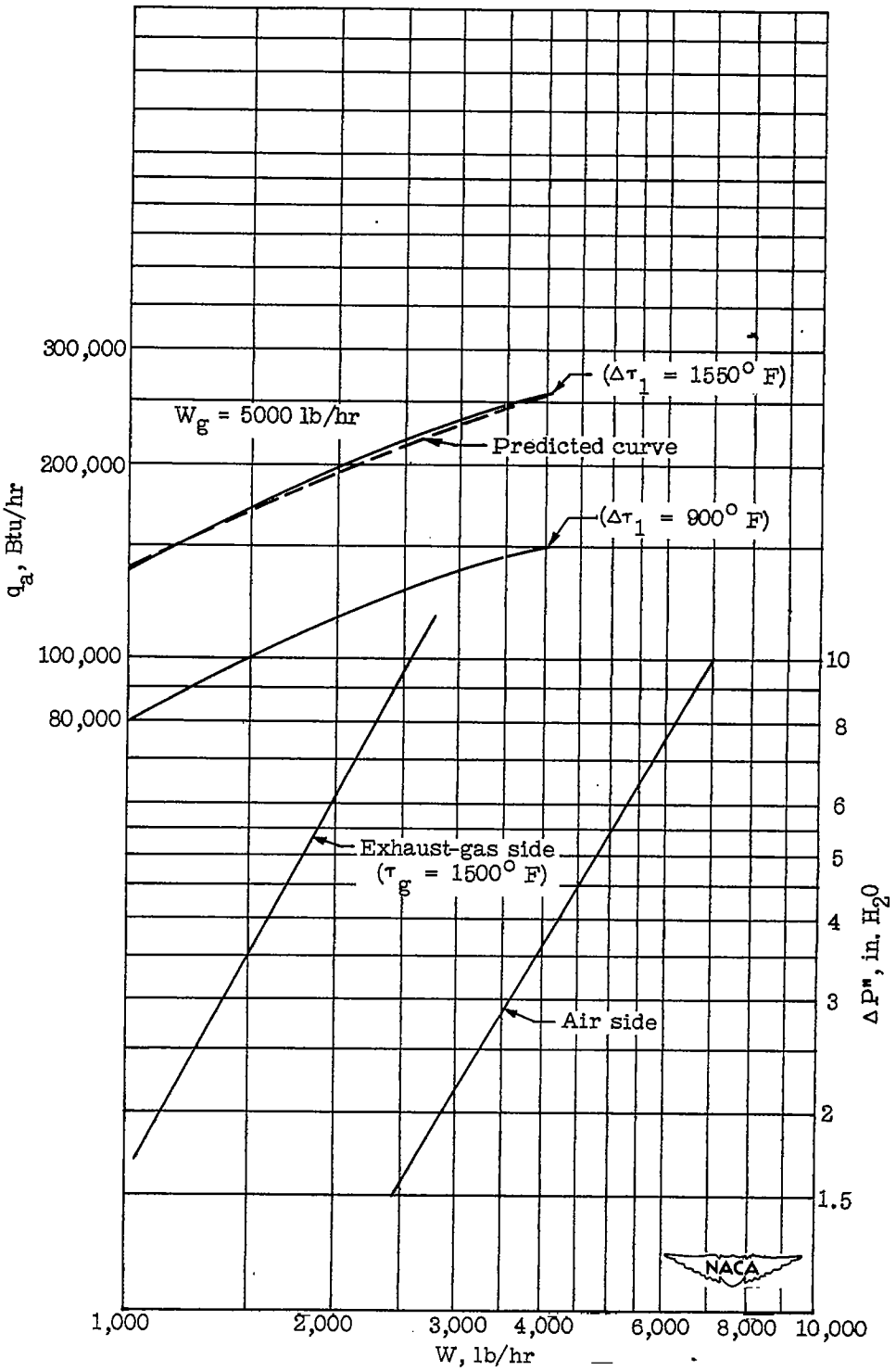

Figure 51.- Thermal output and isothermal frictional pressure drops of cast-aluminum fin heat-exchanger M.

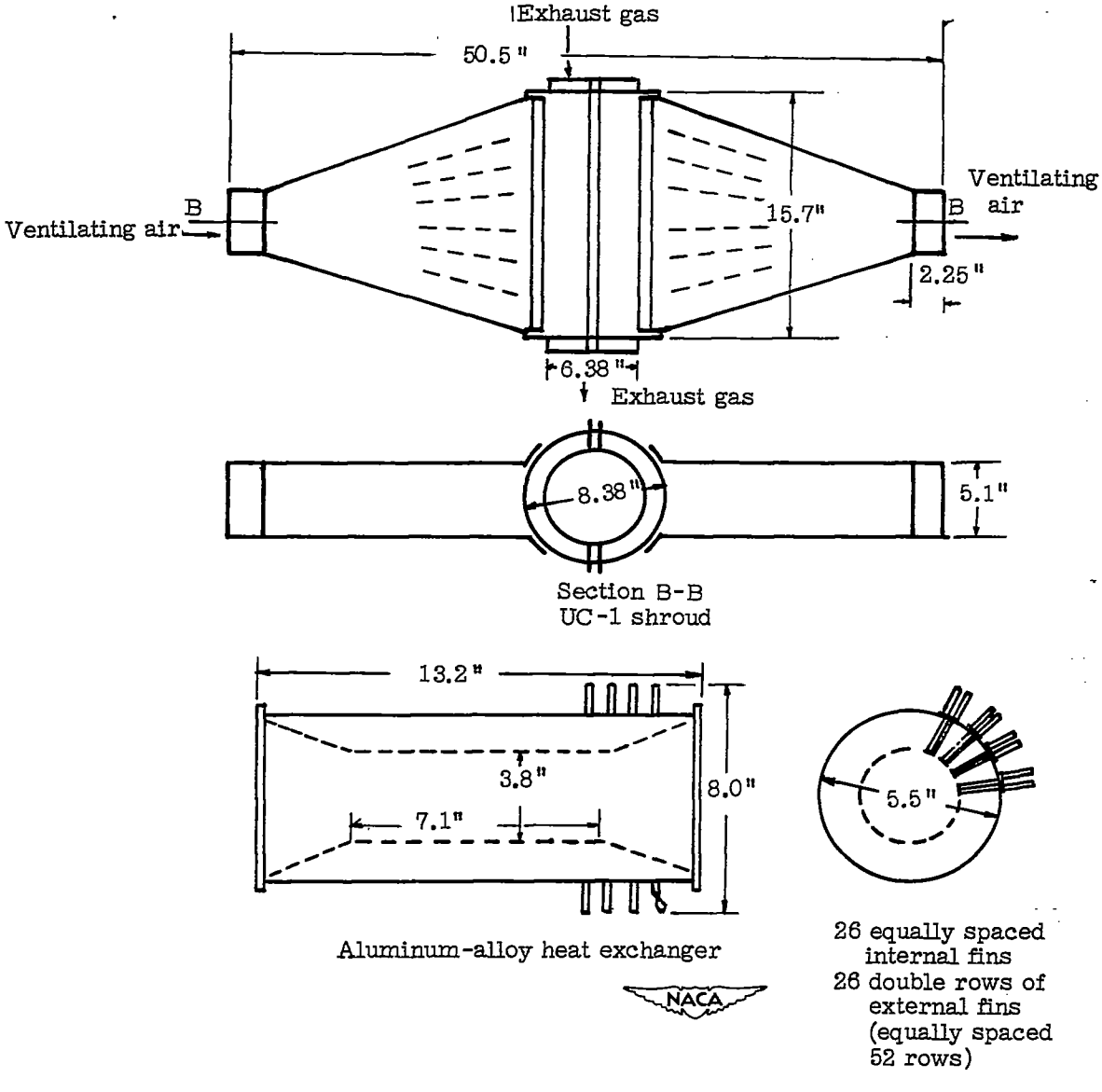

Figure 52.- Schematic diagram of fin heat exchanger N and air shroud. Weight of heat exchanger, 10 pounds.

	Air side	Gas side
Cross-sectional area, sq ft	0.302	0.109

Figure 53.- Aluminum-alloy fin heat exchanger N.

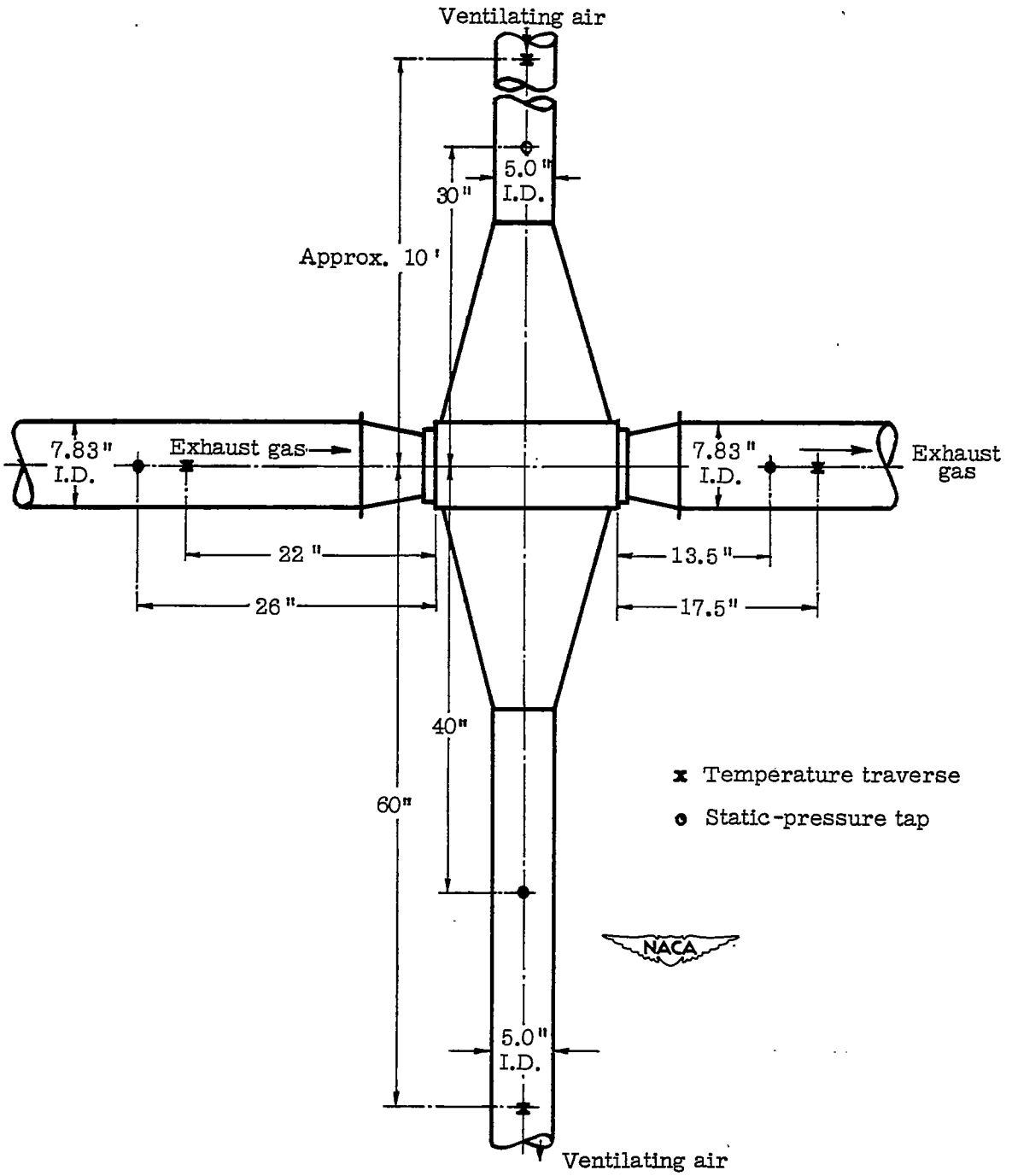

Figure 54.- Schematic diagram of test setup of heat exchanger N and air shroud, showing location of static-pressure and temperature measuring stations.

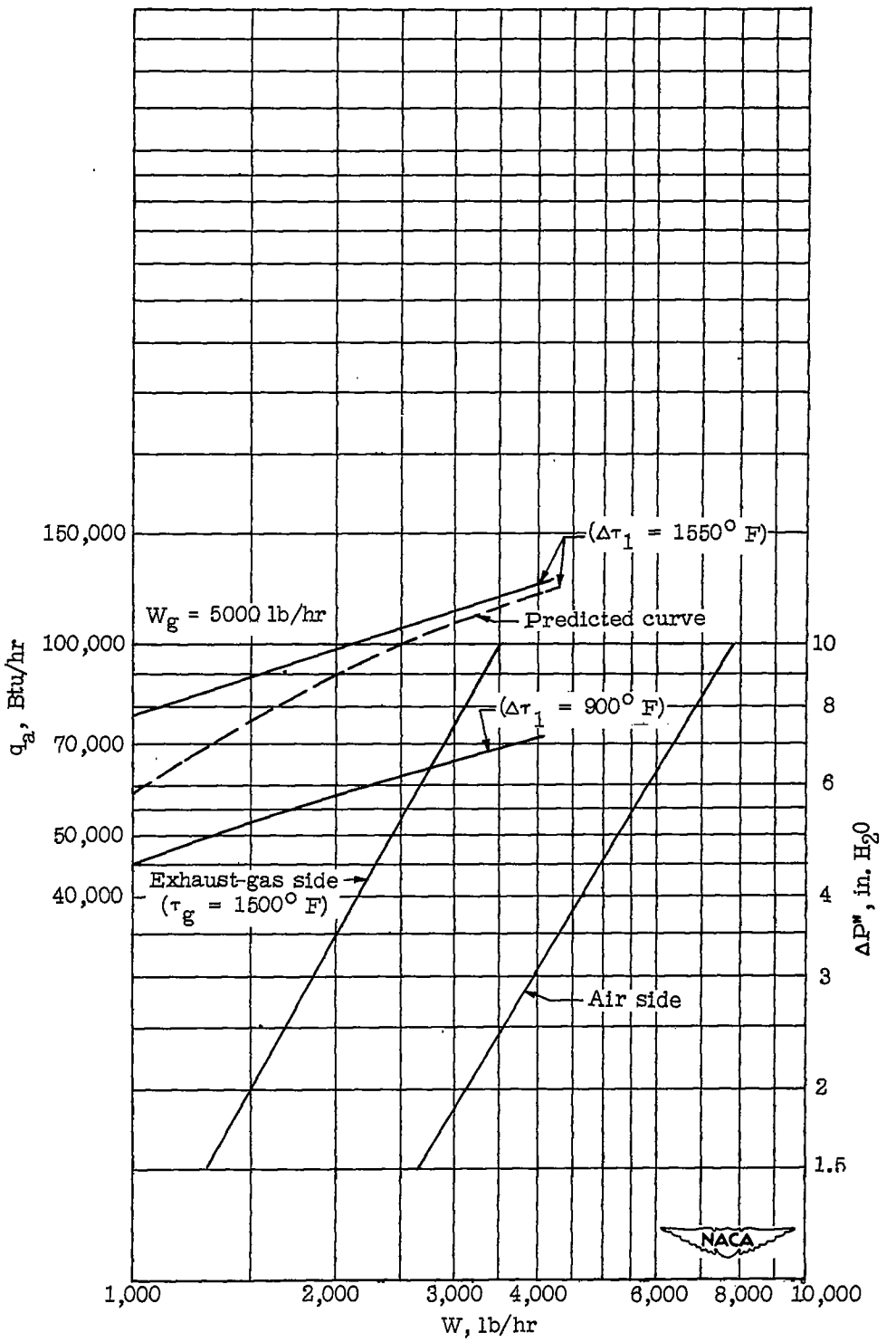

Figure 55.- Thermal output and isothermal frictional pressure drops of aluminum-alloy fin heat exchanger N.

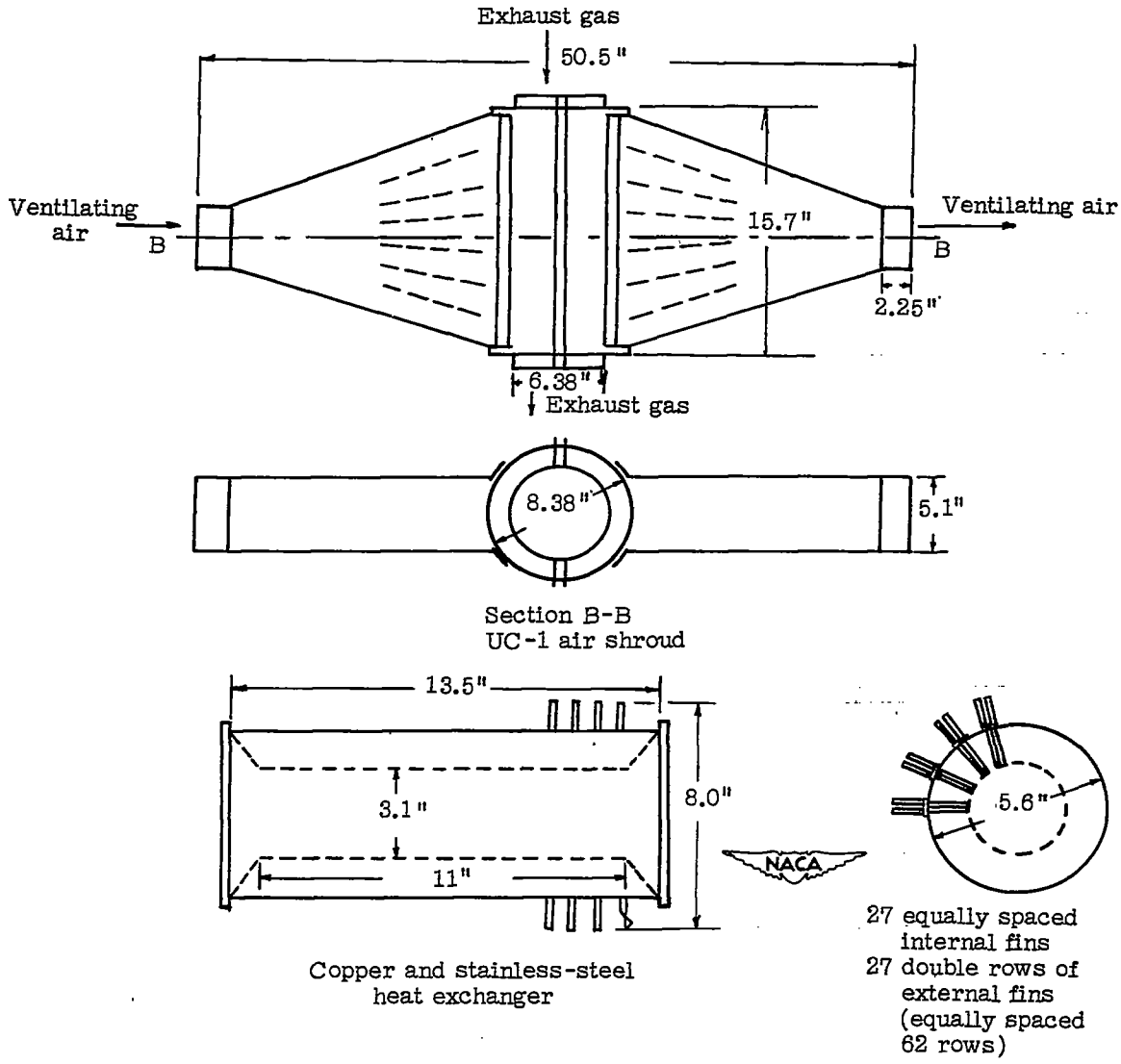

Figure 56.- Schematic diagram of fin heat exchanger O and air shroud. Weight of heat exchanger, 24.5 pounds.

	Air side	Gas side
Cross-sectional area, sq ft	0.262	0.142

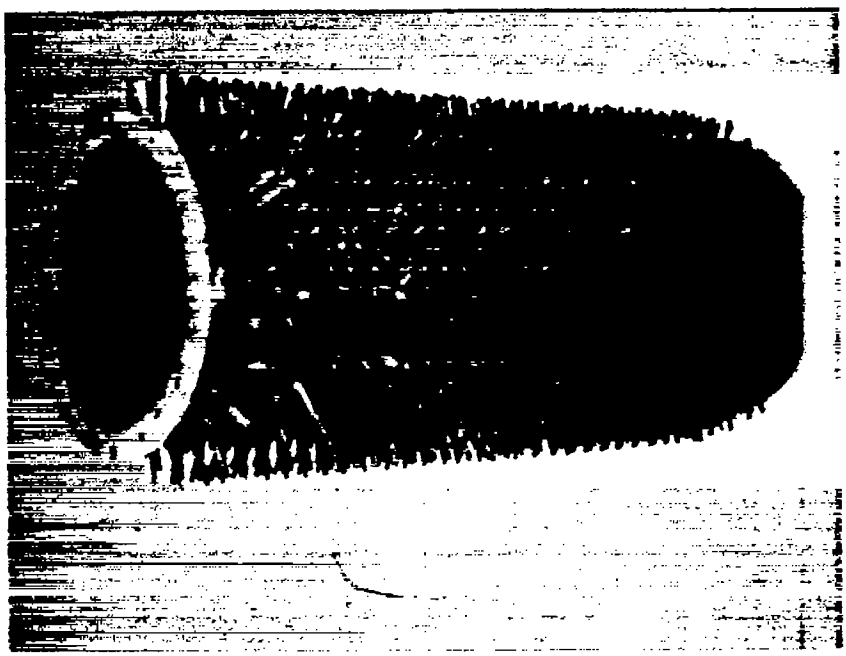

Figure 57.- Copper and stainless-steel heat exchanger O.

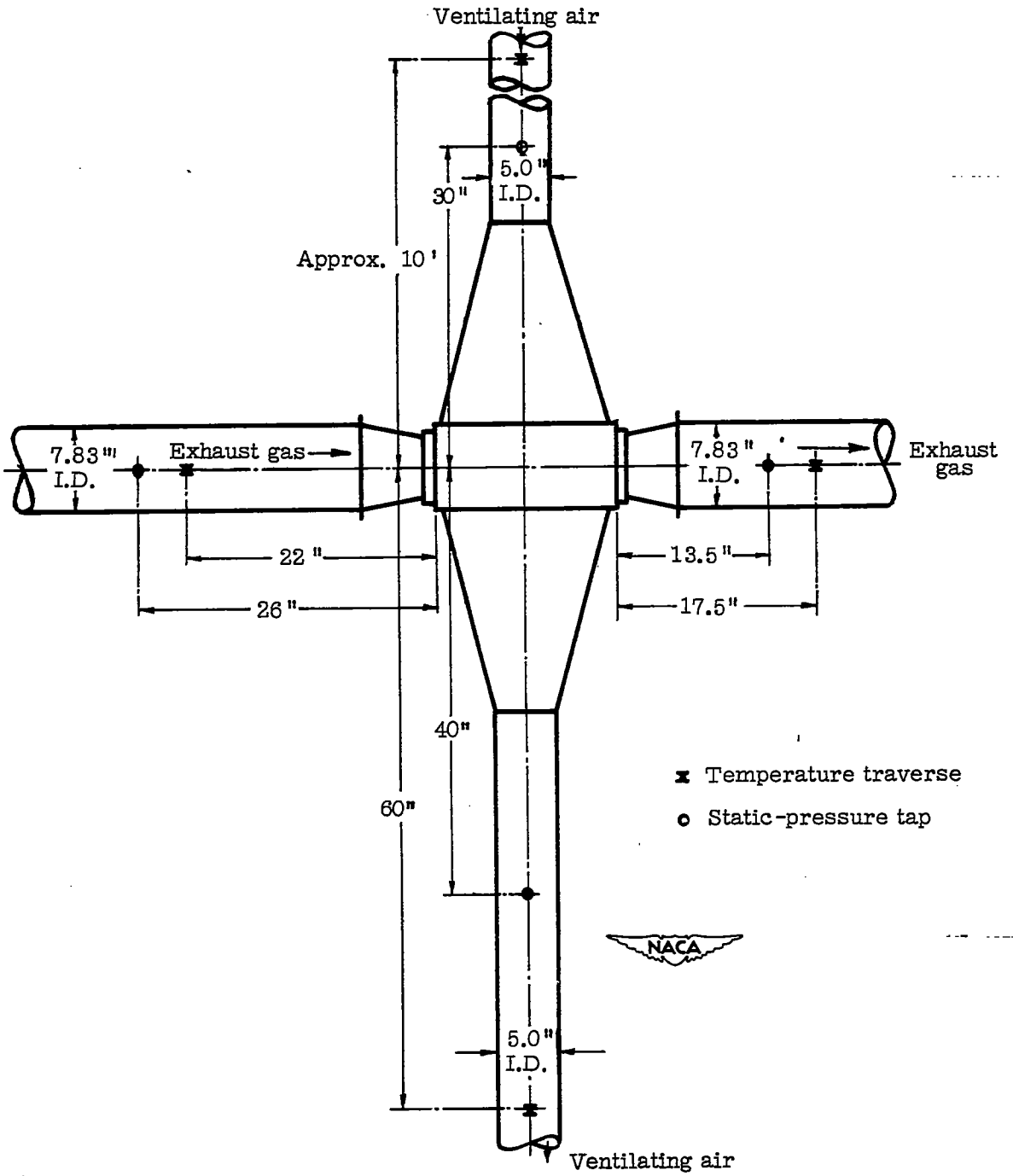

Figure 58.- Schematic diagram of test setup of heat exchanger O and air shroud, showing location of static-pressure and temperature measuring stations.

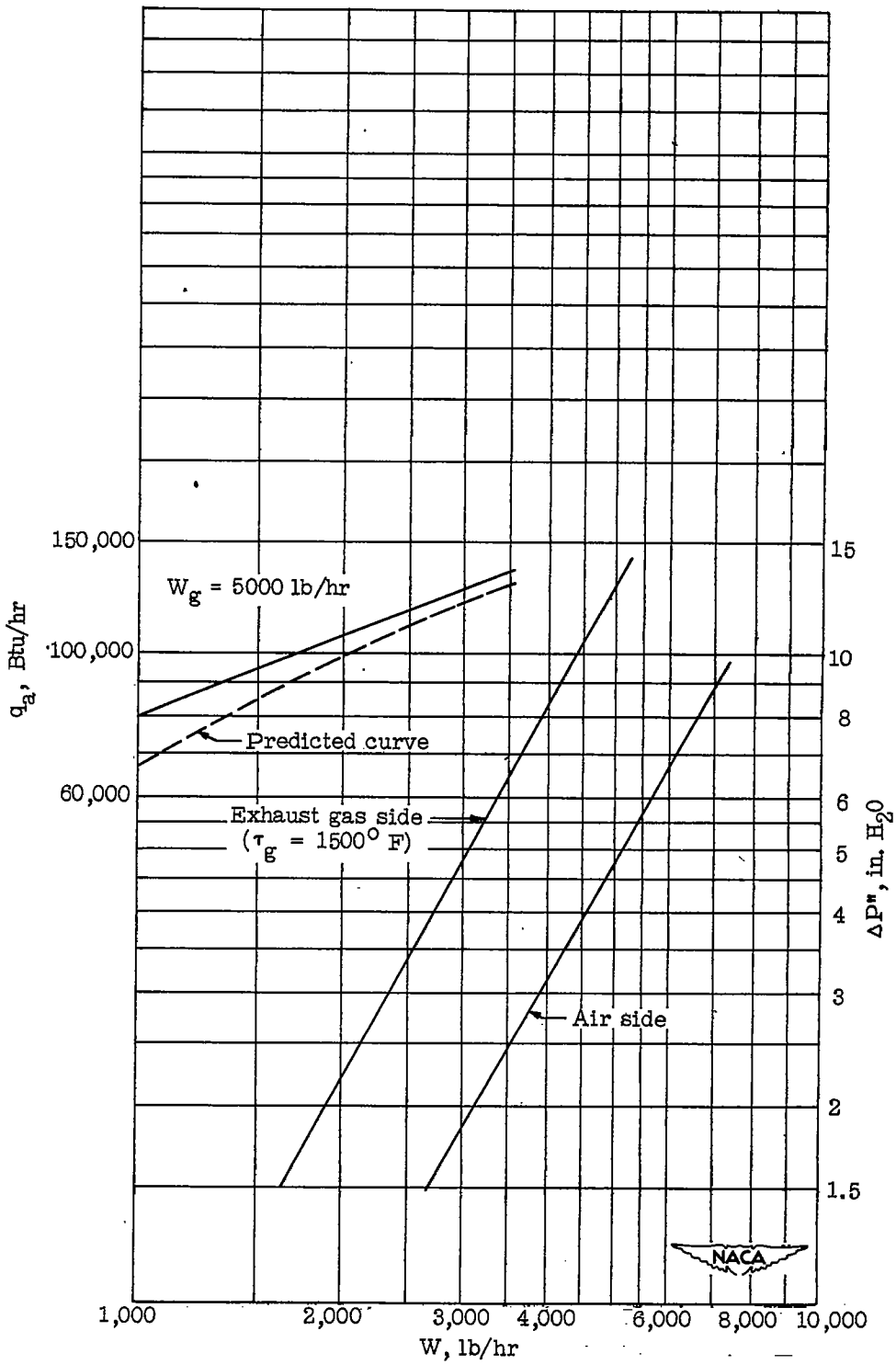

Figure 59.- Thermal output and isothermal frictional pressure drops of copper and stainless-steel fin heat exchanger O.

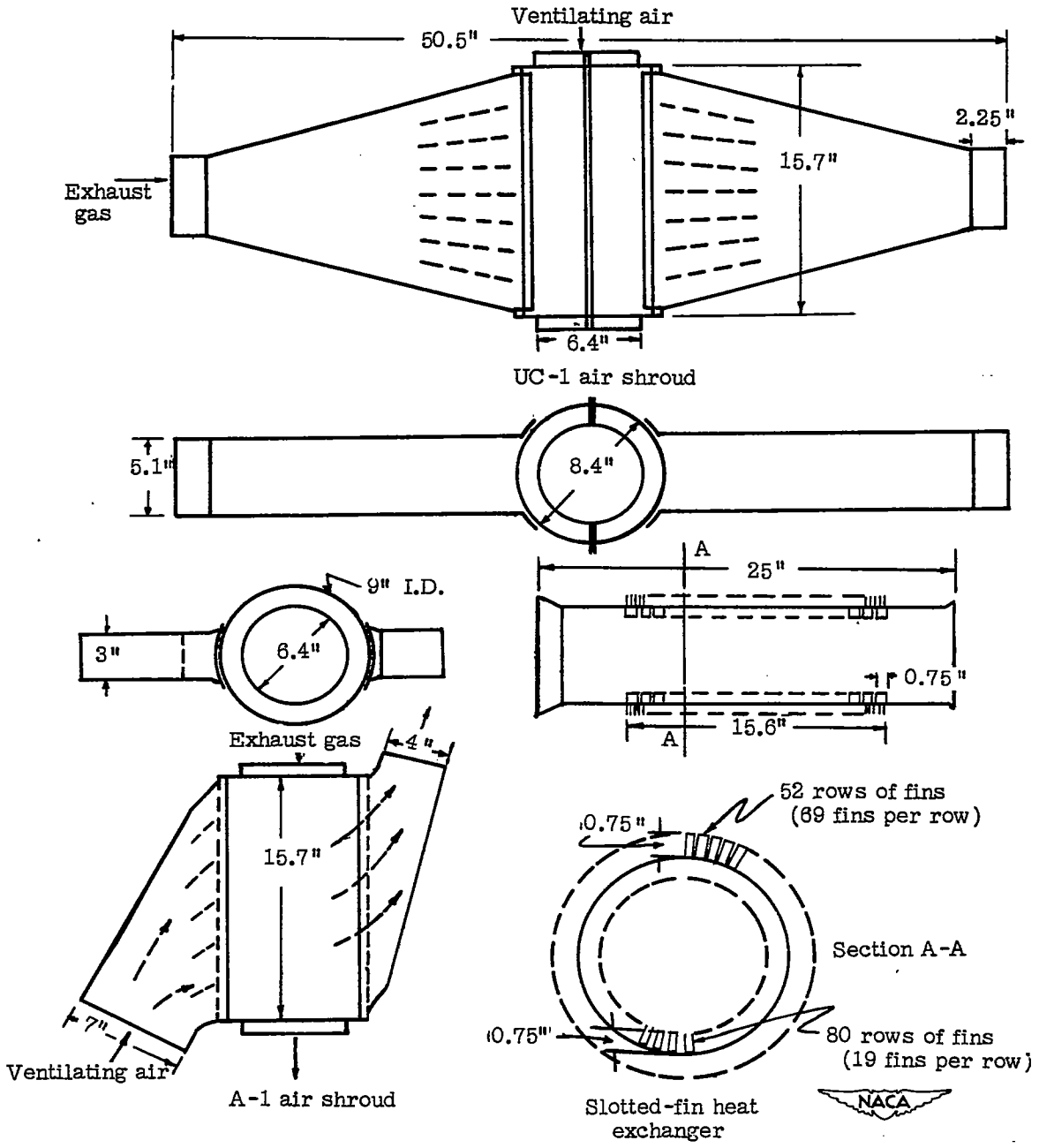

Figure 60.- Schematic diagram of slotted-fin heat exchanger P and air shrouds UC-1 and A-1. Weight of heat exchanger, 32.5 pounds.

	Air side		Gas side
	UC-1	A-1	
Cross-sectional area, sq ft	0.203	0.271	0.203

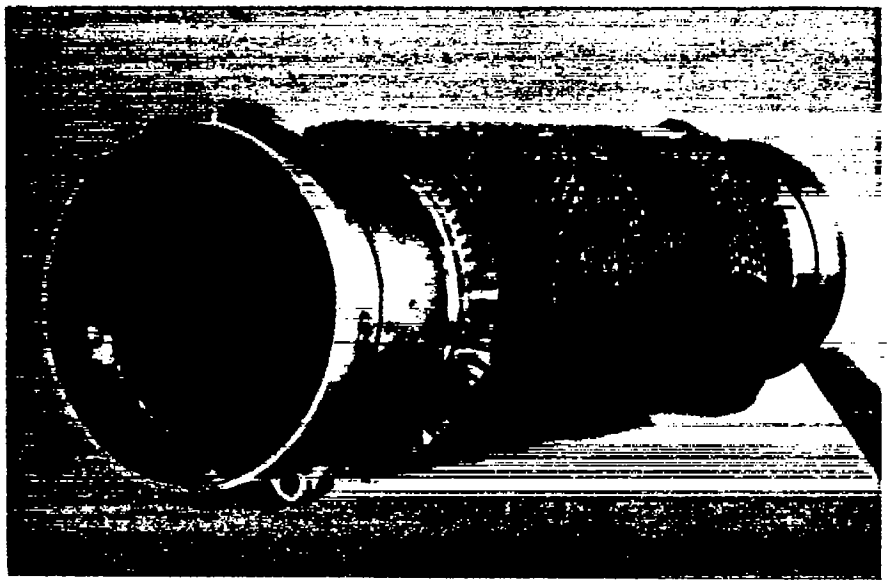

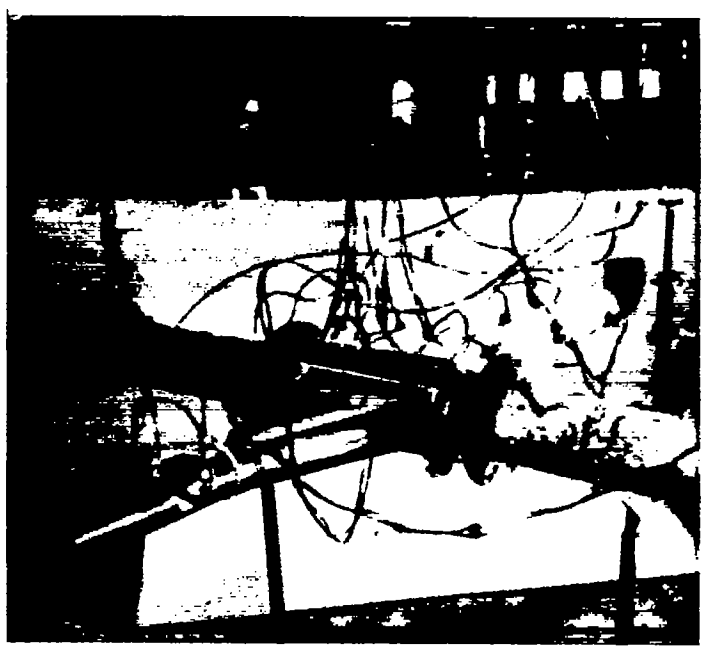

Figure 61.- Slotted-fin heat exchanger P and test setup.

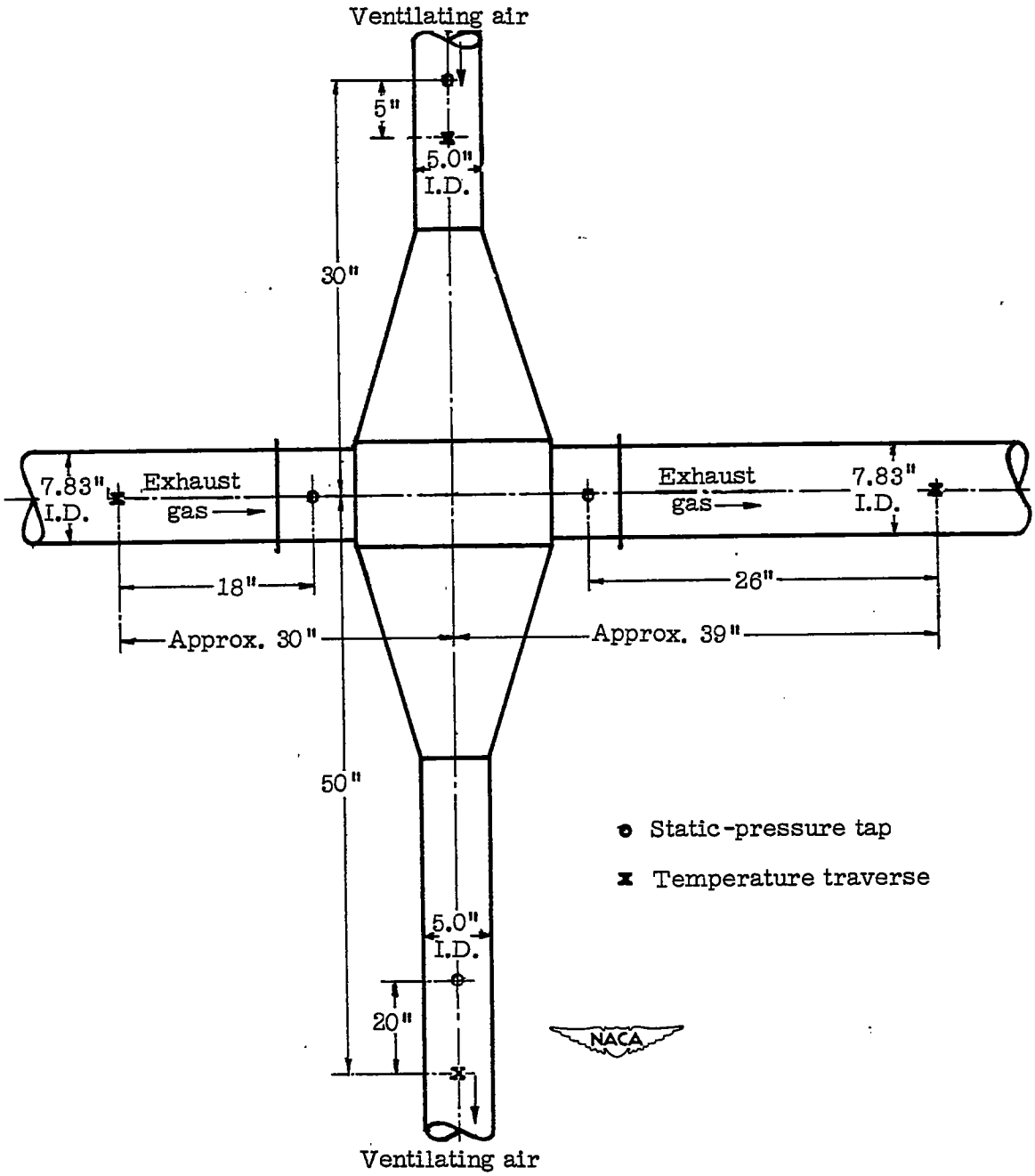

Figure 62.- Schematic diagram of test setup of heat exchanger P using UC-1 air shroud, showing location of static-pressure and temperature measuring stations.

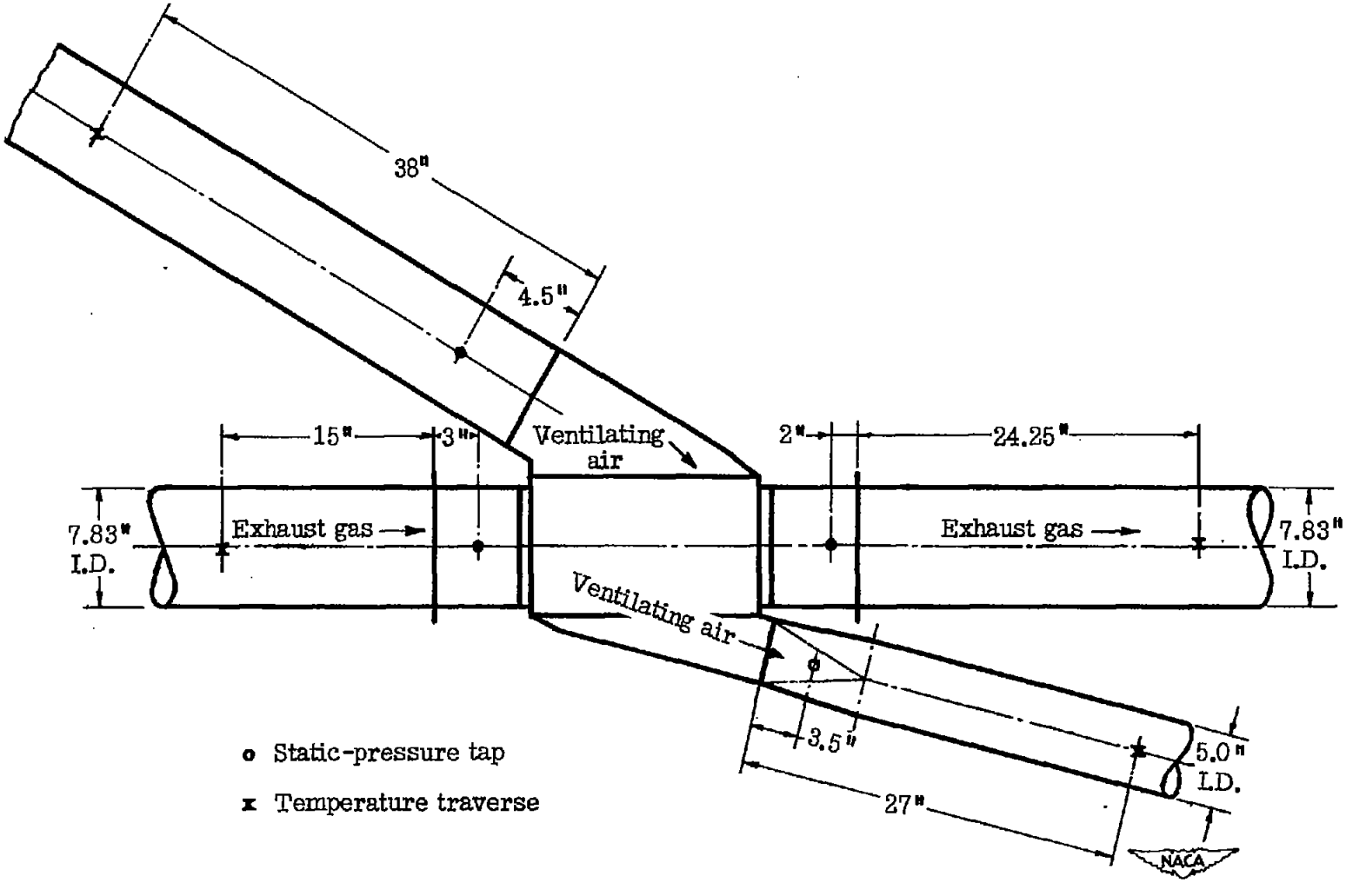

Figure 63.- Schematic diagram of test setup of heat exchanger P and air shroud, showing location of static-pressure and temperature measuring stations.

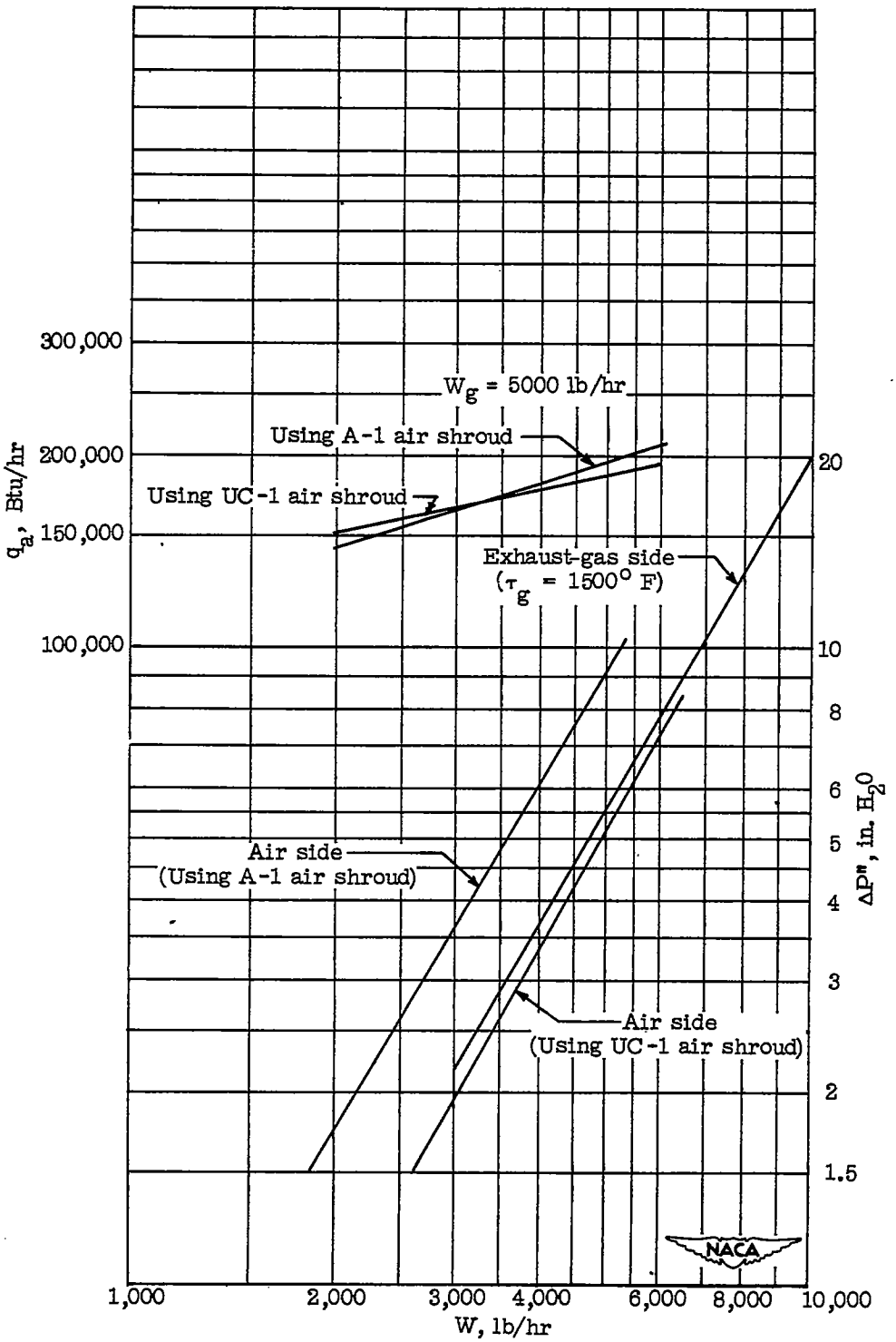

Figure 64.- Thermal output and isothermal frictional pressure drops of slotted-fin heat exchanger P.